

Asymmetric Synthesis of Substituted Pyrrolidines
via Kinetic Resolutions

Athanasia Agora

Master of Science (by Research)

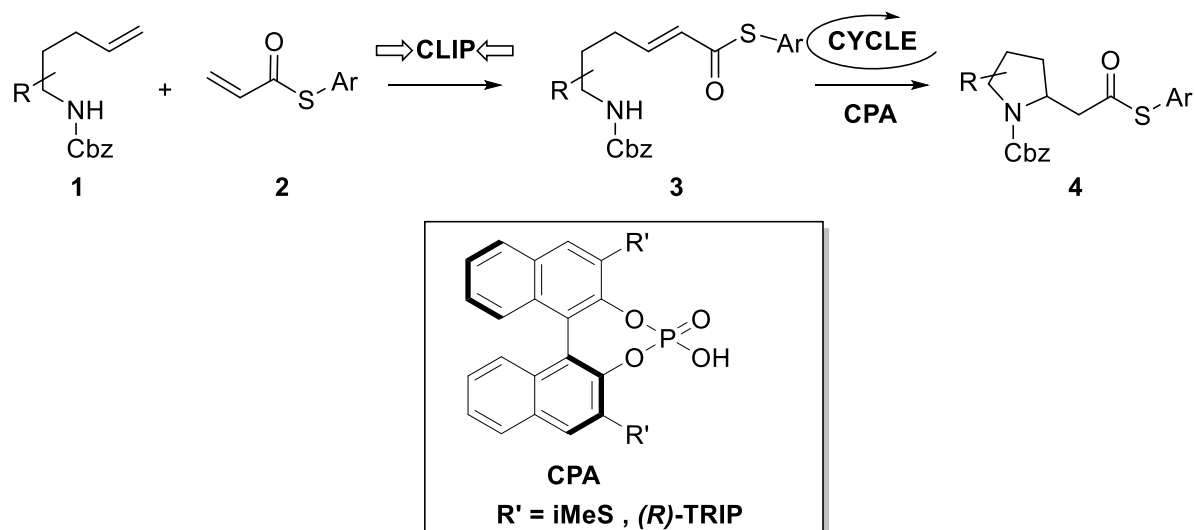
University of York

Chemistry

April 2020

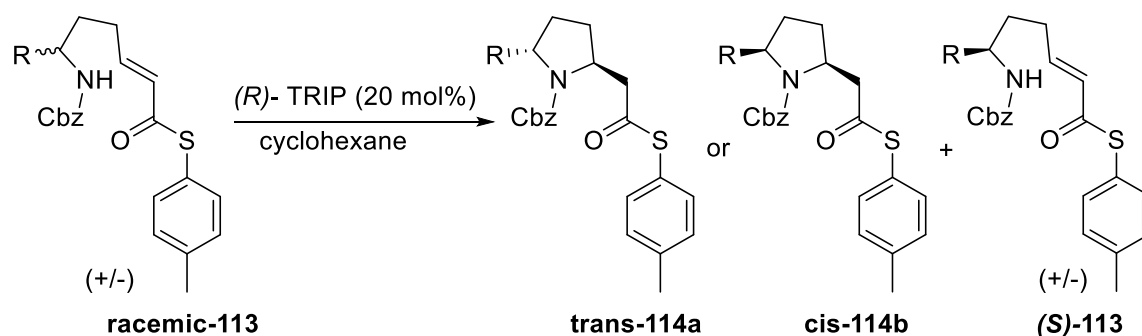
1. Abstract

The pyrrolidine ring is present in a large number of alkaloid natural products and in many pharmaceutical drugs. Building on the asymmetric 'Clip-Cycle' synthesis of spiropyrrolidines, this thesis details our study into the kinetic resolution of racemic 'Clip-Cycle' substrates to give enantioenriched chiral pyrrolidines.



Scheme 1: 'Clip-Cycle' asymmetric reaction

'Clip-Cycle' involves an unsaturated Cbz-protected 'allyl' amine being 'clipped' with an activating unsaturated thioester group by an alkene metathesis reaction, followed by a chiral phosphoric acid (CPA) catalyzed aza-Michael 'cycle' reaction. Racemic 2-, and 3-substituted cyclisation precursors were cyclized using (*R*)-TRIP and the conversion monitored until 50% of the substrate had been consumed. Analysis of the reaction mixture by chiral HPLC indicated that kinetic resolution had occurred in all cases studies with up to 90% ee and $s=122$.



Scheme 2: Asymmetric kinetic resolution reaction

2. Contents

| | |
|--|------------|
| 1. Abstract | 2 |
| 2. Contents | 3 |
| 3. List of Figures | 4 |
| 4. List of Schemes | 6 |
| 5. List of Tables | 9 |
| 6. Acknowledgements | 11 |
| 7. Declaration | 13 |
| 8. Introduction | 14 |
| 8.1 Pyrrolidines in Natural Products | 14 |
| 8.2 Asymmetric Synthesis of Chiral Pyrrolidines..... | 15 |
| 8.3 Asymmetric aza-Michael reactions for the synthesis of N-heterocycles..... | 27 |
| 8.4 Kinetic Resolutions | 35 |
| 8.4.1. Concept of Kinetic Resolutions..... | 35 |
| 8.4.2 Examples of Kinetic Resolutions..... | 36 |
| 8.5 Background Work..... | 42 |
| 8.6 Aim of Project..... | 48 |
| 9. Results and discussion | 49 |
| 9.1 Retrosynthetic Analysis of the Pyrrolidine Precursors | 49 |
| 9.2 Synthesis of the Pyrrolidine Precursors..... | 50 |
| 9.3 Brønsted Acid Catalyzed Cyclisation of Pyrrolidine Precursors | 56 |
| 9.4 Kinetic Resolutions of the Pyrrolidine Precursors..... | 61 |
| 9.5 Determination of stereochemistry..... | 77 |
| 9.6 Conclusions and future work | 88 |
| 10. Experimental | 91 |
| 10.1 General Experimental | 91 |
| 10.2 Experimental procedures..... | 92 |
| 11. Abbreviations | 102 |
| 12. References | 105 |

3. List of Figures

| | |
|---|----|
| Figure 1: Common N-heterocycles | 14 |
| Figure 2: Structures of pyrrolidine moieties in alkaloids and natural products | 14 |
| Figure 3: Structures of pyrrolidine moieties in pharmaceutical drugs | 15 |
| Figure 4: Plausible reaction mechanism | 28 |
| Figure 5: Iminium intermediate..... | 29 |
| Figure 6: Proposed reaction mechanism..... | 31 |
| Figure 7: Different transition state energies in kinetic resolution..... | 35 |
| Figure 8: Transition states under TBAF and TFA cyclisations | 42 |
| Figure 9: Computational work on cyclisation selectivity..... | 45 |
| Figure 10: Hoveyda Grubbs II Catalyst | 52 |
| Figure 11: HPLC trace of 113a precursor | 54 |
| Figure 12: HPLC trace of 113b precursor | 54 |
| Figure 13: HPLC trace of 113c precursor..... | 55 |
| Figure 14: HPLC trace of racemic 114a pyrrolidine | 57 |
| Figure 15: HPLC trace of racemic 114b pyrrolidine | 58 |
| Figure 16: HPLC trace of racemic 114c pyrrolidine..... | 59 |
| Figure 17: HPLC trace of racemic 113a + racemic 114a | 60 |
| Figure 18: HPLC trace of racemic 113b + racemic 114b | 60 |
| Figure 19: HPLC trace of racemic 113c + racemic 114c | 61 |
| Figure 20: Conversion of Starting Material 113a and Product 114a | 63 |
| Figure 21: %ee of Starting Material 113a and Product 114a | 63 |
| Figure 22: Conversion of Starting Material 113a and Product 114a | 65 |
| Figure 23: %ee of Starting Material 113a and Product 114a | 65 |
| Figure 24: HPLC trace of enantioenriched 114a | 66 |
| Figure 25: HPLC trace of enantioenriched 113a | 66 |
| Figure 26: HPLC trace of enantioenriched 126 | 67 |
| Figure 27: Conversion of Starting Material 113b and Product 114b | 69 |
| Figure 28: %ee of Starting Material 113b and Product 114b | 69 |
| Figure 29: Conversion of Starting Material 113b and Product 114b | 70 |
| Figure 30: %ee of Starting Material 113b and Product 113b | 71 |
| Figure 31: HPLC trace of enantioenriched 114b | 71 |
| Figure 32: HPLC trace of enantioenriched 113b | 71 |
| Figure 33: HPLC trace of enantioenriched 127 | 73 |
| Figure 34: Conversion of Starting Material 113c and Product 114c | 74 |

| | |
|--|----|
| Figure 35: %ee of Starting Material 113c and Product 114c | 75 |
| Figure 36: HPLC trace of enantioenriched 114c | 75 |
| Figure 37: HPLC trace of enantioenriched 113c | 76 |
| Figure 38: HPLC trace of enantioenriched 128 | 77 |
| Figure 39: ^1H NMR (CDCl_3) spectrum of 114a | 83 |
| Figure 40: ^1H NMR (CDCl_3) spectrum of 140 | 83 |
| Figure 41: ^1H NMR (CDCl_3) spectrum of 114a | 84 |
| Figure 42: ^1H NMR (CDCl_3) spectrum of 140 | 85 |
| Figure 43: ^1H NMR (CDCl_3) spectrum of 139 | 86 |
| Figure 44: ^1H NMR (CDCl_3) spectrum of 141 | 86 |
| Figure 45: ^1H NMR (CDCl_3) spectrum of 139 | 87 |
| Figure 46: ^1H NMR spectrum of 141 | 87 |

4. List of Schemes

| | |
|---|----|
| Scheme 1: 'Clip-Cycle' asymmetric reaction..... | 2 |
| Scheme 2: Asymmetric kinetic resolution reaction | 2 |
| Scheme 3: Sparteine mediated asymmetric deprotonation/cyclisation to form N-Boc pyrrolidines | 16 |
| Scheme 4: Pathway of the asymmetric deprotonation-Cyclization of 19 to (S)- 20 | 16 |
| Scheme 5: Asymmetric Lithiation of N-Boc Pyrrolidine using (-)-sparteine..... | 16 |
| Scheme 6: Asymmetric Lithiation of N-Boc Pyrrolidine using (+)-sparteine surrogate | 17 |
| Scheme 7: Ag/phosphoramidite catalyzed exo selective asymmetric 1,3-dipolar cycloaddition of azomethine ylides with nitroalkenes | 18 |
| Scheme 8: 1, 3-dipolar cycloaddition of azomethine ylides..... | 19 |
| Scheme 9: Representative examples of Fe-catalyzed 1, 3-dipolar cycloadditions of azomethine ylides | 20 |
| Scheme 10: Formation of pyrrolidines from keto acid and (R)-phenylglycinol..... | 20 |
| Scheme 11: Proposed mechanism of the alane reduction to afford the pyrrolidines..... | 21 |
| Scheme 12: Alternative procedure for 2-phenylpyrrolidine | 21 |
| Scheme 13: Gold catalyzed tandem cycloisomerization/hydrogenation of chiral homopropargyl sulfonamides | 22 |
| Scheme 14: Proposed reaction mechanism | 22 |
| Scheme 15: Reaction scope representative examples..... | 22 |
| Scheme 16: Enantioselective pyrrolidine synthesis via successive nucleophilic and electrophilic allylation..... | 23 |
| Scheme 17: Redox-Neutral coupling of alcohols with bis-Boc-carbonate to form adducts 44 | 23 |
| Scheme 18: Representative examples of corresponding adducts 44a-d | 24 |
| Scheme 19: Tsuji-Trost allylation reaction followed by Mitsunobu cyclisation | 24 |
| Scheme 20 : Representative examples of the corresponding pyrrolidine rings..... | 24 |
| Scheme 21: Ring-closing metathesis reaction..... | 25 |
| Scheme 22: Representative examples of the ring-closing metathesis reaction..... | 25 |
| Scheme 23: Enantioselective synthesis of 2-substituted pyrrolidines via intramolecular reductive amination | 26 |
| Scheme 24: Representative examples of scope of the reaction | 27 |
| Scheme 25: A microwave-assisted organocatalytic enantioselective intramolecular aza-Michael reaction | 28 |
| Scheme 26: The total synthesis of (+)-myrtine..... | 29 |

| | |
|--|----|
| Scheme 27: Asymmetric oxa-Michael and aza-Michael addition catalyzed by boronic acid 68 and thiourea 69 | 30 |
| Scheme 28: Asymmetric hetero atom Michael reaction via organocatalysis | 30 |
| Scheme 29: Representative examples of the reaction scope | 31 |
| Scheme 30: Synthetic methodology of β -proline derivatives | 31 |
| Scheme 32: Domino hydroformylation/Wittig olefination reaction | 32 |
| Scheme 33: Representative examples of domino hydroformylation/Wittig olefination reaction .. | 32 |
| Scheme 34: Selective deprotonation and intramolecular aza-Michael reaction | 33 |
| Scheme 35: Enantioselective synthesis of piperidines catalyzed by chiral phosphoric acids | 34 |
| Scheme 36: Representative examples of the enantioselective synthesis of piperidines catalyzed by chiral phosphoric acids..... | 34 |
| Scheme 37: A classical kinetic resolution..... | 35 |
| Scheme 38: Jacobsen's hydrolytic kinetic resolution | 36 |
| Scheme 39: Kinetic resolution of allylic alcohols by a non-enzymatic acylation catalyst..... | 37 |
| Scheme 40: Unreacted alcohols-major enantiomer of the kinetic resolution of allylic alcohols by a non-enzymatic acylation catalyst..... | 38 |
| Scheme 41: Catalytic kinetic resolution of cyclic secondary amines..... | 38 |
| Scheme 42: Kinetic resolution of disubstituted 1-pyrrolidines catalyzed by a chiral titanocene catalyst | 40 |
| Scheme 43: Stereodivergent oxy-Michael Cyclisation..... | 42 |
| Scheme 44: Asymmetric tetrahydropyran cyclisation | 43 |
| Scheme 45: 'Clip-Cycle' Approach and proton shuttle transition state with the chiral phosphoric acid..... | 43 |
| Scheme 46: Asymmetric synthesis of substituted pyrrolidines using α , β -unsaturated thioesters as Michael acceptors and (R)-TRIP as the catalyst..... | 44 |
| Scheme 47: Methyl ester synthesis | 45 |
| Scheme 48: Chiral phosphoric acid cyclisation of the 2, 2-dimethyl substituted precursor..... | 46 |
| Scheme 49: Chiral phosphoric acids | 47 |
| Scheme 50: Spirocyclic substituted pyrrolidines synthesized | 47 |
| Scheme 51: Enantioselectivity and Diastereoselectivity in our Kinetic Resolution | 48 |
| Scheme 52: Retrosynthetic Analysis of 2-substituted cyclisation precursor | 49 |
| Scheme 53: Retrosynthetic Analysis of 3-substituted cyclisation precursor | 49 |
| Scheme 54: Structures of 2- and 3-substituted Cbz-protected amines..... | 50 |
| Scheme 55: Representative reaction route to 2-substituted Cbz-amines | 50 |
| Scheme 56: Representative reaction route to 3-substituted Cbz-amines | 51 |
| Scheme 57: Synthesis of the thioacrylic acid S-p-tolyl ester | 51 |

| | |
|---|----|
| Scheme 58: Cross metathesis reaction for 2-substituted precursors..... | 52 |
| Scheme 59: Cross metathesis reaction for 3-substituted precursor | 52 |
| Scheme 60: Cross metathesis reaction for 115a | 53 |
| Scheme 61: Cross metathesis reaction for 115b | 54 |
| Scheme 62: Cross metathesis reaction for 115c | 55 |
| Scheme 63: Cyclisation of 113a-c precursors using CSA..... | 56 |
| Scheme 64: Cyclisation of 113a precursor using CSA | 57 |
| Scheme 65: Cyclisation of precursor 113b using CSA | 57 |
| Scheme 66: Cyclisation of 114c precursor using CSA | 58 |
| Scheme 67: Kinetic resolution of 113a using 20 %mol (R)-TRIP at 50 °C..... | 62 |
| Scheme 68: Kinetic resolution of 113a using 20 %mol (R)-TRIP at 80 °C..... | 64 |
| Scheme 69: Cyclisation of enantioenriched 113a using CSA..... | 67 |
| Scheme 70: Kinetic resolution of 113b using 20 %mol (R)-TRIP at 50 °C..... | 68 |
| Scheme 71: Kinetic resolution of 113b using 20 %mol (R)-TRIP at 80 °C..... | 70 |
| Scheme 72: Cyclisation of enantioenriched 113b using CSA | 72 |
| Scheme 73: Kinetic resolution of 113c using 20 %mol (R)-TRIP at 50 °C | 74 |
| Scheme 74: Cyclisation of enantioenriched starting material 113c using CSA | 76 |
| Scheme 75: Plan of determination of absolute stereochemistry..... | 78 |
| Scheme 76: Attempted synthesis of alcohol 129 | 78 |
| Scheme 77: Attempted synthesis of alcohol 129 | 79 |
| Scheme 78: Attempted synthesis of aldehyde 129 | 79 |
| Scheme 79: Attempted synthesis of aldehyde 129 | 80 |
| Scheme 80: Liebeskind–Srogl coupling reaction | 80 |
| Scheme 81: Liebeskind–Srogl coupling reaction between phenylboronic acid and 114c | 81 |
| Scheme 82: Intramolecular aza-Michael reaction | 81 |
| Scheme 83: Intramolecular aza-Michael reaction..... | 81 |
| Scheme 84: Methyl ester 139 synthesis..... | 82 |
| Scheme 85: Intramolecular aza-Michael cyclisation reaction | 82 |
| Scheme 86: Methyl ester 141 synthesis..... | 85 |
| Scheme 87: A dynamic kinetic resolution | 90 |

5. List of Tables

| | |
|--|----|
| Table 1: Different set of conditions used in asymmetric deprotonation..... | 17 |
| Table 2: Different set of conditions used in asymmetric deprotonations | 17 |
| Table 3: Scope of the enantioselective 1, 3-dipolar cycloaddition between imino esters and nitroalkenes..... | 19 |
| Table 4: Formation of pyrrolidines 38 from keto acid 34 and (R)-phenylglycinol 33 | 21 |
| Table 5: Representative examples of selective deprotonation and intramolecular aza-Michael reaction | 33 |
| Table 6: Representative examples of Jacobsen's hydrolytic kinetic resolution | 37 |
| Table 7: Representative examples of the catalytic kinetic resolution of cyclic secondary amines . | 39 |
| Table 8: Representative examples of the kinetic resolution of disubstituted 1-pyrrolidines catalyzed by a chiral titanocene catalyst..... | 40 |
| Table 9: Conditions screened for the 2, 2-dimethyl substituted precursor 105 | 46 |
| Table 10: HPLC conditions of racemic 113a precursor..... | 53 |
| Table 11: Retention times of 113a precursor..... | 54 |
| Table 12: HPLC conditions of racemic 113b precursor | 54 |
| Table 13: Retention times of 115b precursor | 55 |
| Table 14: HPLC conditions of racemic 113c precursor..... | 55 |
| Table 15: Retention times of 113c precursor | 55 |
| Table 16: HPLC conditions of racemic 114a pyrrolidine | 57 |
| Table 17: HPLC retention times of racemic 114a pyrrolidine..... | 57 |
| Table 18: HPLC conditions of racemic 114b pyrrolidine | 58 |
| Table 19: HPLC retention times of racemic 114b pyrrolidine | 58 |
| Table 20: HPLC conditions of racemic 114c pyrrolidine..... | 58 |
| Table 21: HPLC retention times of racemic 114c pyrrolidine..... | 59 |
| Table 22: HPLC retention times of racemic 114a pyrrolidine and racemic 113a precursor | 60 |
| Table 23: Table: HPLC retention times of racemic 114b pyrrolidine and racemic 113b precursor | 60 |
| Table 24: HPLC retention times of racemic 114c pyrrolidine and racemic 113c precursor | 61 |
| Table 25: HPLC conditions of racemic mixtures 113a-c, 114a-c | 61 |
| Table 26: Conversion and %ee of Starting Material 113a and Product 114a | 62 |
| Table 27: Conversion and %ee of Starting Material 113a and Product 114a | 64 |
| Table 28: HPLC conditions of enantioenriched 113a+114a | 66 |
| Table 29: HPLC retention times of enantioenriched 114a | 66 |
| Table 30: HPLC retention times of enantioenriched 113a | 67 |
| Table 31: HPLC conditions of enantioenriched 126 | 67 |

| | |
|--|----|
| Table 32: HPLC retention times of enantioenriched 126 | 68 |
| Table 33: Conversion and %ee of Starting Material 113b and Product 114b | 68 |
| Table 34: Conversion and %ee of Starting Material 113b and Product 114b | 70 |
| Table 35: HPLC conditions of enantioenriched 113b+114b | 71 |
| Table 36: HPLC retention times of enantioenriched 113b+114b | 72 |
| Table 37: HPLC conditions of enantioenriched 127 | 72 |
| Table 38: HPLC retention times of enantioenriched 127 | 73 |
| Table 39: Conversion and %ee of Starting Material 113c and Product 114c | 74 |
| Table 40: HPLC conditions of enantioenriched 113c+114c | 75 |
| Table 41: HPLC retention times of enantioenriched 113c+114c | 76 |
| Table 42: HPLC conditions of enantioenriched product 128 | 76 |
| Table 43: HPLC retention time of enantioenriched 128 | 77 |

6. Acknowledgements

Firstly, I would like to thank my supervisor Prof Paul Clarke for giving me the opportunity to work on his group and on this exciting project. Constantly, he provided a lot of guidance and advice about this project and helping to overcome some of the challenges. Throughout the year, he was patient and his office door was always open for me to go and ask many many questions/share my results. I want to thank him for proofreading every draft that formed this thesis, providing feedback, especially over the quite difficult last couple of months.

I would like to thank my IPM Prof Ian Fairlamb, for giving feedback and guidance with the project during my TAP meetings, and for making me feel comfortable that I could reach him at any point during the year.

I would also like to thank Heather Fish, for her assistance with acquiring NMR and for patiently reminding me that there is a time limit per person in the NMR. I would also like to thank Karl Heaton for all the help in acquiring mass spectrometry data, and for either listening to my complaints when I couldn't get the reaction to work and cheering with me when I finally got the right product.

This project would not have been possible without the warmth and camaraderie of the Clarke group who have made me, look forward to come back to the lab every day. I begin with Saikiran, my mentor, for all the help, guidance and support that she gave me since the very first day in the lab. From teaching me how to use needles/N₂ balloons to the last days, still helping me sort out my columns/TLC's/results. We shared some of our top and lowest days together, eating cake and donuts! Christopher, thank you for always putting your work on hold to help me and annoy me. Thank you for always looking at my messy NMRs/HPLCs, for showing me irrelevant YouTube videos that ended up with us crying of laughter and for all of our dancing/singing. Nik, my buddy, thank you for being the first friend I got when I came to York. Thank you for always proofreading every single thing I wrote, for introducing me to the lab and for always answering to my questions. You and Maggie really helped me through the year, not enough pints and donuts will pay you back!! Chloe, thank you for your help and support, for teaching me how to organize my stuff/listening to my complaints and making chemistry with me! All of our lab sing-alongs, cake and coffee/gin trips will be missed. Kirsten and (Br)Anna thank you for all the help, for all of the laughs we shared during lunchtime/cake time and for always inviting me to the pub quiz! All you guys have been wonderful and your kindness and friendship will never be forgotten. To the rest of the Clarke group, thank you for making the lab a better an enjoyable place to be!

Finally, I would like to thank my family for providing me the opportunity to study abroad for a Master's degree. They constantly supported me, believing in me and always being there for me! I cannot express my gratitude and I'm very thankful for their help throughout the year. I, also, want to thank my sister who she told me one million times to mention that she is a physicist in my thesis.

7. Declaration

I hereby declare that the substance of this thesis has not been submitted, nor is currently being submitted, in candidature for any other degree.

I also declare that the work embodied in this thesis is the result of my own investigations and in the event the work of others has been used this has been fully acknowledged in the text as references.

8. Introduction

8.1 Pyrrolidines in Natural Products

The most predominant heterocycles in medicinal chemistry and natural/pharmaceutical products are nitrogen-based heterocycles, five- and six-membered systems, such as pyrrolidine and piperidine. Also prominent are structures containing two heteroatoms within the carbocyclic ring, such as morpholines, and piperazines (Figure 1).

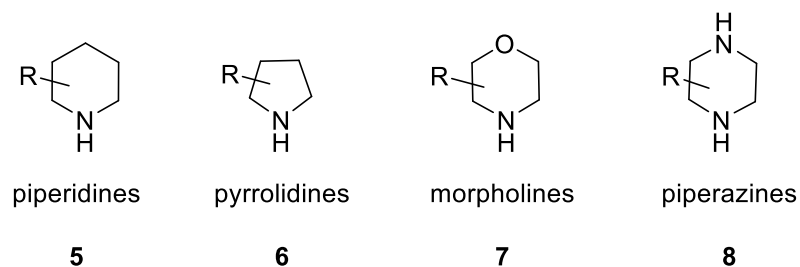


Figure 1: Common *N*-heterocycles

Nitrogen-containing heterocyclic structures are increasingly desirable scaffolds for drug discovery as they are present in many drug molecules and biologically active natural products. A recent report demonstrated that 59% of FDA approved drug molecules are cyclic amines; piperidines are in the 1st place while pyrrolidines are the 5th most frequent approved drugs.¹

The pyrrolidine ring has become a privileged structure in medicinal chemistry. The great interest in this heterocycle is based on the fact that pyrrolidines form the central structure of the amino acid proline, and are present in plenty of natural products and alkaloids^{2,3} (Figure 2).

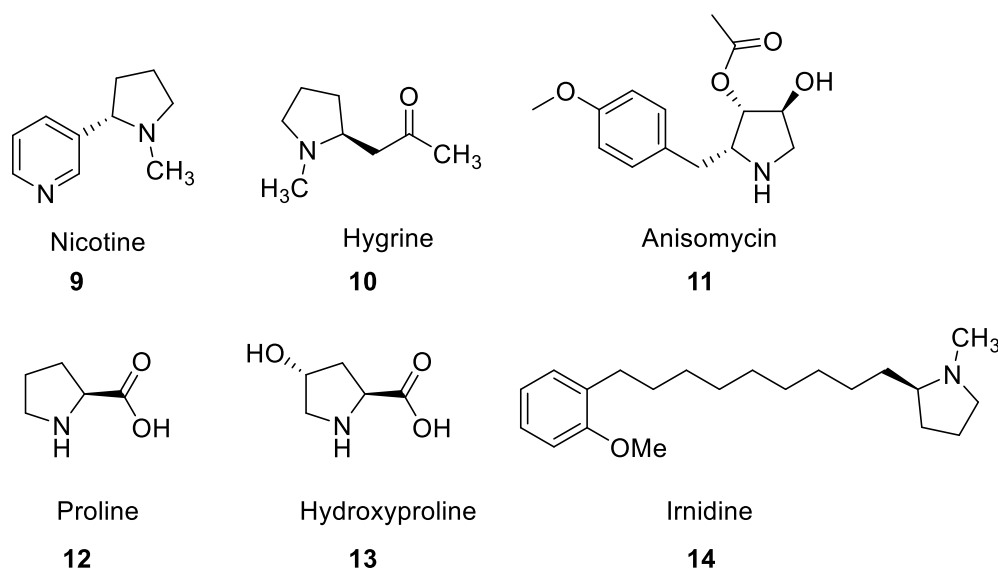


Figure 2: Structures of pyrrolidine moieties in alkaloids and natural products

Additionally, many substituted pyrrolidine derivatives are acknowledged to possess a wide range of bioactivities, such as antibiotic, antibacterial, antifungal and cytotoxic effects, and consequently offer an excellent opportunity for the discovery of new pharmaceutical agents^{4,5,6} (Figure 3).

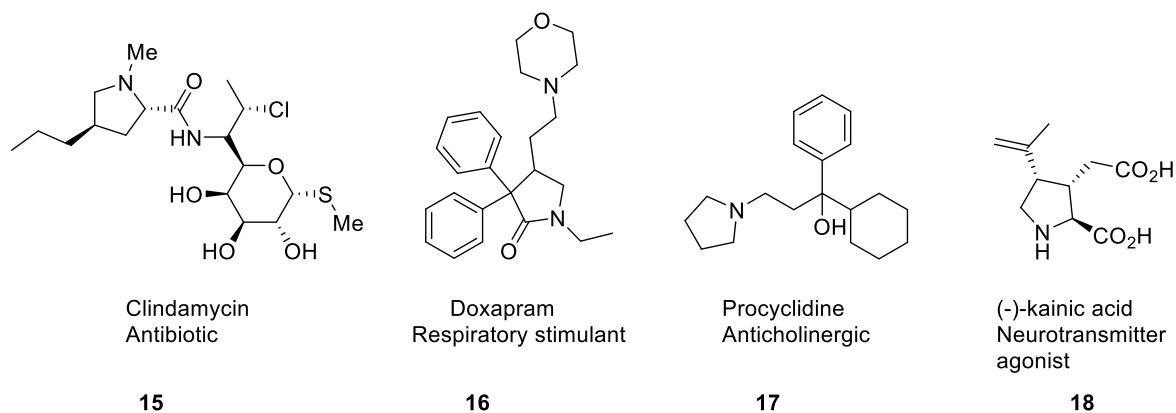


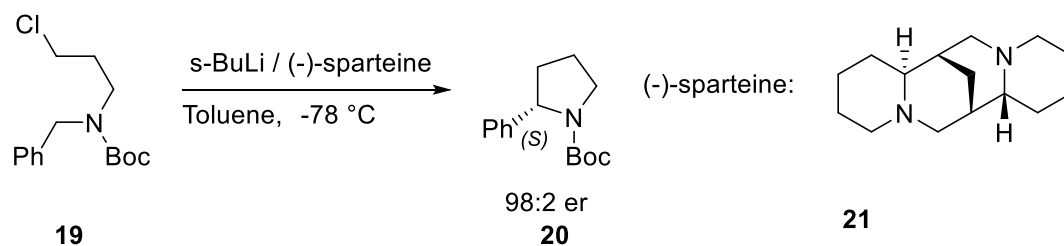
Figure 3: Structures of pyrrolidine moieties in pharmaceutical drugs

Enantiopure polyfunctionalized pyrrolidines are also found in pharmaceuticals and in numerous natural products; they are useful chiral auxiliaries and ligands for asymmetric syntheses, too. Although many methods have been reported for the synthesis of pyrrolidines, the continuing challenge is to design more concise methods, particularly enantiopure examples that have ring functionality that can provide access to more complex derivatives.

8.2 Asymmetric Synthesis of Chiral Pyrrolidines

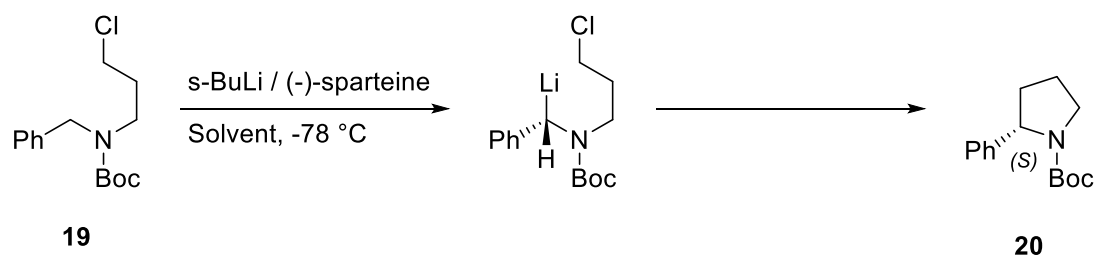
In recent years, several reports for the asymmetric formation of pyrrolidine rings have appeared in the literature. A selection of these methodologies is presented below to demonstrate the scope of enantioselective synthesis of these *N*-heterocycles in as a powerful tool in organic chemistry.

One successful method in asymmetric synthesis is using asymmetric deprotonation to form *N*-Boc pyrrolidines *via* a chiral ligand like (-)-sparteine **21** to induce stereochemistry. An example from Beak's⁷ work is illustrated: an asymmetric deprotonation-cyclisation of the *N*-Boc amino chloride **19** using (-)-sparteine and *sec*-butyllithium (*s*-Buli) to yield (*S*)-pyrrolidine **20** in toluene (96% ee). These enantioselective lithiation-cyclizations were applied to a range of substrates with good to low yields and % ee's (Scheme 3).



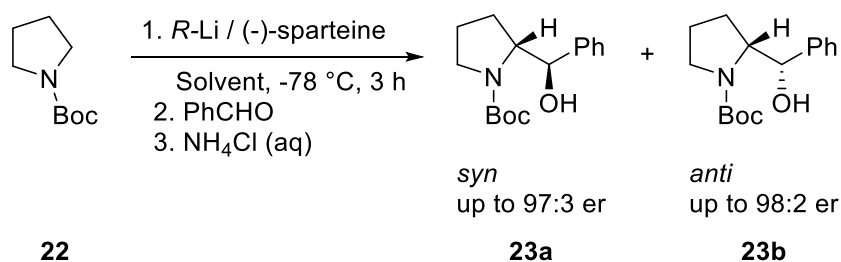
Scheme 3: Sparteine mediated asymmetric deprotonation/cyclisation to form N-Boc pyrrolidines

The key step of the reaction in the enantioselective induction is enantioselective deprotonation by *s*-BuLi/ (-)-sparteine complex to yield an enantioenriched lithiated species which undergoes cyclization more rapidly than racemization. Mechanistic studies, also, shows that the enantioselectivity is introduced by the asymmetric deprotonation at the benzylic position by the *s*-BuLi/ chiral ligand complex (Scheme 4).



Scheme 4: Pathway of the asymmetric deprotonation-Cyclization of **19** to (*S*)-**20**

Carbone *et. al.* investigated a series of asymmetric deprotonations of *N*-Boc-pyrrolidine followed by functionalisations using *s*-BuLi or *i*-PrLi and (-)-sparteine- or (+)-sparteine surrogate that yielded pyrrolidine rings with high enantioselectivity. Lithiation of *N*-Boc-pyrrolidine **22** with *s*-BuLi/ (-)-sparteine **21** or (+)-sparteine surrogate **24** affects an asymmetric deprotonation which yields the anion which reacts with electrophiles to provide the 2-substituted *N*-Boc-pyrrolidines **23a**, **23b** and in enantiomeric ratios which generally are >90%.^{8,9} Below are shown two representative examples of asymmetric deprotonation reactions that were investigated; different solvents and *R*-Li reagents were tested (Scheme 5, Scheme 6).



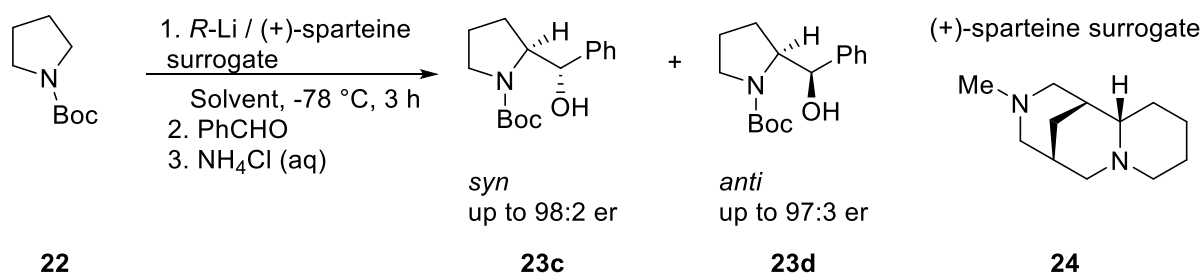
Scheme 5: Asymmetric Lithiation of *N*-Boc Pyrrolidine using (-)-sparteine

It was found that reactions with (-)-sparteine in tetrahydrofuran and 2-methyl-tetrahydrofuran proceeded with low enantioselectivity and yields for both *syn* and *anti* products (Table 1, Entries 4-6). Upon use with diethyl ether or methyl *tert*-butyl ether yielded in increased enantioselectivities; moderate yields were obtained in all cases (Table 1, Entries 1-3).

| Entry | Solvent | R-Li | Yield of <i>syn</i> | %ee of <i>syn</i> | Yield of <i>anti</i> | %ee of <i>anti</i> |
|-------|-------------------|----------------|---------------------|-------------------|----------------------|--------------------|
| 1 | Et ₂ O | <i>i</i> -BuLi | 64 | 97:3 | 22 | 95:5 |
| 2 | Et ₂ O | <i>s</i> -BuLi | 63 | 97:3 | 23 | 97:3 |
| 3 | TBME | <i>s</i> -BuLi | 51 | 97:3 | 24 | 98:2 |
| 4 | THF | <i>i</i> -BuLi | 65 | 63:37 | 22 | 60:40 |
| 5 | THF | <i>s</i> -BuLi | 50 | 51:49 | 14 | 51:49 |
| 6 | 2-methyl-THF | <i>s</i> -BuLi | 50 | 59:41 | 29 | 55:45 |

Table 1: Different set of reaction conditions used in asymmetric deprotonation

Conversely the corresponding reactions with the (+)-sparteine surrogate occurred with high enantioselectivity in all cases (Table 2, Entries 1-6). However, the yields remained moderate in every different set of conditions.



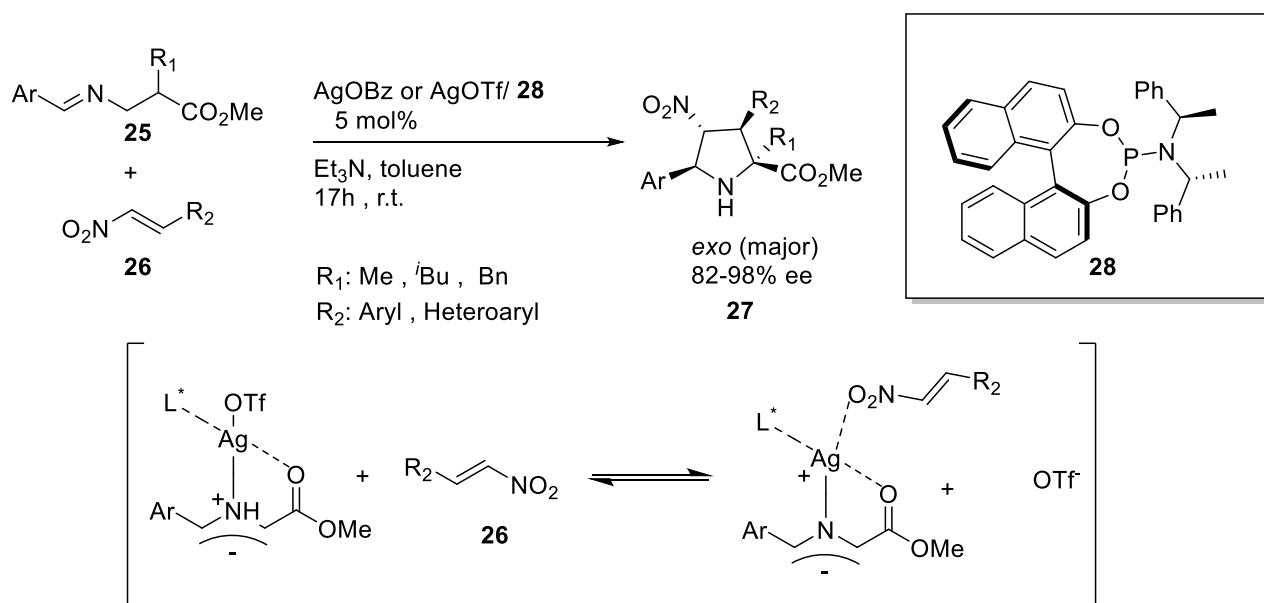
Scheme 6: Asymmetric Lithiation of *N*-Boc Pyrrolidine using (+)-sparteine surrogate

| Entry | Solvent | RLi | Yield of <i>syn</i> | %ee of <i>syn</i> | Yield of <i>anti</i> | %ee of <i>anti</i> |
|-------|-------------------|----------------|---------------------|-------------------|----------------------|--------------------|
| 1 | Et ₂ O | <i>i</i> -BuLi | 68 | 98:2 | 23 | 95:5 |
| 2 | Et ₂ O | <i>s</i> -BuLi | 58 | 95:5 | 23 | 94:6 |
| 3 | TBME | <i>s</i> -BuLi | 56 | 94:6 | 31 | 93:7 |
| 4 | THF | <i>i</i> -BuLi | 66 | 97:3 | 21 | 97:3 |
| 5 | THF | <i>s</i> -BuLi | 45 | 95:5 | 20 | 95:5 |
| 6 | 2-methyl-THF | <i>s</i> -BuLi | 43 | 93:7 | 22 | 93:7 |

Table 2: Different set of reaction conditions used in asymmetric deprotonations

The catalytic asymmetric 1,3-dipolar cycloaddition reaction is conceptually an efficient strategy for the enantioselective construction of five-membered heterocycles. Of particular interest is the reaction between azomethine ylides and activated alkenes to form functionalised pyrrolidines.¹⁰ Copper(I) complexes together with a silver-based catalyst, are the most widely employed catalysts in asymmetric 1,3-dipolar cycloadditions of azomethine ylides. Two representative examples of the cycloadditions using Copper (I) and silver catalysts are shown below.

Nájera *et. al.* reported an *exo*-selective 1,3-dipolar cycloaddition between iminoesters **25** and nitroalkenes **26**, using silver triflate or silver benzoate phosphoramidite complexes.¹¹ Computational work (DFT calculations) suggested that the triflate anion remained coordinated to the silver atom along the reaction pathway avoiding the stabilizing *endo* interaction between the metal and the nitro group of the dipolarophile (Scheme 7).



Scheme 7: Ag/phosphoramidite catalyzed *exo* selective asymmetric 1,3-dipolar cycloaddition of azomethine ylides with nitroalkenes

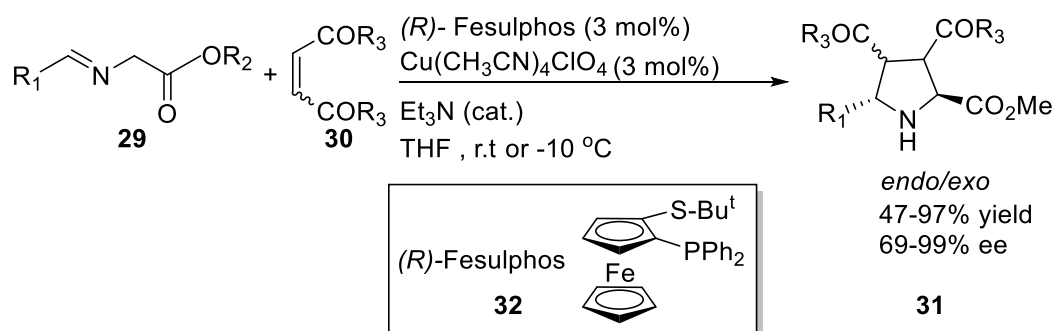
The scope of the reaction was investigated with different nitroalkenes, α -amino esters and benzylideneimino esters (Scheme and Table). Parallel studies were carried out for the reaction catalyzed by ligand **28** and AgOTf or AgOBz and 19 different substrates were tested. A few representative examples are shown in the table below (Table 3). The variation of the aryl substituent of the dipolarophile induced higher chemical yields, *exo*-diastereoselectivities and enantioselections in products **18** (Table 3, entries 1-3, 5 and 6). When an alanine derived imino ester was employed as azomethine ylide precursor, an increment of the *endo*-diastereoisomer was observed with moderate yield and %ee (Table 3, Entry 4). A tolyl- substituent was obtained in an ee up to 82% with moderate *exo*-selectivity and low yield (Table 3, Entry 5). Finally, in the case

of the 2-naphthyl substituent, *exo*-product was obtained with up to 85% ee and 70% yield (Table 3, Entry 6).

| Entry | Ar | R ₁ | R ₂ | <i>exo/endo</i> | %yield | %ee |
|-------|-----------------------------------|----------------|-----------------------------------|-----------------|--------|-----|
| 1 | Ph | H | Ph | 90:10 | 80 | 96 |
| 2 | Ph | H | 4-MeC ₆ H ₄ | 70:30 | 52 | 89 |
| 3 | Ph | H | 4-FC ₆ H ₄ | 89:11 | 74 | 97 |
| 4 | Ph | Me | Ph | 21:79 | 14 | 87 |
| 5 | 2-MeC ₆ H ₄ | H | Ph | 56:44 | 33 | 82 |
| 6 | 2-naphthyl | H | Ph | 86:14 | 70 | 85 |

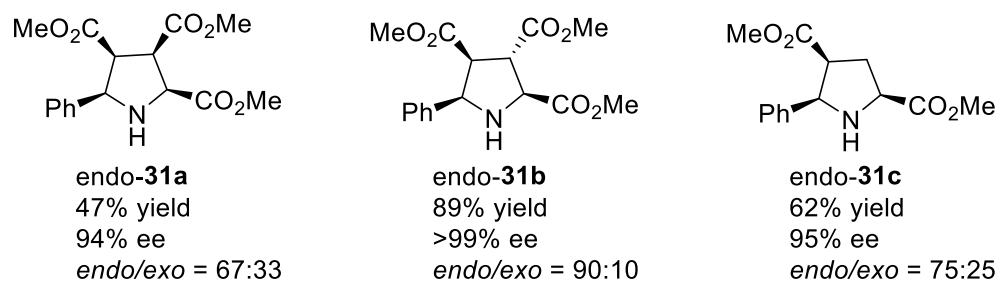
Table 3: Scope of the enantioselective 1, 3-dipolar cycloaddition between imino esters and nitroalkenes

Cabrera, Gómez and Carretero demonstrated an interesting enantioselective 1, 3-dipolar cycloaddition of azomethine ylides catalysed by a copper(I)-Fesulphos catalyst system.¹² (Scheme 8) The catalyst system behaves as an efficient chiral Lewis acid on the catalytic cycloaddition reaction and shows a good reactivity at low catalyst loadings (3 mol%) affording *endo/exo* selectivity and high enantioselectivity (>99% ee). This catalytic asymmetric procedure has a broad structural scope with regard to both azomethine and dipolarophile substitution.



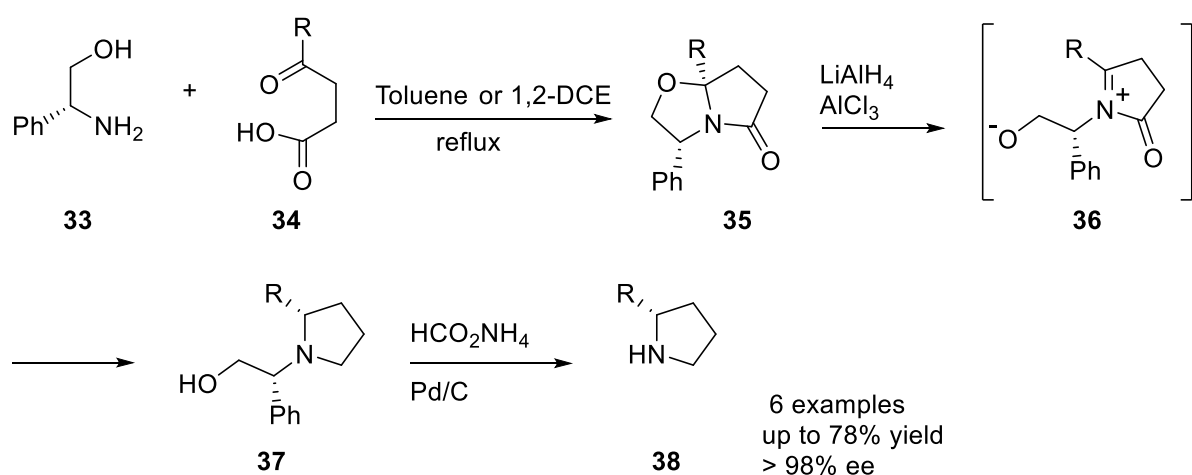
Scheme 8: 1, 3-dipolar cycloaddition of azomethine ylides

This protocol provided high levels of diastereoselectivity and enantioselectivity with a wide variety of imino esters and dipolarophiles and a few of them are presented below. (Scheme 9) The *endo/exo* selectivity proved to be dependent on the dipolarophile. The *endo*-fumarate adduct **31a** was yielded in excellent %ee and diastereoselectivity, whereas the *endo*-maleate **31b** and *endo*-acrylate **31c** products gave lower diastereoselectivity and %ee (*endo/exo*: 90/10, 67/33 and 75/25, respectively).



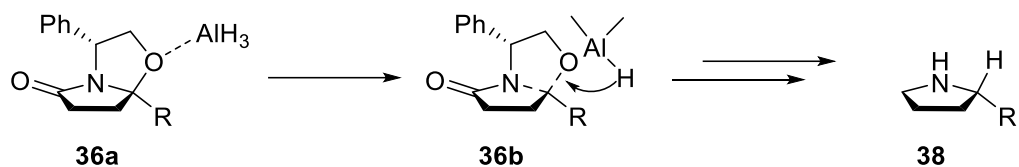
Scheme 9: Representative examples of Fe-catalyzed 1,3-dipolar cycloadditions of azomethine ylides

A simple, yet efficient procedure for the asymmetric synthesis of 2-substituted pyrrolidines with high enantiomeric purity has been investigated by Burgess and Meyers in 1991¹³ (Scheme 10).



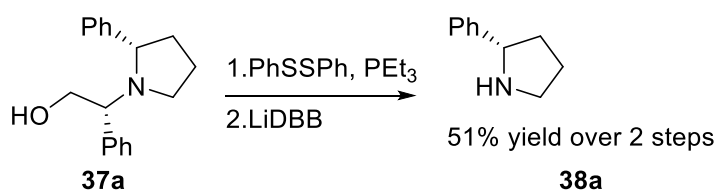
Scheme 10: Formation of pyrrolidines from keto acid and (*R*)-phenylglycinol

Starting from 3-acylpropionic acids "...**34**, using (*R*)-phenylglycinol **33**, as a chiral auxiliary, yielded..." yielded the bicyclic lactam **35**. Reacting the intermediate **36** under Lewis acid conditions, followed by hydrogenolysis conditions provided the desired *N*-substituted pyrrolidines **38**. In this transformation, the alane which was prepared *in situ* from aluminum trichloride and lithium aluminum hydride, acts as the necessary Lewis acid to form the intermediate **36** and as a hydride source to yield the **37**. The alane, weakens the C-O bond in **36a** promoting *N*-acyliminium ion formation to **36b**. Subsequent delivery of the hydride from the same face as the departing oxygen then provides the observed pyrrolidine products (Scheme 11). The enantiomeric purity of these compounds was determined to be >98% by chiral stationary-phase HPLC. This method was also applied for the preparation of pyrrolidinones.



Scheme 11: Proposed mechanism of the alane reduction to afford the pyrrolidines

In the table below, three different substrates' results are presented (Table 4). In the case of the 2-phenyl derivative (Entry 1), an alternative procedure for benzyl-*N* bond cleavage was devised. Diphenyl disulfide and triethylphosphine converted the primary alcohol **37a** to the corresponding phenyl sulfide followed by treatment with lithium di-*tert*-butyl biphenylide which resulted in lithiation and elimination of styrene to yield the 2-phenylpyrrolidine **38a** in 51% yield over the two steps (Scheme 12).



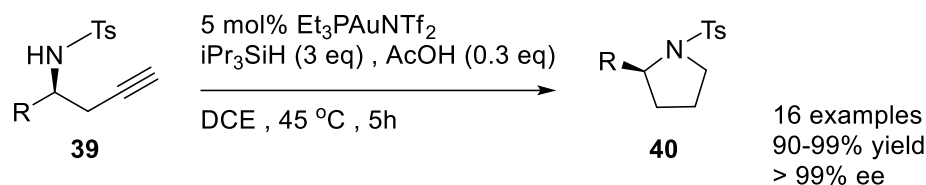
Scheme 12: Alternative procedure for 2-phenylpyrrolidine

The synthesis of the other two pyrrolidine substrates (Entries 2, 3) proceeded smoothly under the revised conditions. The assignment of the absolute configuration of the pyrrolidines was based on comparison of the observed optical rotation with those from literature and the designation of *R* or *S* was made.

| Entry | R | %yield | Configuration | %ee |
|-------|------------------|--------|---------------|-----|
| 1 | Phenyl | 51 | <i>S</i> | >98 |
| 2 | <i>n</i> -propyl | 78 | <i>R</i> | |
| 3 | Cyclopentyl | 65 | <i>S</i> | |

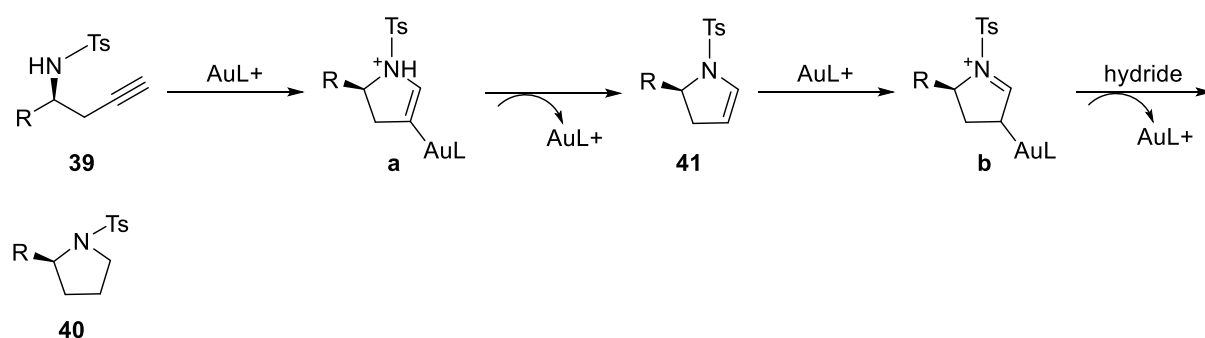
Table 4: Formation of pyrrolidines **38** from keto acid **34** and (*R*)-phenylglycinol **33**

Yu *et. al.* developed a method for the enantioselective synthesis of various pyrrolidine rings *via* a gold-catalysed tandem cycloisomerisation/hydrogenation of chiral homopropargyl sulfonamides¹⁴ (Scheme 13). Chiral pyrrolidines were obtained in excellent yields and enantioselectivities by successfully combining gold catalysis with a chiral *tert*-butylsulfinimine. Optimization of reaction conditions led to employing Et₃PAuNTf₂ as the gold catalyst, triisopropyl silane as the organosilane and acetic acid as the additive. The starting homopropargyl sulfonamides **39** underwent a direct 5-*endo*-dig *anti*-Markovnikov cyclisation / hydrogenation to yield the desirable chiral pyrrolidines **40**.



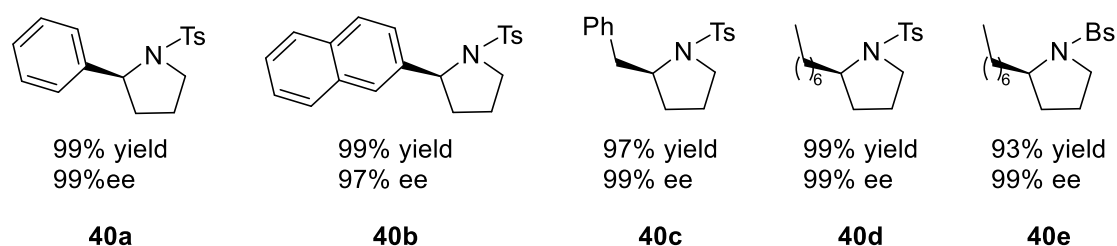
Scheme 13: Gold catalyzed tandem cycloisomerization/hydrogenation of chiral homopropargyl sulfonamides

Consequently, a possible reaction mechanism to explain the formation of **40** was proposed (Scheme 14). Initially, the gold catalyst catalyzed the 5-*endo*-dig cycloisomerization followed by the *in situ* generation of the intermediate **41**, which was then converted to the iminium intermediate **b** catalyzed by gold and acid. The iminium intermediate was then reduced by hydride to afford the pyrrolidine **40**.



Scheme 14: Proposed reaction mechanism to rationalize the formation of **40**

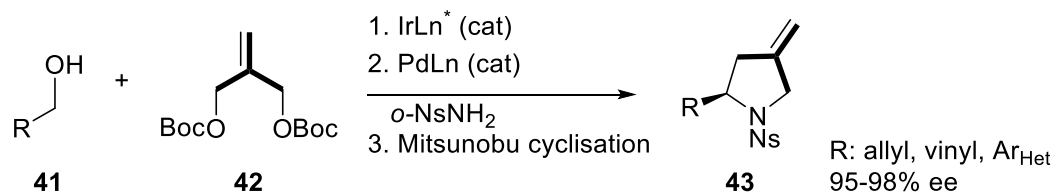
The scope of this gold-catalysed cycloisomerization/hydrogenation reaction was examined and 16 different substrates were tested, a few of them presented in the scheme below (Scheme 15). In particular excellent enantioselectivities and yields were achieved in almost all cases and no epimerization of the precursors was observed. Besides the tosyl group, the reaction proceeded well for *p*-bromobenzenesulfonyl-protected (Bs) substrate **40e**, resulting in the efficient formation of the desired product.



Scheme 15: Reaction scope representative examples

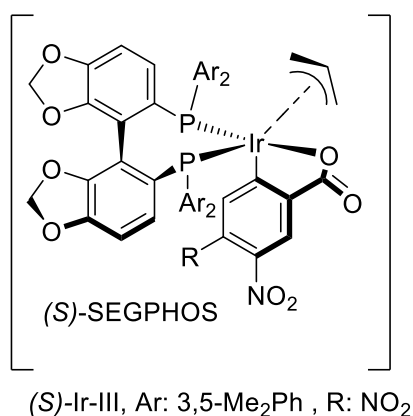
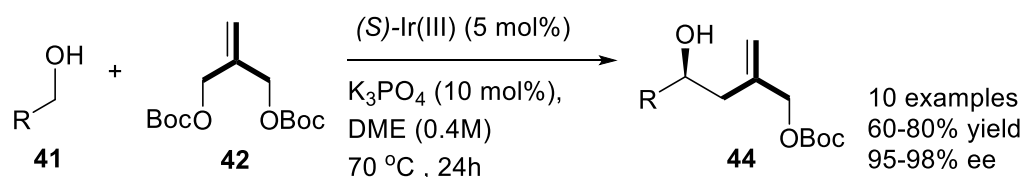
In early 2019, Krische *et. al.* demonstrated a successive nucleophilic and electrophilic allylation for the catalytic enantioselective synthesis of *N*-protected 2,4-disubstituted pyrrolidines¹⁵ (Scheme

16). The allylation, mediated by the *bis*-Boc-carbonate **42** derived from 2-methylene-1, 3-propane diol enables the formation of enantiomerically enriched 2,4-disubstituted pyrrolidines **43**. The enantioselective iridium-catalyzed transfer hydrogenative carbonyl C-allylation is followed by Tsuji–Trost *N*-allylation using 2-nitrobenzenesulfonamide; a Mitsunobu cyclization provides the *N*-protected 2, 4-disubstituted pyrrolidines.



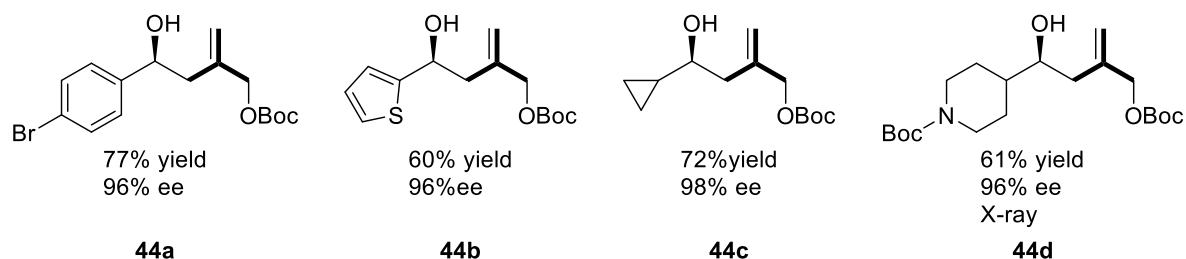
Scheme 16: Enantioselective pyrrolidine synthesis *via* successive nucleophilic and electrophilic allylation

Initially a variety of alcohols **41** were coupled with *bis*-Boc-carbonate **42** *via* alcohol mediated hydrogen transfer to form the corresponding adducts **44** (Scheme 17). Selected optimization experiments led to using the (*S*)-Ir(III) catalyst with 5 mol% loading. The conversion of starting alcohols to adducts represents redox-neutral processes.



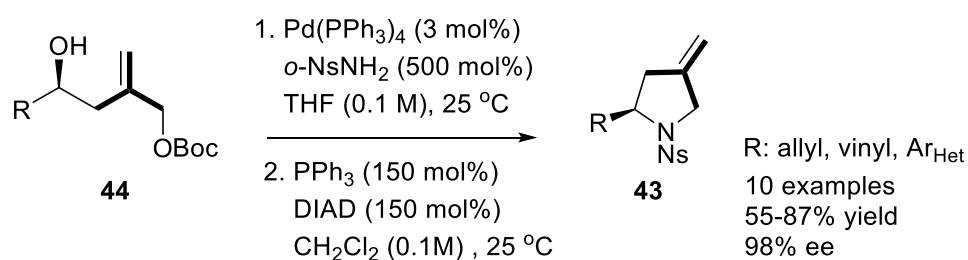
Scheme 17: Redox-Neutral coupling of alcohols with *bis*-Boc-carbonate to form adducts **44**

The optimized conditions were applied to a range of alcohols **41** which were coupled with *bis*-Boc-carbonate **42** and a few representative examples are shown below (Scheme 18). The benzylic alcohols delivered the respective adducts **44a**, **44b** with moderate yields but excellent enantioselectivity. The **44c**, **44d** adducts were generated with moderate yields and high %ee's from the respective aliphatic alcohols. The absolute stereochemistry of adducts was assigned in comparison to adduct **44d**, which was determined by single-crystal X-ray diffraction analysis.



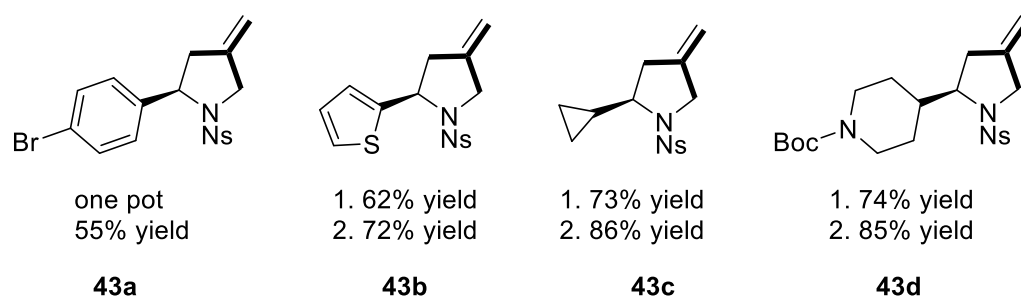
Scheme 18: Representative examples of corresponding adducts **44a-d**

Subsequently, adducts **44a-d** were converted to the 2-substituted 4-methylenepyrrolidines **43** via a Tsuji – Trost palladium-catalyzed allylation followed by a Mitsunobu cyclisation (Scheme 19).



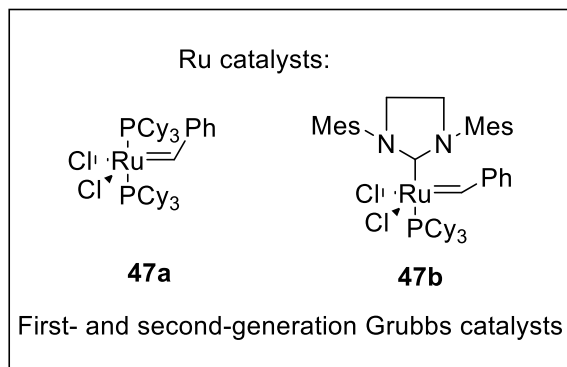
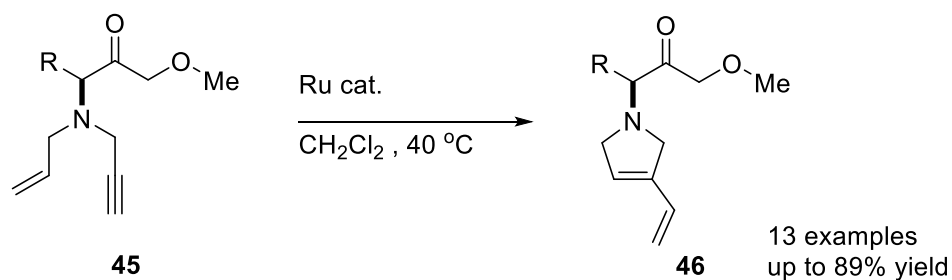
Scheme 19: Tsuji-Trost allylation reaction followed by Mitsunobu cyclisation

The palladium-catalyzed allylation reactions of *o*-nitrobenzenesulfonamide proceeded well, providing in good yields the *o*-nosyl adducts. The following cyclisations under Mitsunobu conditions generated the 2-substituted 4-methylenepyrrolidines **43a-d** with no erosion in enantiomeric purity. In the scheme below, representative examples of the corresponding pyrrolidine rings are shown (Scheme 20).



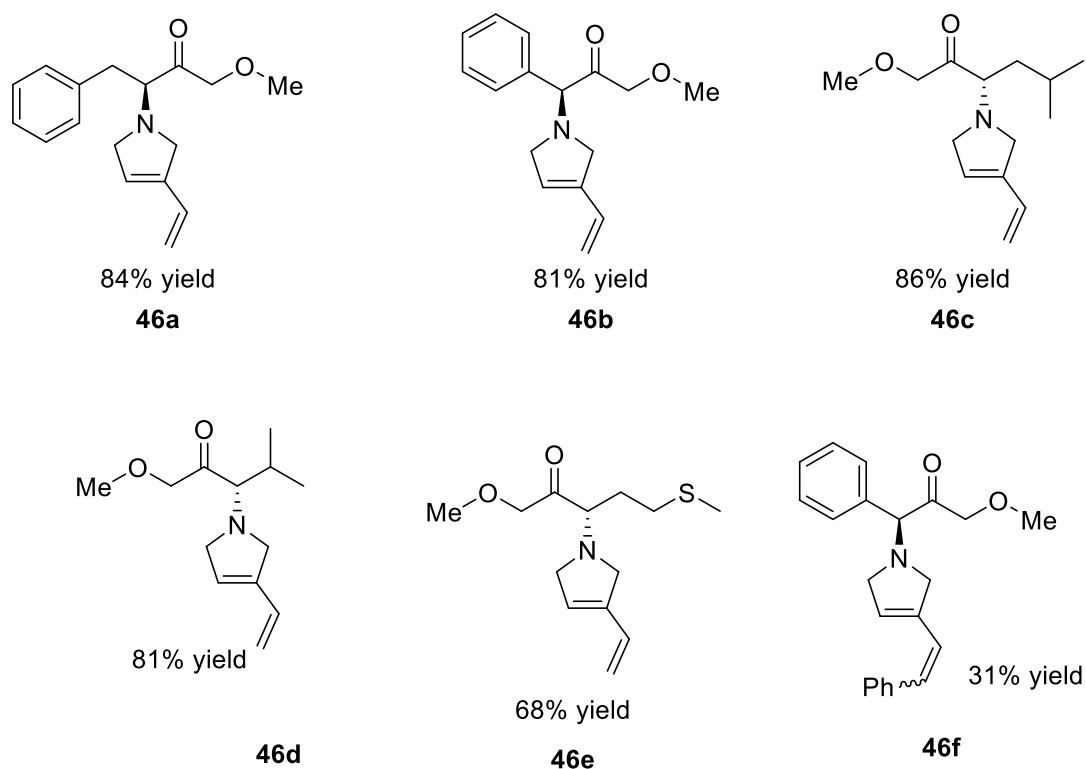
Scheme 20 : Representative examples of the corresponding pyrrolidine rings

A common method to synthesize cyclic products from acyclic diene or enyne precursors is via a ring-closing metathesis reaction catalyzed by highly active ruthenium catalysts such as first-generation Grubbs catalyst **47a** and second-generation Grubbs catalyst **47b**.¹⁶ Yang *et. al.* synthesized a series of pyrrolidine derivatives prepared in good yields via a ring-closing enyne metathesis reaction¹⁷ (Scheme 21).



Scheme 21: Ring-closing metathesis reaction

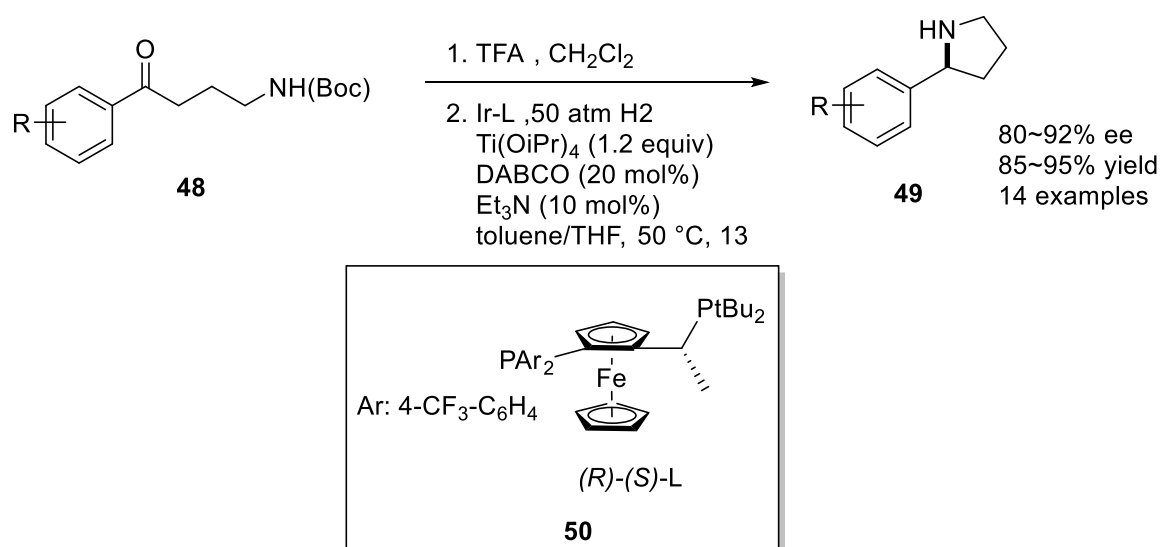
Initially, several enyne substrates were generated from commercially available chiral amino acids, based on literature procedures. A variety of chiral pyrrolidine derivatives were prepared from the enyne substrates containing a basic or nucleophilic *N* atom *via* ring-closing enyne metathesis reaction under mild reaction conditions and a few of them are presented in the scheme below (Scheme 22).



Scheme 22: Representative examples of the ring-closing metathesis reaction

Enynes containing aromatic rings or alkane chains afforded the corresponding pyrrolidines in good yields. (**46a-e**). To further expand the scope, substrates with substituents on the alkene bond were tested **46f**. When **46f** was subjected to the reaction conditions, starting material was recovered due to the steric effect, resulting in low yield (31%). Additionally, the **46e** substrate which contains a sulfur atom gave no reaction under the conditions, but when 40 mol % of $\text{Ti}(\text{O}^i\text{Pr})_4$ was added to the reaction the pyrrolidine was generated successfully in 68% yield. This may be due to the fact that the sulfur atom is a stronger electron donor, therefore causing the alkylidene ruthenium carbene to coordinate with the sulfur atom and deactivation of the catalyst.

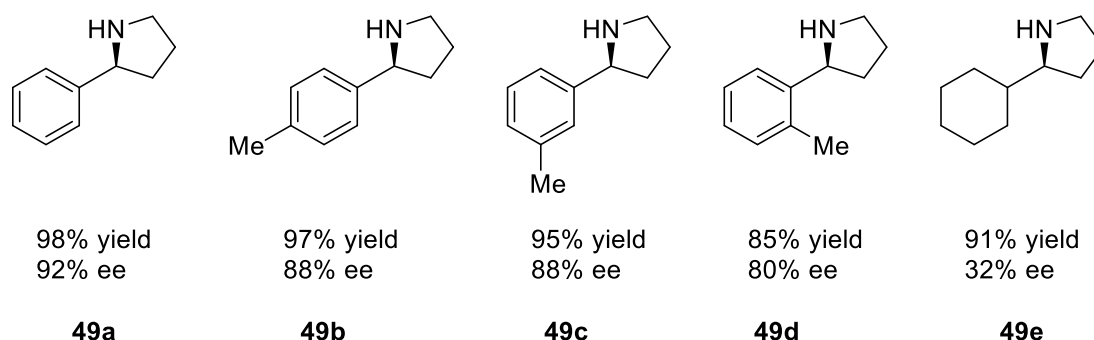
An enantioselective synthesis of 2-substituted pyrrolidines *via* an intramolecular reductive amination was reported by Chang *et. al.*¹⁸ (Scheme 23). This concise, one-pot synthesis is catalyzed by an iridium/chiral ferrocene ligand to yield the 2-aryl pyrrolidines in excellent enantioselectivities. The starting carbamates **48** were subjected to *N*-deprotection under trifluoroacetic acid conditions and cyclized to form 2-substituted aryl pyrrolidines **49**, in which the intramolecular reductive amination was the key step. The use of the three additives $\text{Ti}(\text{O}i\text{Pr})_4$, Et_3N and KI enhanced the conversion and the stereoselectivity of the reaction. A range of chiral pyrrolidines were synthesised up to 98% yield and 92% ee.



Scheme 23: Enantioselective synthesis of 2-substituted pyrrolidines *via* intramolecular reductive amination

A few representative examples are shown in the scheme below (Scheme 24). For the *para*-substituted substrate **49b**, the steric properties or their electronic effect of the substituent had almost no effect on the reaction enantioselectivity or reactivity and excellent yield and %ee were obtained. Similarly, the substituent on the *meta*-position **49c** converted smoothly into the corresponding pyrrolidine with no difference in reactivity and enantioselectivity. However, the

ortho-substituted substrate **49d** was generated in a decreased yield and %ee, which might be from the steric hindrance of the position. The catalytic system did not work well for the piperidine-substituted product **49e** and only 32% was achieved.

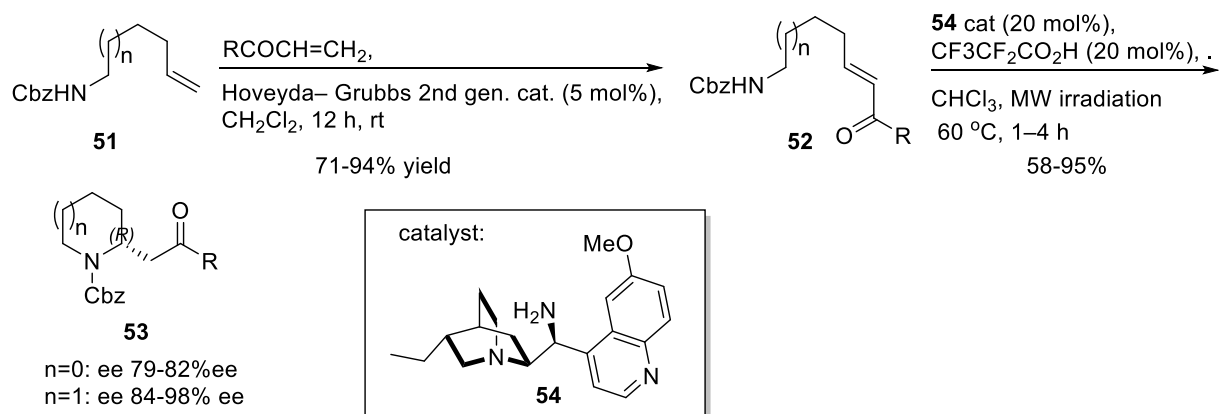


Scheme 24: Representative examples of scope of the reaction

8.3 Asymmetric aza-Michael reactions for the synthesis of N-heterocycles

The aza-Michael reaction; the 1,4-addition of a nitrogen nucleophile to an α,β -unsaturated carbonyl compound, is an excellent and useful way of forming C-N bonds and is of great significance in asymmetric synthesis. Indeed, the reaction in its intramolecular version constitutes a quite straightforward methodology to construct nitrogen-containing heterocycles.¹⁹

Fustero *et. al.* reported general procedures for highly enantioselective organocatalysed intramolecular aza-Michael reaction to access different nitrogen containing ring sizes, such as pyrrolidines and piperidines.²⁰ In a recent report they demonstrated an example of asymmetric intramolecular aza-Michael reactions of carbamates bearing α, β -unsaturated ketones as Michael acceptors²¹ (Scheme 25). The carbamate **51** undergoes a cross metathesis reaction using Hoveyda-Grubbs 2nd generation catalyst to form the enone **52**. The organocatalyst **54** combined with pentafluoropropionic acid as co-catalyst drive the stereoselective aza-Michael attack. The process is also affected by microwave irradiation which provides an accelerating effect.



Scheme 25: A microwave-assisted organocatalytic enantioselective intramolecular aza-Michael reaction

A plausible mechanism reaction was suggested and described the iminium intermediate **55** which can be seen in the figure below: a hydrogen bond is formed between the carbamate carbonyl oxygen group and the acidic proton from the quinuclidinium group of the catalyst and that could drive a stereoselective aza-Michael attack. The conjugate addition of the nucleophilic nitrogen would happen on the *Re* face of the less sterically hindered iminium to generate the Michael product in *R*-configuration (Figure 4).

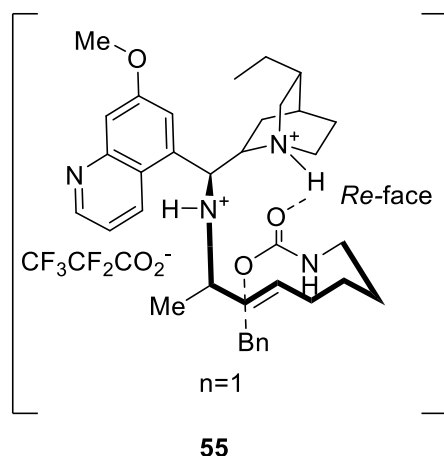
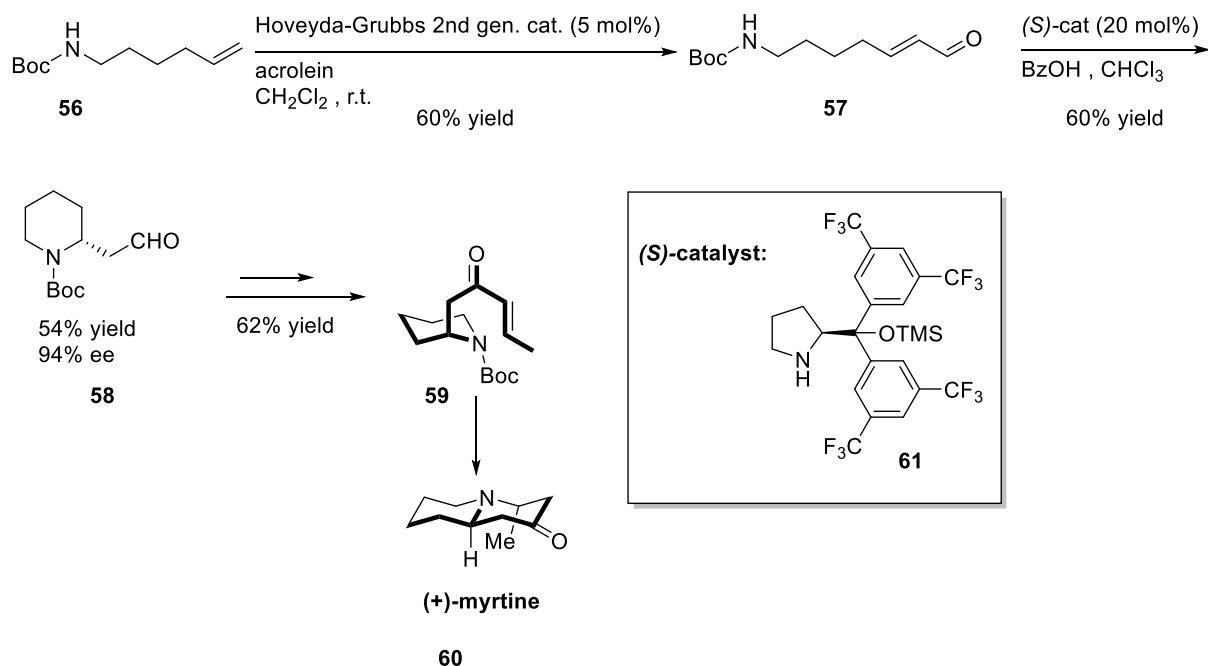


Figure 4: A model of the transition state

Fustero²² and Carter²³, demonstrated the transformation of carbamates bearing α , β -unsaturated aldehydes into the enantiomerically enriched nitrogen heterocycles *via* an organocatalysed intramolecular aza-Michael reaction (Scheme 26). The conjugate aldehyde **57** with Jorgensen diarylpropinol catalyst **61** and benzoic acid as co-catalyst yielded the piperidine **58** in excellent enantioselectivity. The piperidine **58** was further exploited for the synthesis of the piperidine alkaloids, (+)-myrtine **60**.



Scheme 26: The total synthesis of (+)-myrtine

The aza-Michal reaction takes place via an iminium intermediate that favors the attack of the nucleophilic nitrogen onto the less hindered Re-face of activated olefin **63**, as shown in the figure below. (Figure 5)

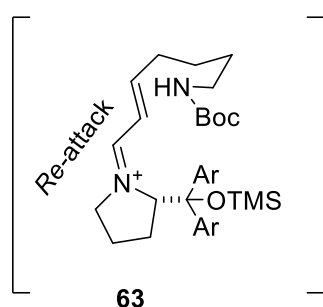
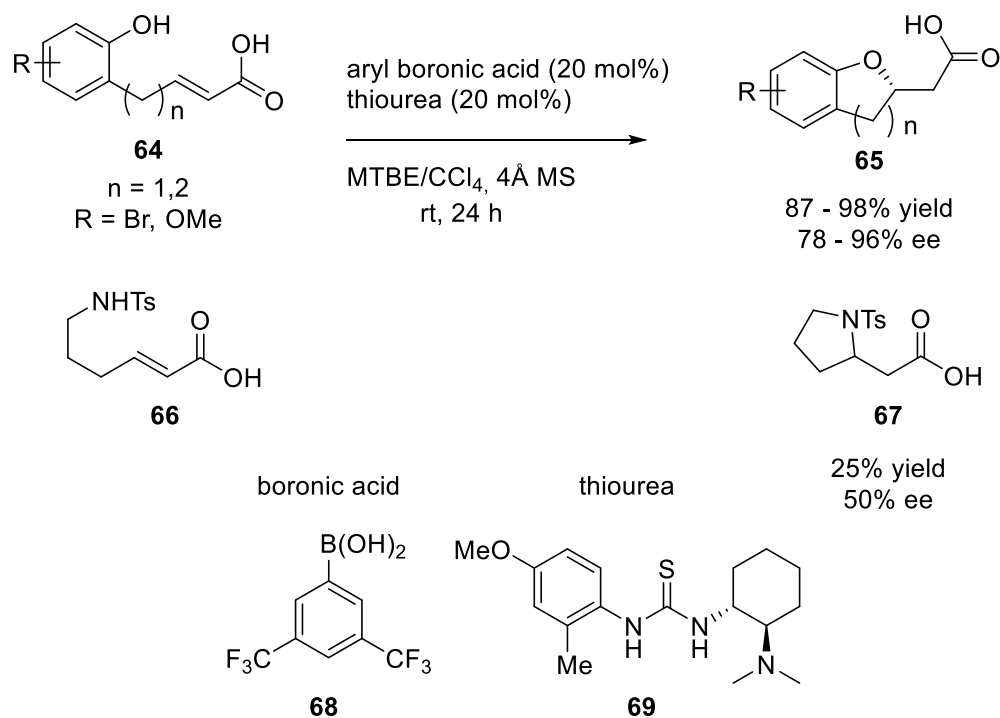


Figure 5: Iminium intermediate

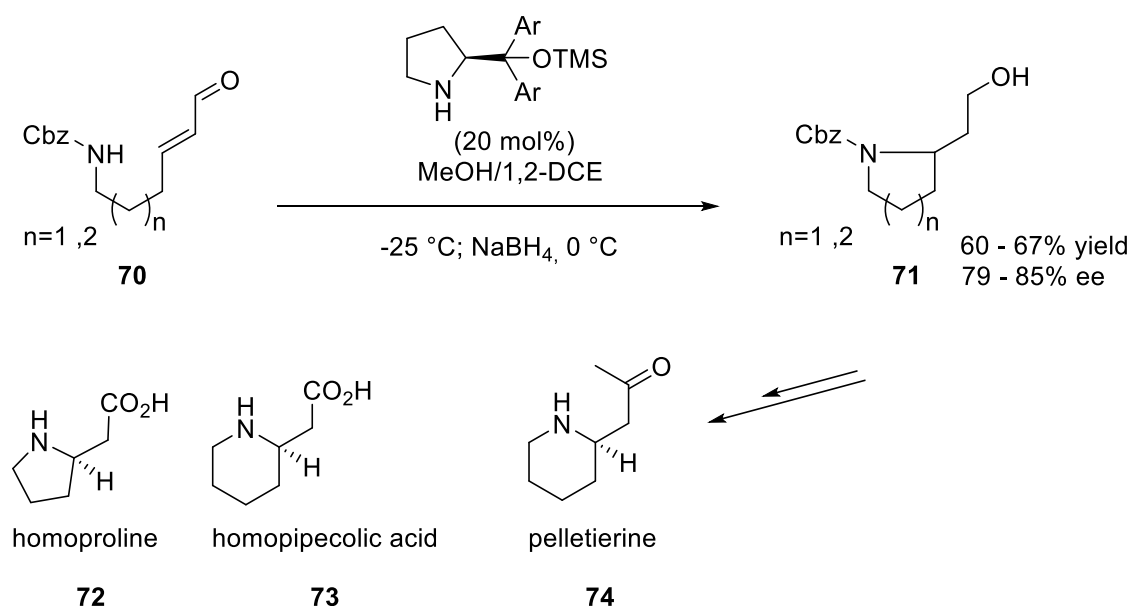
In 2014, Azuma *et al.* demonstrated an asymmetric intramolecular heteroMichael reaction of α,β -unsaturated carboxylic acids²⁴ (Scheme 27). A combination of an aryl boronic acid **68** with a chiral aminothiouria **69** catalyzed the intramolecular oxa- and aza-Michael reactions to yield the desired heterocycles **65,67** in high yields and enantioselectivities. Upon screening different catalysts and conditions, they established that the yields and the enantioselectivities could be improved with a dual catalytic system of boronic acid **68** and thiourea **69**. Solvent screening led to using a mixed solvent system of methyl *tert*-butyl ether (MTBE) and carbon tetrachloride (CCl₄). The reaction worked well for oxy-Michael reaction as the benzofuran and chromane derivatives **65** were

obtained in high yields and enantioselectivities; whereas the formation of the *N*-tosyl pyrrolidine **67** afforded poor %ee's and yields. The reaction also uses CCl₄, a solvent not widely used due to its carcinogenicity and environmental concerns.



Scheme 27: Asymmetric oxa-Michael and aza-Michael addition catalyzed by aryl boronic acid **68** and thiourea **69**

Carlson *et. al.* reported a procedure for enantioselective intramolecular hetero atom Michael addition *via* organocatalysis²⁵ (Scheme 28).



Scheme 28: Asymmetric hetero atom Michael reaction *via* organocatalysis

The organocatalyst, a diaryl TMS-proline derivative facilitated the asymmetric synthesis of pyrrolidines, indolines and piperidines **71** with good yields (60-70%) and enantioselectivities (79-

95%). The method was further extended to the enantioselective synthesis of homoproline **72**, homopipercolic acid **73** and pelletierine **74**. The proposed mechanism for the reaction is shown in the figure below (Figure 6). The catalyst is a Jørgensen's trifluoromethyl derivative, forms a chiral α , β -unsaturated iminium species **75** to activate the Michael acceptor and utilises sterically demanding groups to force attack from one side of the molecule.

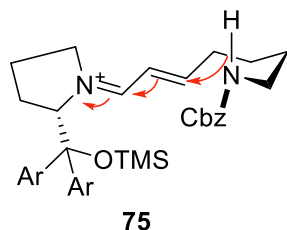
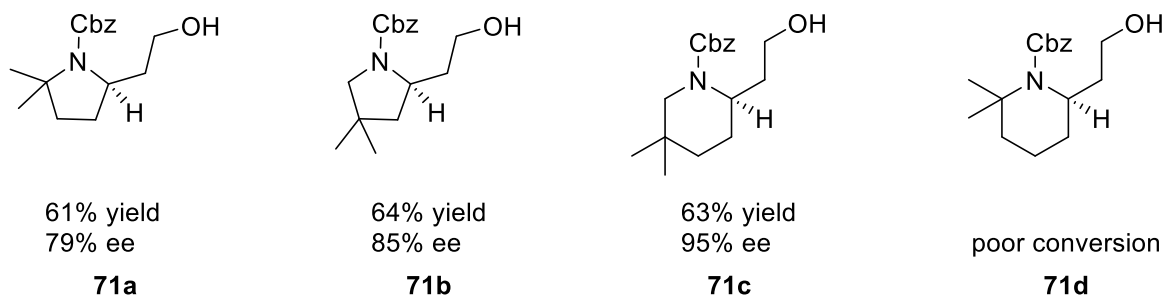


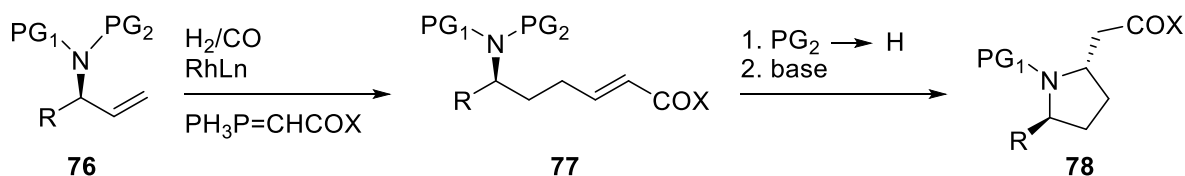
Figure 6: Key step from the proposed reaction mechanism

The reaction scope was extended and a few examples are presented below (Scheme 29). It was found that dimethyl substitution in the second position on the ring led to reduced reactivity, due to steric effects. The 2-dimethyl pyrrolidine **71a** required an extended reaction time to proceed to completion (4 days) and led to reduced enantioselectivity whereas the synthesis of 2-dimethyl piperidine **71d** was not successful even under extended reaction times and increased catalyst loading. Dimethyl substitution on the third position **71b**, **71c** yielded increased reactivity and good levels of enantiomeric excess.



Scheme 29: Representative examples of the asymmetric hetero atom Michael reaction scope

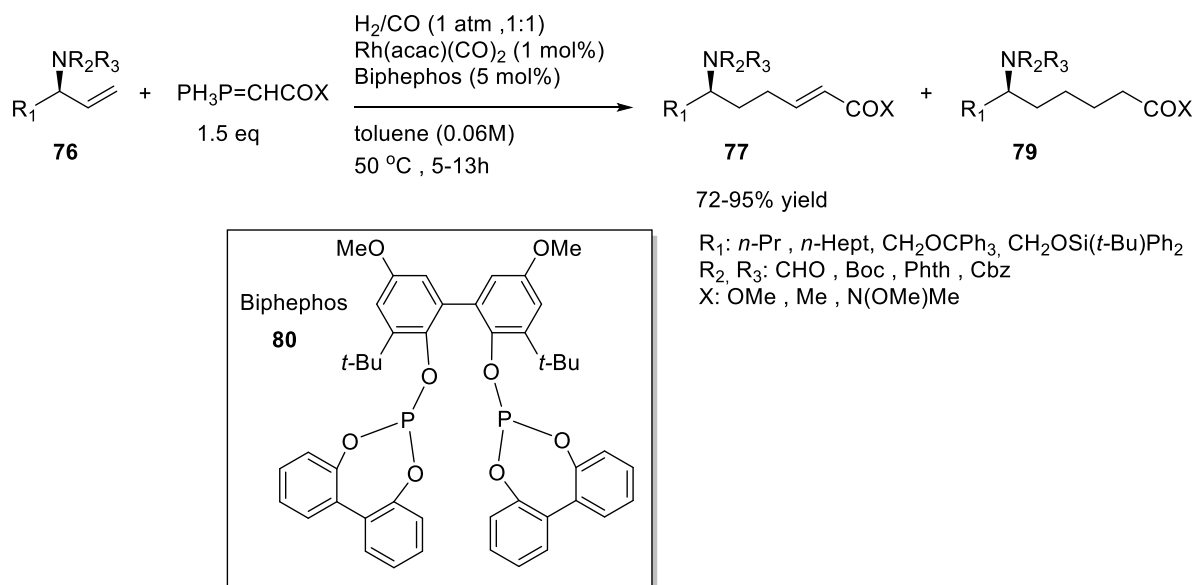
In 2010, Farwick and Helmchen introduced a stereoselective synthetic methodology of β -proline derivatives from allylamines²⁶ (Scheme 30). The route proceeds *via* a domino hydroformylation/Wittig olefination, followed by a separate intramolecular aza-Michael addition.



Scheme 30: Synthetic methodology of β -proline derivatives

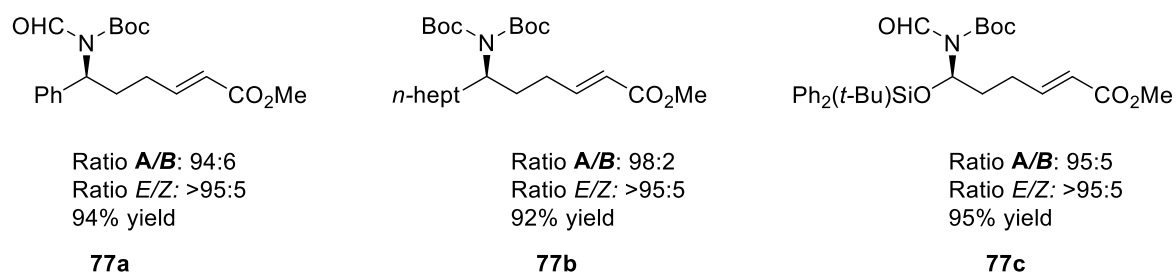
The intramolecular aza-Michael reaction proceeds with high *trans*-diastereoselectivity if 2, 5-substituted pyrrolidines are formed; the cyclisation of urethanes PG₁: Boc/Cbz proceeds to give a product containing a *trans*-configuration at a reaction temperature of -78 °C and use of potassium *tert*-butoxide (*t*-BuOK) as a base.

The domino hydroformylation/Wittig olefination under optimized reaction conditions afforded the *N,N*-diacylamines **77** in excellent yield (72-95% yield) with *E/Z* selectivity (Scheme 31).



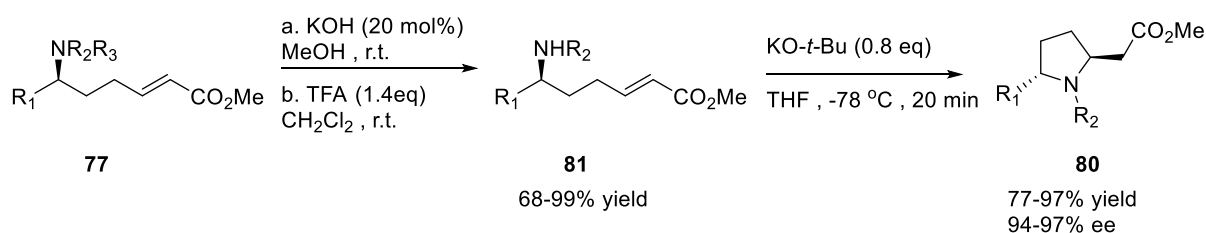
Scheme 31: Domino hydroformylation/Wittig olefination reaction

The rhodium-catalyzed hydroformylation reaction was catalyzed by the ligand Biphephos **80** in a ratio 5:1 (ligand: Rh) to ensure stereoselectivity. Short reaction times reaction times (5-13 h) and low temperatures with a combination of synthesis gas (H₂/CO 1:1) led to full conversion of the starting allylamine derivatives. Those set of conditions were used to expand the scope of the domino reaction with a variety of allylamine derivatives and representatives stabilized Wittig ylides. Three representative examples of the Domino reaction are presented in the scheme below (Scheme 32). *E/Z* selectivity was typical for the Wittig olefination. The aromatic substituent **77a** was afforded in excellent yield as well as the alkane chain **77b** and the *tert*-butyldiphenylsilyl **77c** ones.



Scheme 32: Representative examples of domino hydroformylation/Wittig olefination reaction

The *N,N*-diacylamines **77** were converted to the mono-protected amides which were used as the starting materials for the aza-Michael reaction (Scheme 33).



Scheme 33: Selective deprotonation and intramolecular aza-Michael reaction

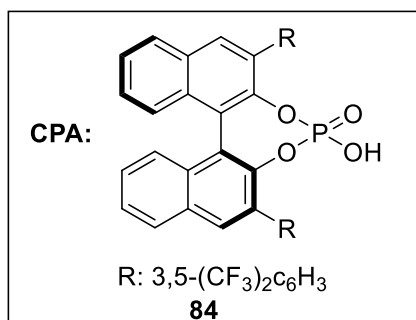
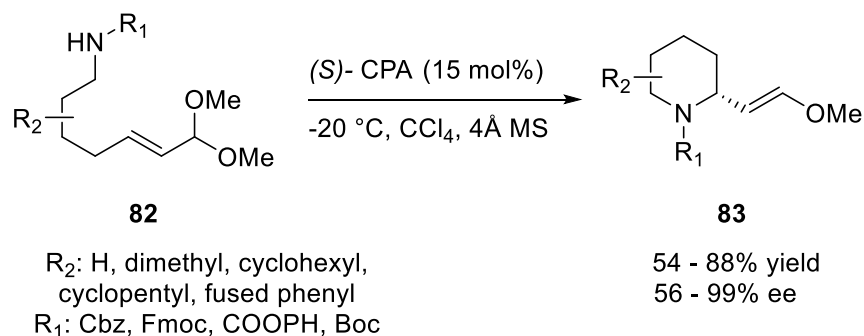
The selective deprotection of the formyl or Boc group was effected with KOH (cat.)/methanol or with TFA/CH₂Cl₂ respectively. The aza-Michael reactions were effected with KO-*t*-Bu (0.8 equiv.) as base at a reaction temperature of -78 °C in THF as solvent at a reaction time of 20 min. The *trans*-diastereoisomers **80** were generated in good to excellent yields (68–97%). No *cis*-isomers were detected by ¹H NMR under the reaction conditions. The enantiomeric excess was determined for a few of the 2,5-disubstituted pyrrolidines and it was found to be equal to that of the starting chiral allylamine derivatives. Thus, no racemization had occurred in the hydroformylation reaction. The corresponding results are shown in the table below (Table 5). The 2-phenyl substituted pyrrolidine derivative (Entry 1) was obtained in good yield and %ee whereas as the *n*-heptane and *tert*-butyldiphenylsilyl groups (Entries 2, 3) were afforded in excellent enantiomeric excess and yield.

| Entry | R ₁ | R ₂ | R ₃ | Deprotonation method | %Yield of B | %Yield of C | % ee of C |
|----------|---|----------------|----------------|----------------------|-------------|-------------|-----------|
| 1 | Ph | Boc | CHO | a | 93 | 80 | 96 |
| 2 | <i>n</i> -hept | Boc | Boc | b | 81 | 97 | 97 |
| 3 | CH ₂ OSi(<i>t</i> -Bu)Ph ₂ | Boc | CHO | a | 71 | 91 | 94 |

Table 5: Representative examples of selective deprotonation and intramolecular aza-Michael reaction

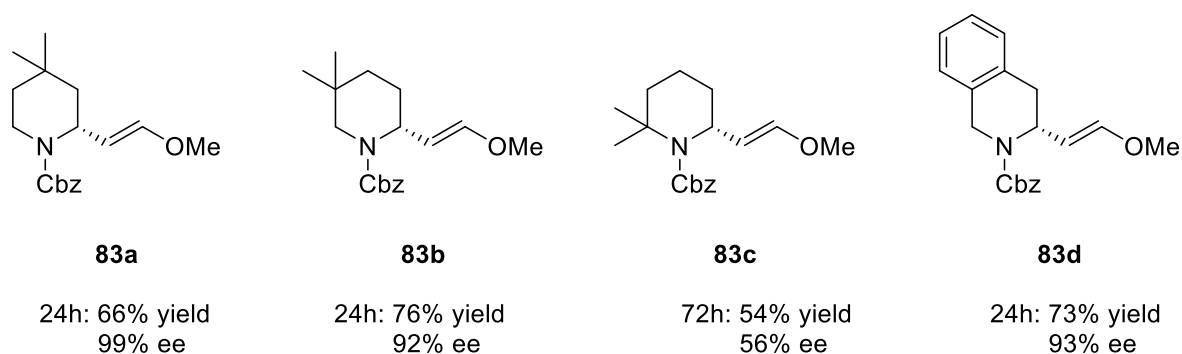
Nagorny *et al.* published an enantioselective synthesis of piperidines catalyzed by chiral phosphoric acids²⁷ (Scheme 34). This report was the first example of the asymmetric cyclisation of unsaturated acetals **82** leading to functionalized piperidines **83** with good enantioselectivities (56–99%). Optimization of the cyclisation reaction conditions lead to carbon tetrachloride as the solvent, the chiral phosphoric acid **84** at -20 °C, as lower reaction temperatures improved selectivity. Computational work revealed that the mechanism involves the formation of a mixed

chiral phosphate acetal which undergoes a concerted asynchronous S_N2' -like displacement yielding the products. Additionally, the axial chirality of the BINOL-based catalyst **84** controls the direction of the Michael addition, leading to high enantioselectivity.



Scheme 34: Enantioselective synthesis of piperidines catalyzed by chiral phosphoric acids

The methodology was applied to the synthesis of a number of substituted piperidines, specifically *gem*-dimethyl, fused phenyl, cyclopentyl and more examples. A few representative examples are shown in the scheme below (Scheme 35). Most examples gave good yields and good ee's although the 6,6'-dimethyl compound **83c** was an exception with 54% yield and 56% ee after 72 h. Substituents of the fourth and fifth position **83a**, **83b**, **83c** had a beneficial effect on the selectivity of the reaction and highly enantioselective products were formed. The reaction was also performed in CCl₄ which raises health concerns.

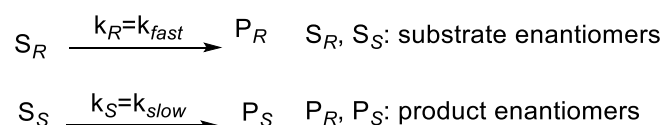


Scheme 35: Representative examples of the enantioselective synthesis of piperidines catalyzed by chiral phosphoric acids

8.4 Kinetic Resolutions

8.4.1. Concept of Kinetic Resolutions

Kinetic resolution is often a valuable alternative for preparing important chiral compounds and can offer many advantages.²⁸ In kinetic resolutions a chiral catalyst or chiral reagent is employed to react with an enantiomeric mixture that is difficult to separate. Ideally, only one enantiomer reacts towards the product. Due to the resulting different physical properties of the two products they can be separated easily with common methods (Scheme 36).



Scheme 36: A classical kinetic resolution

The success of this method depends on the fact that the two enantiomers react at different rates with a chiral catalyst, so one of the two transition states is lower in energy than the other one.

Kinetic resolution occurs when the reaction rate of one enantiomer differs from the reaction rate of the other enantiomer ($k_R \neq k_S$) and the reaction is stopped at 50% conversion. Ideally, one enantiomer reacts much faster than the other; for example, if the starting reactant substrate with the absolute configuration *R* is the only reacting enantiomer ($k_S = 0$). In this case, 50% conversion of the initial 50/50 mixture leads to a final mixture of 50% reactant (*S*) and 50% product (*P*). The quality of the kinetic resolution is typically expressed with the selectivity (*s*-factor). The *s*-factor is a measurement for the effectiveness of a kinetic resolution and relates the rates of the reaction of the two enantiomers with the chiral reagent. It is calculated by the fraction of the rate constant for one enantiomer k_R by the rate constant for the other enantiomer k_S (Figure 7).

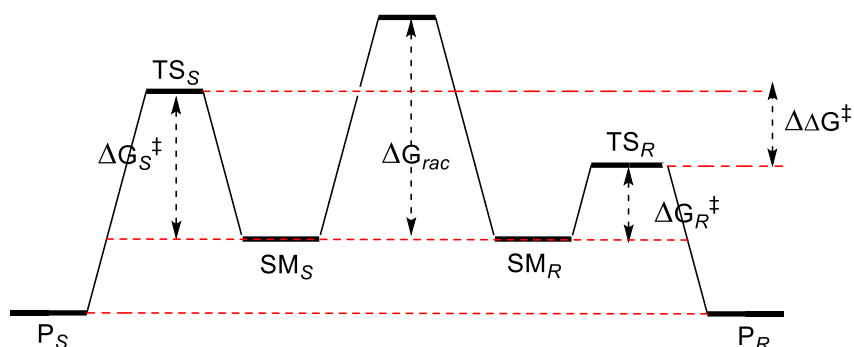


Figure 7: Different transition state energies in kinetic resolution

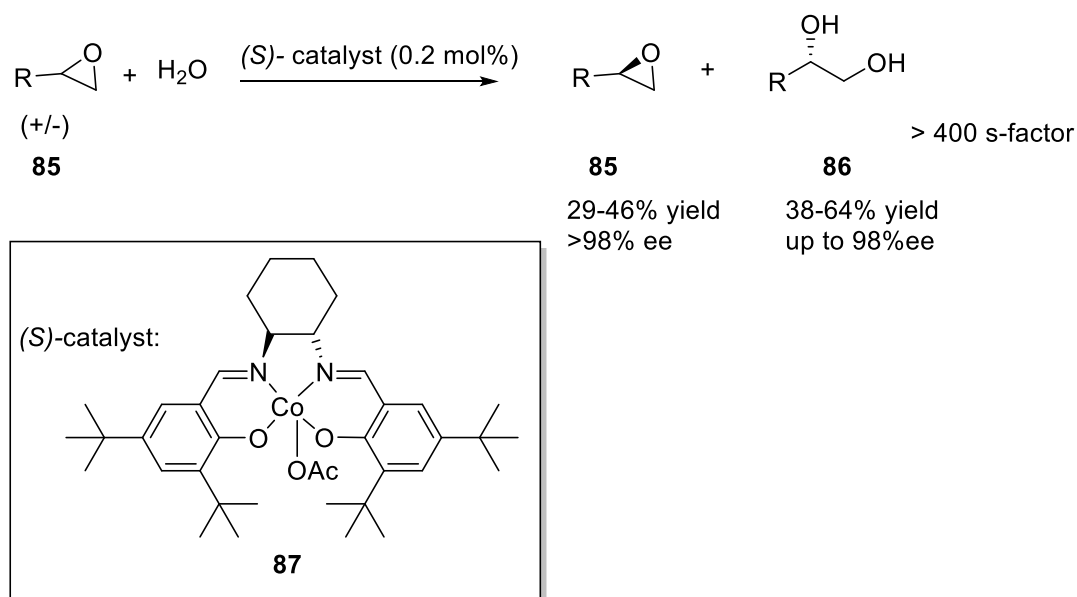
While both enantiomers are at the same Gibbs free energy level by definition, and the products of the reaction with both enantiomers are also at equal levels, the transition state energy (ΔG^\ddagger) can differ. As shown in the figure above, the transition state for the *R* enantiomer has a lower ΔG^\ddagger and

would react faster than the *S* enantiomer. In the ideal kinetic resolution only one enantiomer reacts, i.e. $k_R \gg k_S$. The selectivity (*s*-factor) of a kinetic resolution is related to the rate constants of the reaction of the *R* and *S* enantiomers, k_R and k_S respectively, by $s = k_R/k_S$, for $k_R > k_S$

In kinetic resolutions any enantiomeric ratio can be obtained by sacrificing yield and therefore by controlling the conversion. The enantiomeric ratios of the product and the recovered starting materials after the resolution are dependent on both the *s*-factor and the conversion. In an optimal kinetic resolution (high *s*-factors) enantiopure products can be obtained at 50% conversion. This represents the maximum possible yield in classical kinetic resolutions. Generally, any kinetic resolution with a reasonable selectivity (>20) can deliver 99% ee with in useful yields. Provided that selectivity factors greater than 20 can be obtained, kinetic resolution can be used to separate enantiomers with acceptable yield and outstanding enantiopurity. Despite the 50% maximum yield, kinetic resolutions can be a reliable, effective, and easily implemented method for the production of enantiopure material.²⁹

8.4.2 Examples of Kinetic Resolutions

Jacobsen *et. al.* developed a kinetic resolution of the hydrolytic opening of epoxides *via* nucleophilic ring opening with attack by water and a cobalt complex as catalyst³⁰ (Scheme 37).



Scheme 37: Jacobsen's hydrolytic kinetic resolution

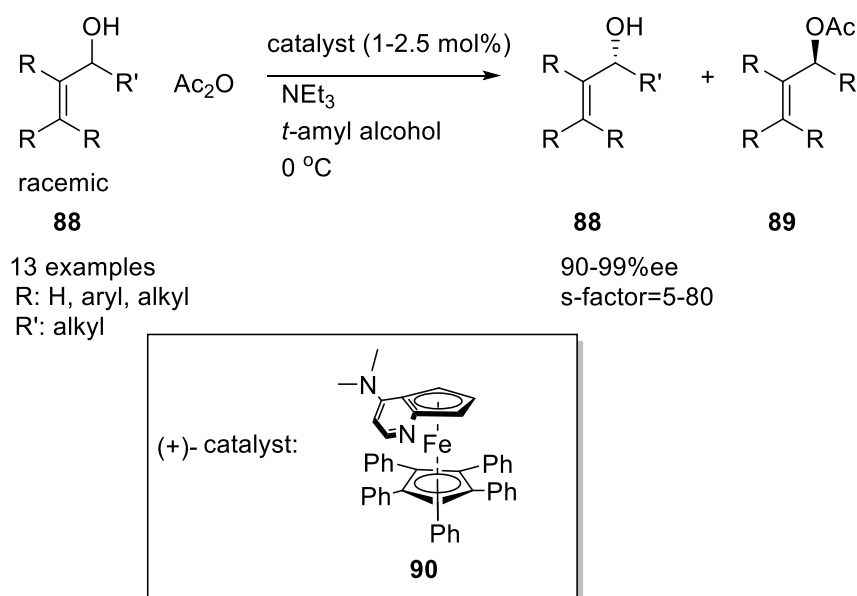
This procedure uses water as the only reagent, no added solvent and low loadings of the chiral catalyst and it affords terminal epoxides and 1, 2-diols in high enantiomeric excess ($>95\%$ in nearly all cases) and quantitative yield. The nucleophile effectively opens the epoxide at the terminal position enantioselectively, providing access to both unreacted epoxide and 1,2-diol products. The hydrolytic kinetic resolution was applicable to a series of terminal epoxides and

representative examples are shown in the table below (Table 6). The alkyl-substituted epoxide underwent efficient resolution with high %ee's for both the diol and the unreacted epoxide and an excellent relative rate constant (Entry 1). The aromatic and the conjugated epoxides were resolved with lower selectivities but highly enantiomerically enriched epoxide and diol were obtained (Entries 2, 3).

| Entry | R | Concentration | | Time (h) | Epoxide | | Diol | | k_{rel} |
|-------|--------------------|---------------|---------------|----------|---------|--------|------|--------|-----------|
| | | Catal (mol%) | Water (equiv) | | %ee | %yield | %ee | %yield | |
| 1 | CH ₃ | 0.2 | 0.55 | 12 | >98 | 44 | 98 | 50 | >400 |
| 2 | Ph | 0.8 | 0.7 | 44 | 98 | 38 | 98 | 39 | 20 |
| 3 | CH=CH ₂ | 0.64 | 0.50 | 20 | 84 | 44 | 94 | 49 | 20 |

Table 6: Representative examples of Jacobsen's hydrolytic kinetic resolution

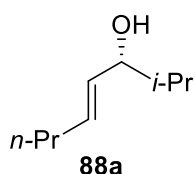
In early 2000s, Fu and co-workers published a catalytic enantioselective acylation focused on application of a planar-chiral DMAP derivative to the kinetic resolution of allylic alcohols³¹ (Scheme 38).



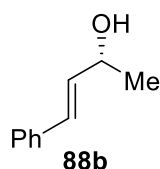
Scheme 38: Kinetic resolution of allylic alcohols by a non-enzymatic acylation catalyst

The catalyst can affect the kinetic resolution of most allylic alcohols with good selectivity. This enantioselective acylation was applied to a variety of substrates with high enantioselectivity and good selectivity for most substrates (90-99% ee). A few representative examples of the recovered enantioenriched alcohols are shown in the scheme below (Scheme 39).

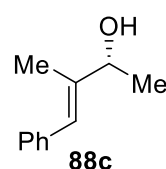
Unreacted alcohols- major enantiomer



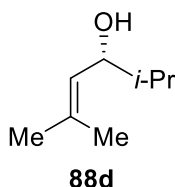
92%ee at 75% conversion
s=5.4



99%ee at 54% conversion
s=64



98%ee at 53% conversion
s=86

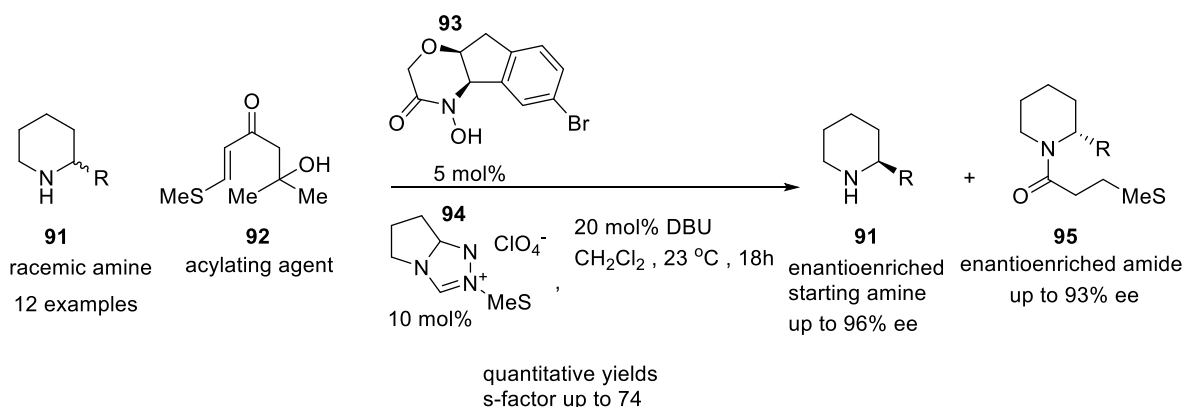


97%ee at 60% conversion
s=18

Scheme 39: Unreacted alcohols-major enantiomer of the kinetic resolution of allylic alcohols by a non-enzymatic acylation catalyst

The allylic alcohol **88a** does not have a substituent geminal or *cis* to the hydroxyl group and was resolved with low selectivity but high enantiomeric excess. However, the phenyl group in the *trans* position **88b** increased the selectivity factor as well as the %ee. Kinetic resolutions of allylic alcohols that are substituted geminal **88c** or *cis* **88d** to the hydroxyl group proceeded with moderate selectivity; the phenyl-group improved the selectivity factor.

Bode *et al.*³² published a method for the catalytic kinetic resolution of cyclic secondary amines (Scheme 40). The methodology employs two catalysts working synergistically to generate enantiopure cyclic amines.



Scheme 40: Catalytic kinetic resolution of cyclic secondary amines

The key advance was the use of a chiral hydroxamic acid **93** and an imidazole **94** co-catalyst as highly enantioselective acylating agent. The starting racemic amines **12** were treated with α' -hydroxyenone **92** (acylating agent) the chiral catalyst **93**, the imidazole co-catalyst **94** and 1,8-diazabicyclo[5.4.0]undec-7-ene (DBU) in dichloromethane (CH_2Cl_2) at 23 °C for 18h and produced enantiomerically enriched amides **95**. These set of conditions were applied for a range of substituted piperidines, piperazines, morpholines, and tetrahydroisoquinolines. The enantiomerically enriched amines **91** and amides **95** were generated with high selectivity factors (s up to 127). Substituted piperazines and morpholines, both of which are were resolved with s factors ranging from 11 to 23. Tetrahydroisoquinolines were resolved with excellent levels of selectivity (up to s = 74).

A few of different substrates tested are presented in the table below (Table 7). The 2-benzyl **91a** and the 2-phenyl **91b** piperidines were resolved with good s-factors and high enantioselectivities for the amides, while the %ee for the recovered amines were moderate (70%). Similarly, the morpholine **91c** was resolved with good s-factor and enantiomeric excess whereas the tetrahydroquinoline **91d** substrate was generated with excellent %ee and higher s-factor than the rest of the substrates mentioned.

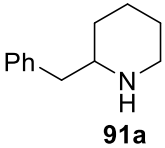
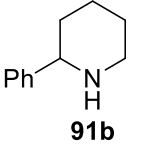
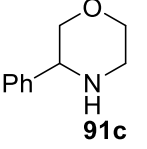
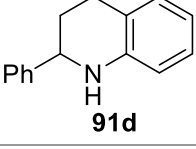
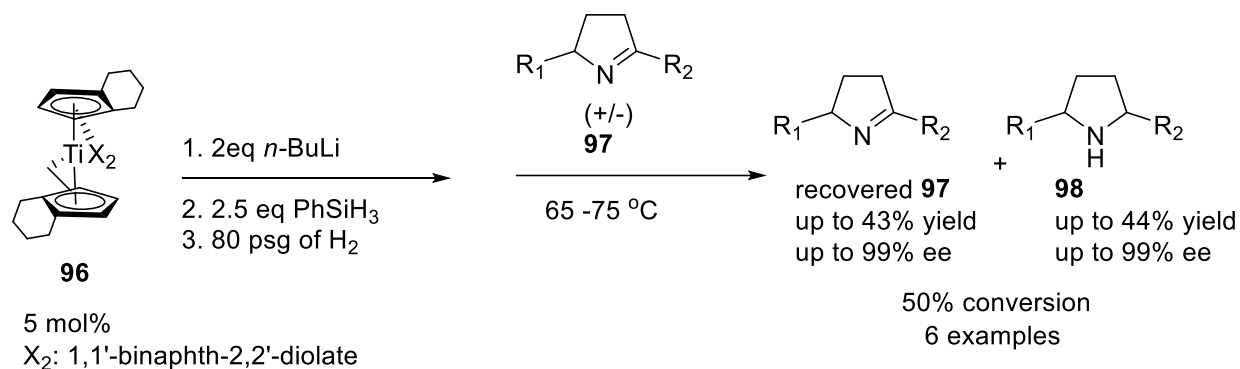
| Substrate | % conversion (% yield) | er amine | er amide | s-factor |
|---|------------------------|----------|----------|----------|
|  91a | 34 (34) | 70:70 | 94:6 | 23 |
|  91b | 41 (41) | 70:30 | 92:8 | 21 |
|  91c | 40 (40) | 79:2 | 93:7 | 24 |
|  91d | 56 (47) | 93:7 | 95:5 | 53 |

Table 7: Representative examples of the catalytic kinetic resolution of cyclic secondary amines

A publication by Buchwald *et. al.* demonstrates a highly enantioselective kinetic resolution of disubstituted pyrrolidines *via* an asymmetric hydrogenation reduction catalyzed by a chiral titanocene catalyst³³ (Scheme 41).



Scheme 41: Kinetic resolution of disubstituted 1-pyrrolidines catalyzed by a chiral titanocene catalyst

The active titanocene catalyst **96** is generated *in situ* and the hydrogenation proceeds in tetrahydrofuran at 65-75 °C with 80 psig of H₂ until the reaction which was monitored by ¹H NMR reached at 50% conversion. This kinetic resolution of 2, 5-disubstituted pyrrolidines **97** was extended to a variety substitution pattern of aromatic groups with high levels of enantiomeric excess. A few of them are shown in the table below (Table 8).

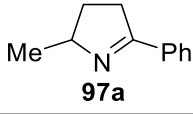
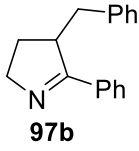
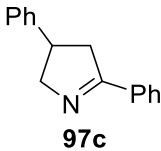
| Substrate | %yield (%ee) recovered 97 | % yield (%ee) 98 |
|---|----------------------------------|-------------------------|
|  97a | 37 (99) | 34 (99) |
|  97b | - (75) | 42 (>95) |
|  97c | 33 (47) | 44 (99) |

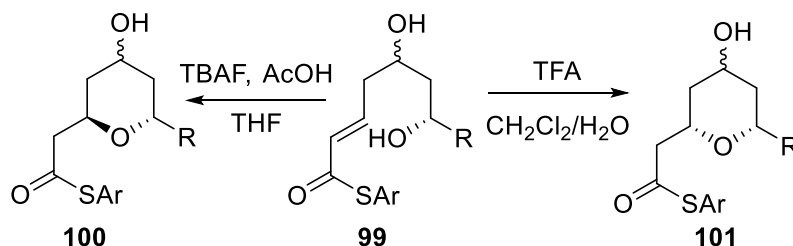
Table 8: Representative examples of the kinetic resolution of disubstituted 1-pyrrolidines catalyzed by a chiral titanocene catalyst

The 2-phenyl 5-alkyl substituted pyrrolidine **97a** underwent an effective kinetic resolution with high levels of enantioselectivity for both recovered pyrrolidine and the *cis*-pyrrolidine product. The 3-benzyl 2-phenyl pyrrolidine **97b** was resolved with modest enantioselectivity for the recovered pyrrolidine but with high %ee for the product **97c**. The yield of the recovered pyrrolidine could not be determined due to racemization on the silica gel column; the %ee was determined by high-performance liquid chromatography (HPLC) analysis. The resolution of 2,4-disubstituted substrate was relatively poor for the recovered pyrrolidine **97c** but the product **98c** was produced in high enantioselectivity. The reduction of **97b**, **97c** substrates produced predominantly *cis* products. Substrate **97b** was reduced with a higher level of diastereoselectivity (*cis:trans* 85:15) than was **97c** (*cis:trans* 75:25). The active Ti(III) hydride catalyst forms two different diastereomeric complexes upon reacting with the starting substrate. Studies on these

complexes revealed that substrates with a substituent at C-3 should be more efficiently kinetically resolved than those with a C-4 substituent. This prediction is consistent with the results that the %ee of the recovered pyrrolidine obtained with substrate **97b** is higher than that for recovered substrate **97c** (Table 8).

8.5 Background Work

The Clarke group has developed a stereodivergent oxy-Michael cyclisation for the stereoselective synthesis of tetrahydropyrans, which converts an alcohol tethered to an α,β -unsaturated thioester into either 2,6-*cis* or 2,6-*trans* tetrahydropyrans³⁴ (Scheme 42).



Scheme 42: Stereodivergent oxy-Michael Cyclisation

The α,β -unsaturated thioester under acetic acid-TBAF conditions produced 2,6-*trans*-tetrahydropyran rings **100** up to 20:1 diastereoselectivity, but, under TFA conditions formed the 2,6-*cis* configuration **101** up to 13:1 diastereoselectivity. In order to explain these interesting results, computational studies were carried out³⁵ (Figure 8). It was then proven, that under TFA conditions the TFA acted as a 'proton shuttle' and played a dual role as it protonates the thioester carbonyl C=O and deprotonates the alcohol OH. The calculations also revealed that the molecule adopts a chair-like transition state and the *cis*-product was favoured, supporting the results seen in the synthetic studies. In contrast, the 2,6-*trans*-configuration was obtained under TBAF conditions; the 4-hydroxyl group was involved in stabilization of the transition state and acted as a hydrogen-bond donor. The calculations predicted that the absolute stereochemistry of these THPs to be (*S*)-configuration and experimental data were compared with literature and confirmed the results.

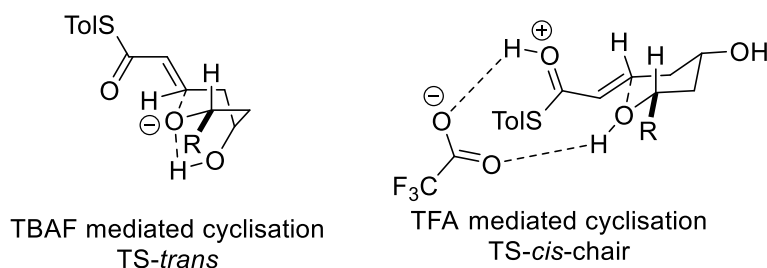
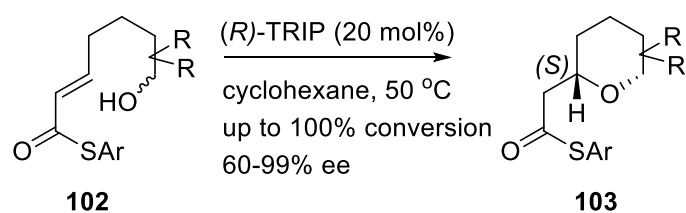


Figure 8: Transition states under TBAF and TFA cyclisations

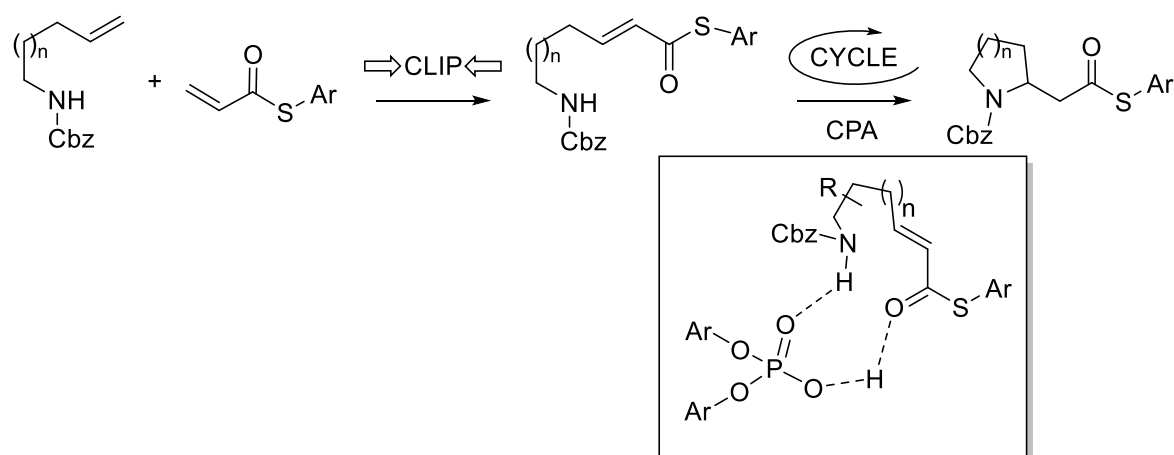
Computational studies (DFT calculations with KE) suggested that the Brønsted acid catalyzed reaction could be made asymmetric by the use of a chiral Brønsted acid that acts as a proton shuttle. The Brønsted acids TFA ($\text{pK}_a = -0.3$) and CSA ($\text{pK}_a = 1.2$) act as proton shuttles in the oxy-Michael reaction, chiral Brønsted acids with similar pK_a values should be able to perform the

same function. Subsequent the cyclisation of alcohols **102** to generate (*S*)-tetrahydropyrans **103** in excellent yields and %ee's³⁶ (Scheme 43).



Scheme 43: Asymmetric tetrahydropyran cyclisation

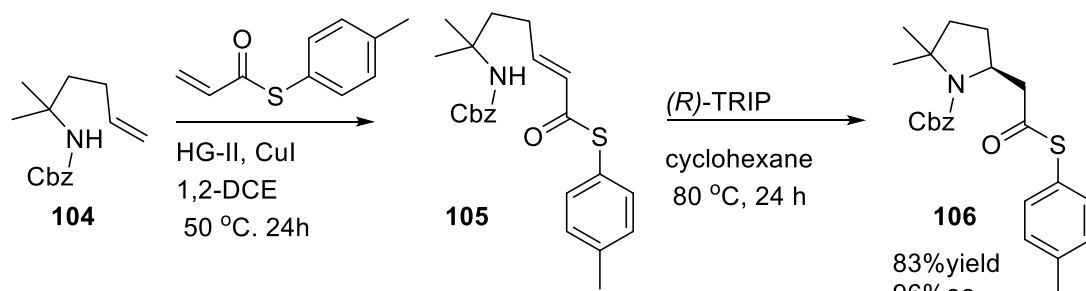
Based on these encouraging results, we decided to extend this approach to the asymmetric synthesis of pyrrolidines *via* an intramolecular aza-Michael reaction.³⁷ A new 'Clip-Cycle' methodology was developed, which an unsaturated protected 'allyl' amine is 'clipped' with an activating unsaturated thioester group by an alkene metathesis reaction, followed by a 'cycle' aza-Michael reaction, which is catalyzed by a chiral Brønsted acid. The chiral phosphoric acid acts as a catalytic proton shuttle, deprotonating the protected amine nitrogen and protonating the thioester carbonyl simultaneously which catalyses the reaction. This strategy can be applied to the synthesis of any ring size cyclic amines and in other heterocycles, too (Scheme 44).



Scheme 44: 'Clip-Cycle' Approach and proton shuttle transition state with the chiral phosphoric acid

The reacting groups were chosen through synthetic and computational studies. The Cbz-protected amine units have similar nucleophilicity and pKa to alcohols and they are easy to deprotect. α,β -unsaturated oxoester, ketones and thioesters were screened to determine which one gives optimum %ee's and yields. It was found that α,β -unsaturated oxoesters are not reactive, lead to decomposition of substrate and gave low yields (8% yield and 90% ee), while α,β -unsaturated ketones are too reactive as they cyclized during the metathesis reaction forming racemic products. However, the α,β -unsaturated thioesters gave excellent results, resulting to 83% yield

and 96% ee and it was concluded that they sit in the 'Goldilocks zone' of reactivity among the Michael acceptors (Scheme 45).



Scheme 45: Asymmetric synthesis of substituted pyrrolidines using α,β -unsaturated thioesters as Michael acceptors and (*R*)-TRIP as the catalyst

Computational work was carried out (with KE, B3LYP/6-31G**, solvent SMD(cyclohexane)) and suggested that the amines should cyclise onto α,β -unsaturated thioesters to form pyrrolidines with high enantioselectivity and indicated formation of (*S*)-product with (*R*)-TRIP (Figure 9). Computational work suggested that the Brønsted acid acts as a proton shuttle and catalyzes the cyclization, which is the stereochemical-determining step. This step can give either the *E* or *Z* enol, depending on whether the thioester adopts an *s-cis* or *s-trans* conformation. It can also have two configurations of the newly formed stereocentre, depending on which face the nitrogen attacks. As demonstrated in the energy diagram below, the energy of the transition state of the *S*, *E* cyclized product (90.8 kcal/mol) is lower than the energy of the *R*, *Z* configuration (96.1 kcal/mol), therefore the catalysed process of the *S*, *E* pathway is the most favorable. The steric clash between the different positions of the thioester α -proton is the main reason the difference in the energies. In the *S*, *E* transition state it is pointing away from the catalyst pocket while in the *R*, *Z* transition state it is pointing inwards allowing the carbamide to approach from the other side. The computational study predicted formation of the (*S*)-product with ~74% ee. Preliminary synthetic studies supported the computational work (Scheme 46).

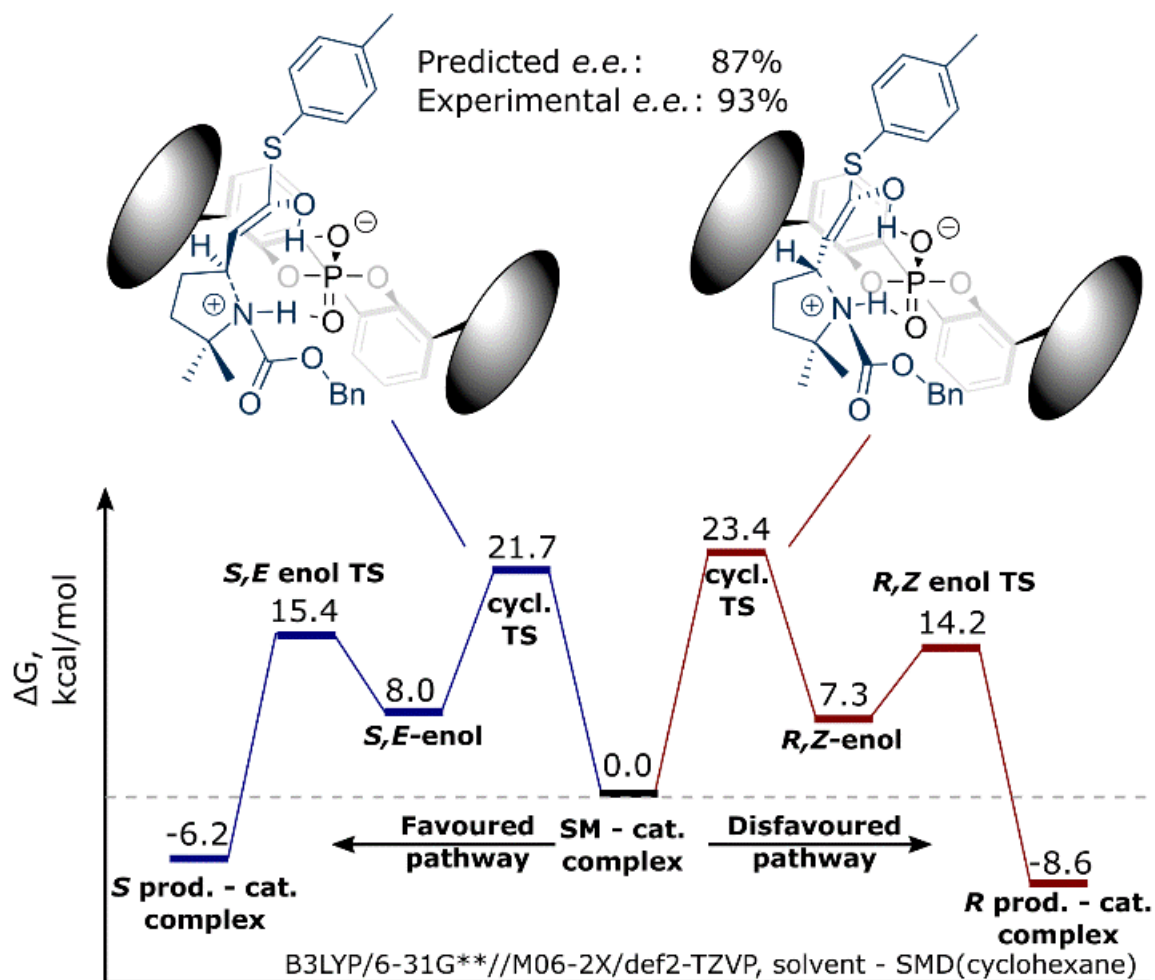
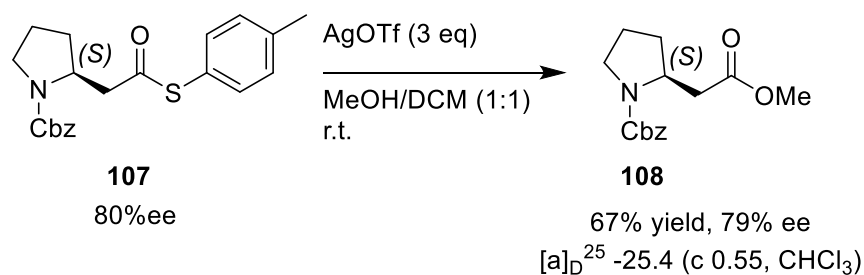


Figure 9: Computational work on cyclisation selectivity

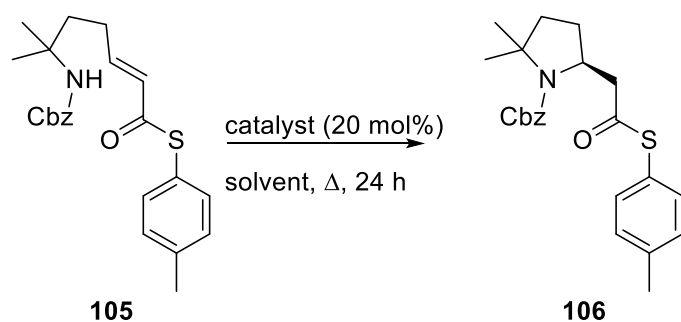
The absolute stereochemistry of the cyclisation was confirmed as (*S*)-configuration by conversion of the thioester group **107** to methyl ester **108** and comparison with literature data³⁸ (Scheme 46).



Scheme 46: Methyl ester synthesis

In the Clarke group, the first project on the 'Clip-Cycle' methodology on pyrrolidines involved an enantioselective synthesis of spirocyclic and non-spirocyclic pyrrolidines.³⁷ The synthetic approaches started with the synthesis of precursors which were subjected to a range of chiral phosphoric acid catalysts with solvents, temperatures and reaction times to find optimal conditions for the reaction. As a representative example, 2, 2-dimethyl substituted precursor **105** was used and the various conditions screened are shown below (Scheme 47, Table 9). Screening

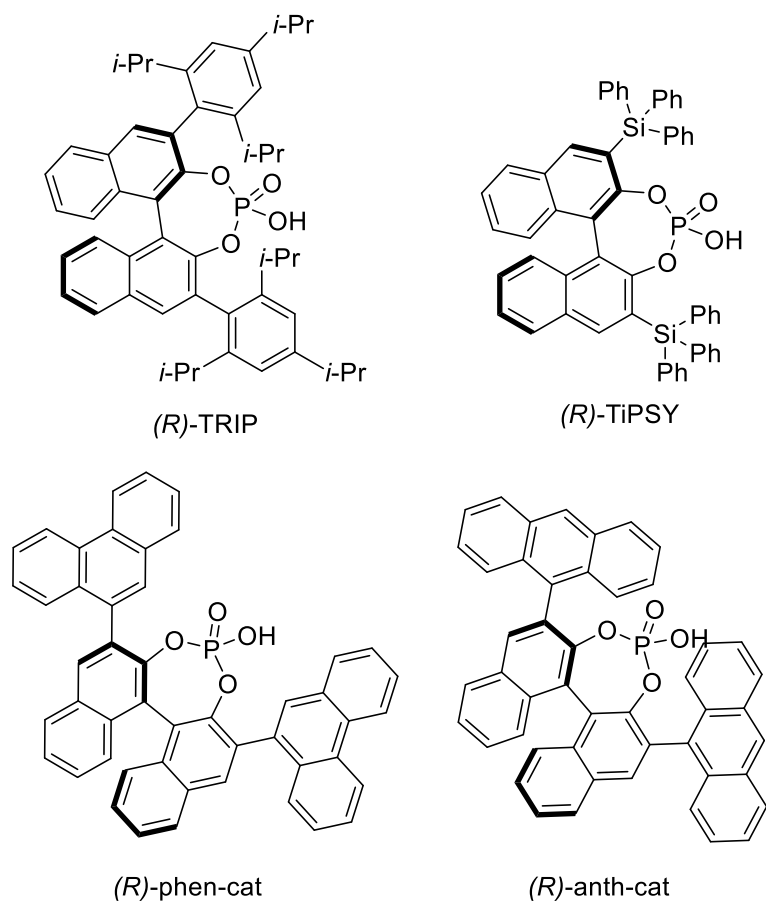
the conditions started with attempts to find a suitable solvent for the system. Initial reaction tests showed that the reaction did not proceed in room temperature, so higher temperatures were required. Previous work in the Clarke group suggested that for chiral Brønsted acids low polarity solvents gave better results.³⁶ This is due to the fact that high polarity solvents may interrupt the ion pairing interaction between the catalyst and substrate. For this reason, cyclohexane (bp. 81 °C), toluene (bp. 111 °C), and 1, 2-DCE (bp. 84 °C), were tested as the initial solvents with 1, 2-DCE being the most polar of the solvents and cyclohexane least polar. For the catalyst screening, the Chiral Brønsted acids that were used are (*R*)-TRIP, (*R*)-TiPSY, (*R*)-phen-cat and (*R*)-anth-cat (Scheme 48). Upon heating the reaction at 50 °C in the four different solvents (Entries 1-3), (*R*)-TRIP gave high enantioselectivities (90-93%) but with poor conversion (15-47%). Increased temperatures (80 °C) lead to increase in conversion with no drop in the %ee (Entry 5). (*R*)-anth-cat gave excellent conversion and yield with low enantioselectivity (Entry 7), while (*R*)-TiPSY and (*R*)-phen-cat gave lower conversions and %ee's (Entries 5,6). Through the process of optimisation, (*R*)-TRIP in cyclohexane at 80°C for 24h was chosen as the standard set of conditions.



Scheme 47: Chiral phosphoric acid cyclisation of the 2,2-dimethyl substituted precursor

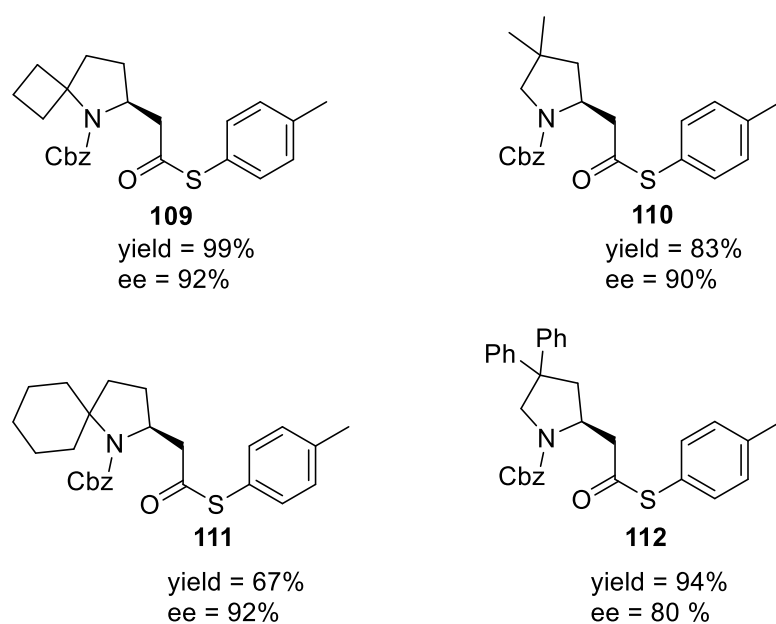
| | Catalyst (20 mol%) | Solvent | T / °C | Conversion% | Yield% | ee% |
|---|------------------------|--------------------|-----------|-------------|-----------|-----------|
| 1 | (<i>R</i>)-TRIP | cyclohexane | 50 | 47 | 38 | 91 |
| 2 | (<i>R</i>)-TRIP | toluene | 50 | 21 | 18 | 93 |
| 3 | (<i>R</i>)-TRIP | 1,2-DCE | 50 | 15 | 12 | 90 |
| 4 | (<i>R</i>)-TRIP | cyclohexane | 80 | 100 | 77 | 93 |
| 5 | (<i>R</i>)-TiPSY | cyclohexane | 80 | 26 | 22 | 58 |
| 6 | (<i>R</i>)-phen-cat | cyclohexane | 80 | 26 | 21 | 45 |
| 7 | (<i>R</i>)-anth-cat | cyclohexane | 80 | 100 | 99 | 63 |

Table 9: Conditions screened for the 2,2-dimethyl substituted precursor **105**



Scheme 48: Chiral phosphoric acids

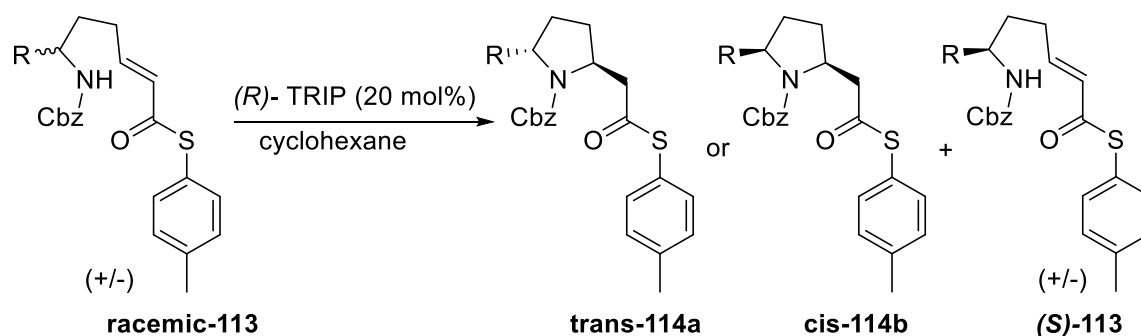
With a set of conditions in hand, the scope was extended to spirocyclic and non-spirocyclic substitutions at the 3,3'- and 2,2'- positions of the pyrrolidine ring. Representative examples of the cyclisation scope are shown below (Scheme 49).



Scheme 49: Spirocyclic substituted pyrrolidines synthesised

8.6 Aim of Project

It was decided to further expand the scope and examine the kinetic resolution of chiral but racemic substrates, given the encouraging results of the 'Clip-Cycle' methodology for the asymmetric synthesis of substituted pyrrolidines (Scheme 50). In our earlier studies achiral substrates were used, however in these studies, there is a stereocentre that could influence the diastereoselectivity of the cyclisation. Each enantiomer of the starting material **113** could cyclize to give either the 2,5-*trans*-cyclic amine **114a** or the 2,5-*cis*-cyclic amine **114b**.



Scheme 50: Enantioselectivity and Diastereoselectivity in our Kinetic Resolution

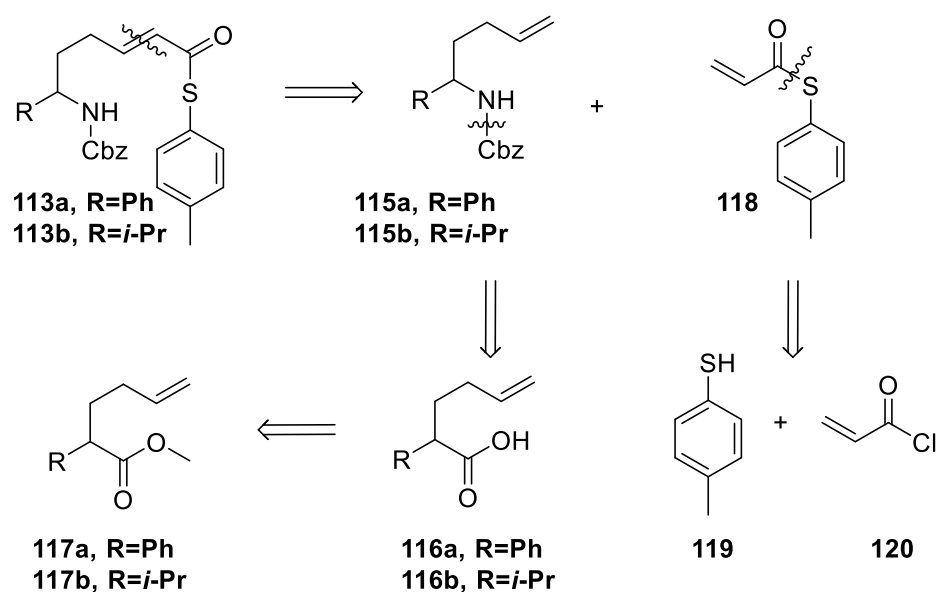
In case of achiral Brønsted acid catalyzed cyclisations, literature examples of cyclic amines such as piperidines, piperazines and morpholins³⁹ indicate the formation of 2,6-*trans*- diastereomer but we are not aware of any example regarding the pyrrolidine forming cyclisations. Our survey of the literature indicates that the diastereoselectivity, in pyrrolidine forming cyclisations, is dependent upon the type of cyclisation reaction used.⁴⁰

The aim of this project was to study the asymmetric synthesis of substituted pyrrolidines using a chiral phosphoric acid *via* a kinetic resolution, which would lead to the formation of enantioenriched pyrrolidine products. Upon completion of the kinetic studies, attempts were made to determine the diastereoselectivity as well as the enantioselectivity in the kinetic resolutions. Chiral HPLC in conjunction with ¹H NMR were used to study the kinetic resolutions, which would allow to build up a kinetic profile of the reaction, calculate s-factors and, determine the conversion for optimal %e.e. of cyclised product, and unreacted starting material.

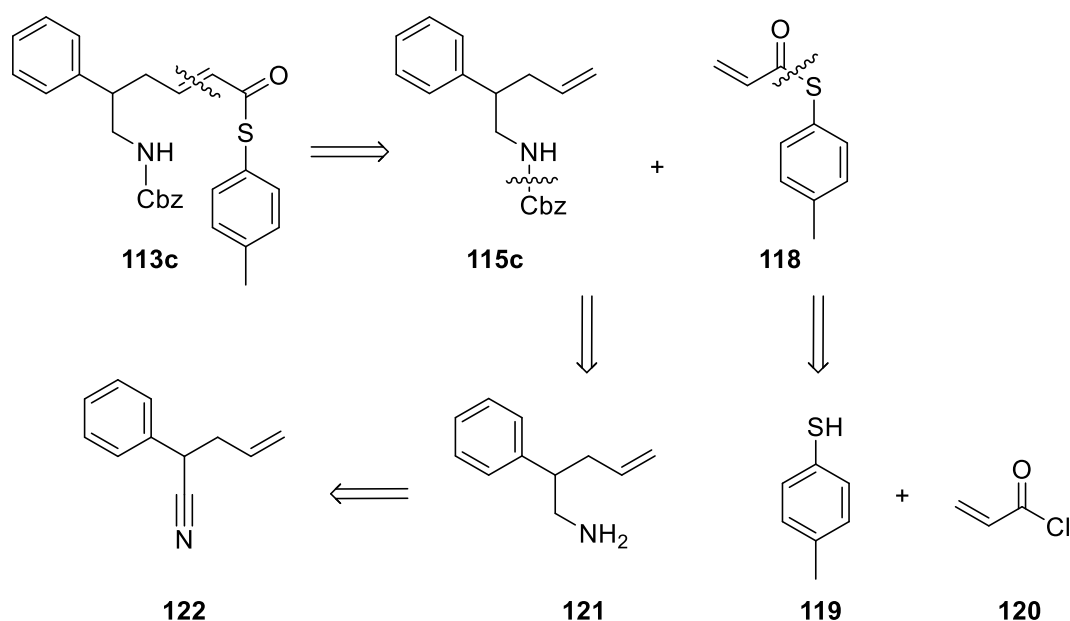
9. Results and discussion

9.1 Retrosynthetic Analysis of the Pyrrolidine Precursors

The cyclisation precursors were synthesized *via* two different straightforward synthetic routes already developed in the Clarke group from commercially available starting materials. Retrosynthetic analysis of the cyclisation precursors simplifies them to the thioacrylate **118** and the corresponding Cbz-protected amines **113a-c**, which can then be joined through a cross metathesis reaction (Scheme 51, Scheme 52). 2-Substituted substrates **113a-b** can be synthesised by allylation of an ester to give **117** followed by a Curtius rearrangement, while 3-substituted substrates **113c** can be formed by allylation of a nitrile to give **122**, followed by reduction and Cbz-protection.



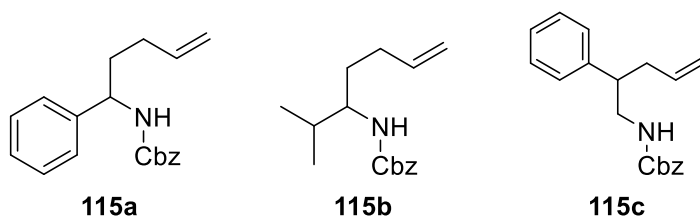
Scheme 51: Retrosynthetic Analysis of 2-substituted cyclisation precursor



Scheme 52: Retrosynthetic Analysis of 3-substituted cyclisation precursor

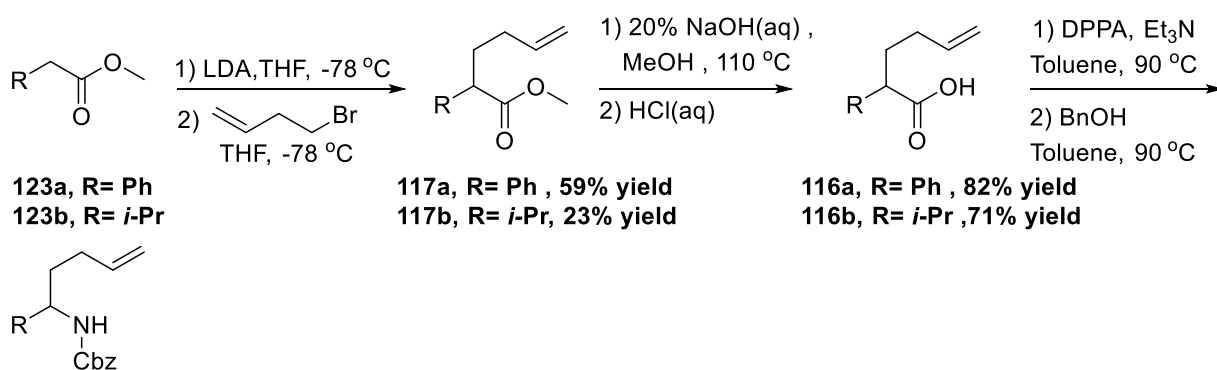
9.2 Synthesis of the Pyrrolidine Precursors

The synthetic route to the precursors started with the synthesis of the 2- and 3-substituted Cbz-protected amines **115a-c** (Scheme 53).



Scheme 53: Structures of 2- and 3-substituted Cbz-protected amines

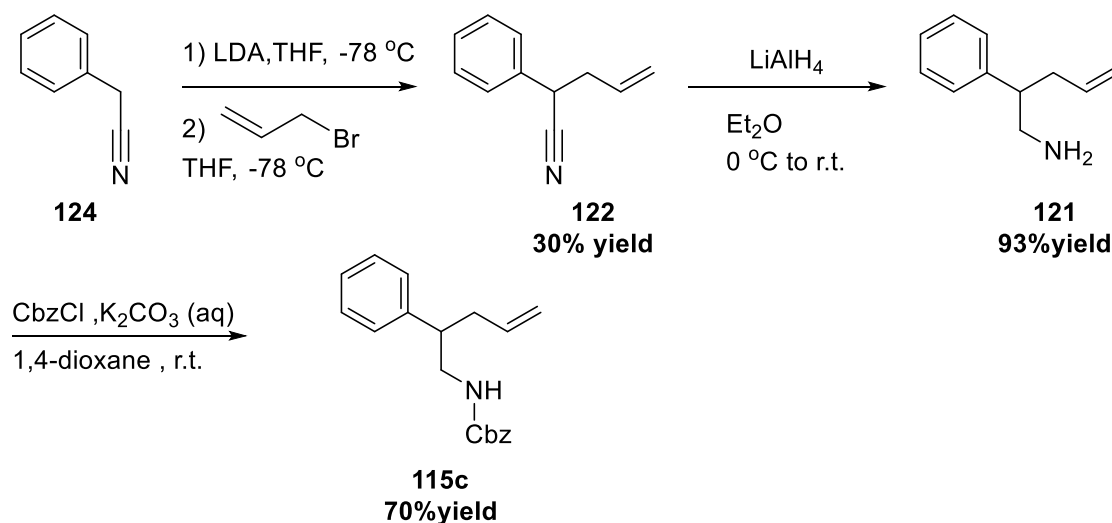
For the 2-substituted amines the route proceeded *via* deprotonation of ester **123** using lithium diisopropylamide (LDA) as a strong base. The LDA was formed using diisopropylamine and *n*-butyllithium at $-78\text{ }^{\circ}\text{C}$ in dry tetrahydrofuran and the solution stirred for 45 min. The starting ester was then added and the resultant enolate was stirred for further 45 min at $-78\text{ }^{\circ}\text{C}$; 1 eq of 4-bromo-1-butene was then added at $-78\text{ }^{\circ}\text{C}$ and the reaction mixture was warmed to room temperature to give the ester **117** after purification. The ester **117** was then hydrolyzed under reflux conditions with 20% sodium hydroxide (aq) in methanol and then acidified with 1M hydrochloric acid to yield the carboxylic acid **116**. The acid **116** underwent the Curtius rearrangement⁴¹ using diphenylphosphoryl azide and triethylamine in dry toluene at $90\text{ }^{\circ}\text{C}$ to form the isocyanate and the reaction mixture was stirred for 2 h; 1.5 eq of benzyl alcohol was then added at $90\text{ }^{\circ}\text{C}$, the reaction was stirred for further 48 h at the same temperature to give the final Cbz-protected amine **116** after purification (Scheme 54).



Scheme 54: Representative reaction route to 2-substituted Cbz-aminines

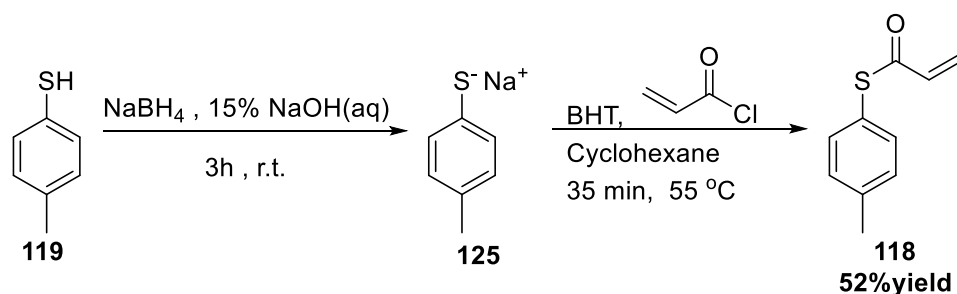
The route to the 3-substituted amines began with deprotonation of the nitrile **124**, a procedure similar to deprotonating the ester **123** as mentioned above, using LDA at $-78\text{ }^{\circ}\text{C}$ in dry THF to give the nitrile anion which was reacted with allyl bromide to give substituted nitrile **122**. The nitrile

was then reduced using lithium aluminium hydride as the reducing agent. The free amine was delivered upon Fieser workup⁴² **121** and it was Cbz-protected⁴³ **115c** with benzyl chloroformate following a standard procedure (Scheme 55).



Scheme 55: Representative reaction route to 3-substituted Cbz-amines

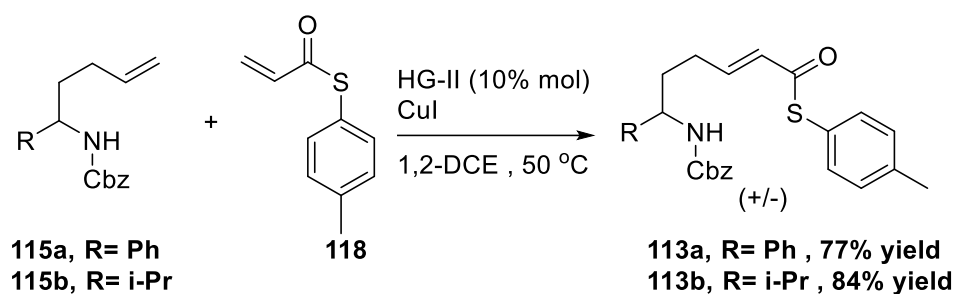
Following the successful synthesis of the 2,3-substituted Cbz-amines, the next step for the “Clip-Cycle” methodology was to make the activating group, the p-tolyl thioacrylate **118**.⁴⁴ The synthetic route proceeds with deprotonation of the thiol **119** by treating it with sodium borohydride and 15% sodium hydroxide to form the sodiated salt of p-thiocresol **125**. The reaction was stirred in room temperature for 3 hours and sodium borohydride used to prevent the formation of disulfides. To this, a solution of acryloyl chloride and 2,4,6-butylated hydroxytoluene (BHT) dissolved in cyclohexane was added and the reaction was stirred for 35 min at 55 °C. The addition of BHT helped prevent radical polymerization of the thioester through oxidation of thiol and the p-tolyl thioester was obtained in moderate yield (Scheme 56).



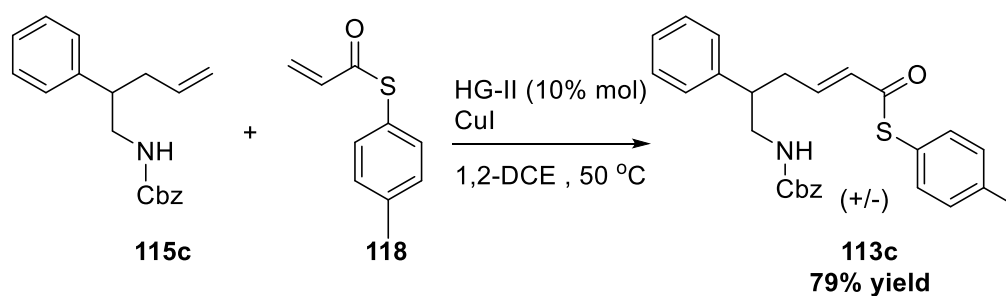
Scheme 56: Synthesis of the thioacrylic acid S-p-tolyl ester

With the synthesis of the thioacrylate **118** and the Cbz-amines **115a-c** complete, the synthesis of the cyclisation precursors **113a**, **113b** and **113c** was attempted *via* an alkene cross metathesis reaction⁴⁵ (Scheme 57, Scheme 58). The reaction conditions have already been optimized within the Clarke group⁴⁶ and the synthesis of the precursors was successful. The unsaturated Cbz-amines **115a**, **115b**, **115c** were “clipped” in a 1:3 ratio with the thioester **118** using Hoveyda

Grubbs II catalyst (10 mol%) **126** and Copper(I) iodide (1 eq) as a co-catalyst in 1,2-dichloroethane (1,2-DCE) at 50 °C to yield the cyclisation precursors **113a-c**.



Scheme 57: Cross metathesis reaction for 2-substituted precursors



Scheme 58: Cross metathesis reaction for 3-substituted precursor

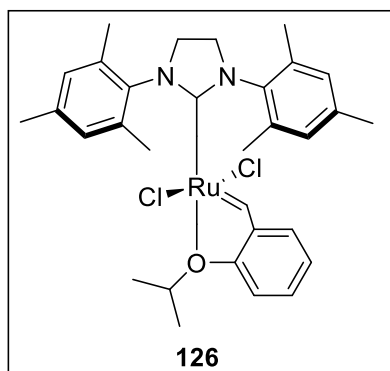
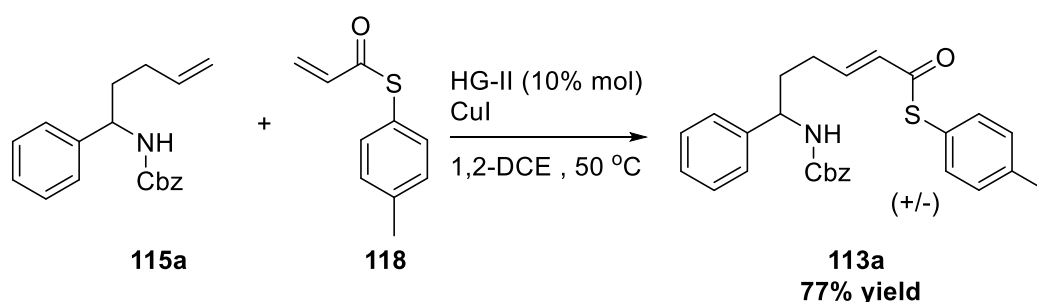


Figure 10: Hoveyda Grubbs II Catalyst

A key part of this project was the asymmetric cyclisation using chiral phosphoric acids and determination of the enantioselectivities of the pyrrolidine products. Therefore, it was necessary to investigate the conditions required to resolve these mixtures. Chiral chromatography refers to the separation of enantiomers using an HPLC column that is packed with a chiral stationary phase. The enantiomers are separated based on the interactions that occur during their exposure to the chiral stationary phase. The stronger the interactions between the enantiomers and the polar stationary phase the longer the elution time. The interaction strength depends on the functional groups of the enantiomers structure, with more polarized groups (*e.g.*, hydroxyl-) and groups capable of hydrogen bonding inducing more retention. Each compound was resolved using various columns (CHIRALPAK IA/IB/IC/IG), and using different eluent concentrations

(hexane:isopropyl alcohol (IPA)) , flow rates and temperatures as the shown in the figures and table below (Figures 11-13, Table 10-15).

Firstly, the synthesis of 2-phenyl-substituted precursor **113a** started from using 1 eq of **115a** and 3 eq of **118** (Scheme 59). The resulted **113a** was yielded successfully after purification. Then attempts were made to resolve the two enantiomers of **113a** and it resolved successfully on IA column (40 °C), at 80:20 hexane:IPA, giving separation of enantiomers as two sharp peaks (Figure 11, Table 10-11). However, two equal 'unknown' peaks with retention times at approximately 9 min and 11 min seemed to appear in every HPLC trace as seen in the figure below. The 'unknown' peaks were separated and determined *via* mass spectrometry to be cyclized product **114a** of the **113a** precursor. However, the **114a** had already been purified by flash column chromatography and analyzed by NMR spectroscopy (^1H , ^{13}C), showing no cyclized product present. That unusual cyclisation effect was tried to be explained and different suggestions were given. One suggested that the precursor was cyclizing inside the HPLC chiral column. The HPLC columns that were used are CHIRALPAK immobilized columns and the chiral stationary phases are amylose-based. Interactions between the polysaccharide stationary phase and the precursor could lead to cyclisation. Another suggestion was that the precursor was actually cyclizing in the solution of eluent, hexane:IPA, when preparing the HPLC sample. Isopropyl alcohol has the polar –OH group in its' molecule and it could cause intermolecular hydrogen bonding interactions with the precursor. In conclusion the solution of eluent upon preparing HPLC samples was needed to be changed to a less polar solvent, the dichloromethane to prevent the cyclisation.



Scheme 59: Cross metathesis reaction for **115a**

| Racemic Substrate | Column (CHIRALPAC) | Hexane:IPA | Flow rate (mL/min) | Temperature (°C) |
|-------------------|--------------------|------------|--------------------|------------------|
| 113a | IA | 80:20 | 1 | 40 |

Table 10: HPLC conditions of racemic **113a** precursor

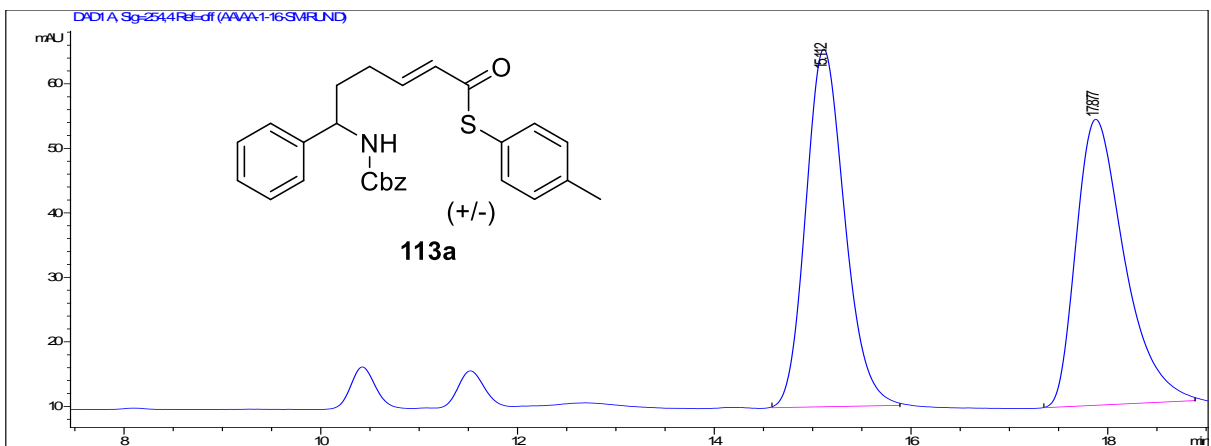
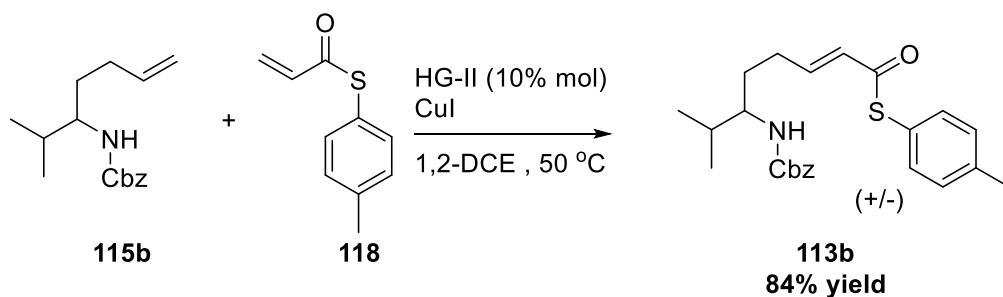


Figure 11: HPLC trace of **113a** precursor

| Racemic Substrate | Peak 1 (Retention time/ min) | Area% | Peak 2 (Retention time/ min) | Area% |
|-------------------|------------------------------|---------|------------------------------|---------|
| 114a | 10.421 | 2.9689 | 11.520 | 2.5287 |
| 113a | 16.112 | 46.8853 | 17.877 | 46.5204 |

Table 11: Retention times of **113a** precursor



Scheme 60: Cross metathesis reaction for **115b**

| Racemic Substrate | Column (CHIRALPAC) | Hexane:IPA | Flow rate (mL/min) | Temperature (°C) |
|-------------------|--------------------|------------|--------------------|------------------|
| 113b | IC | 80:20 | 1 | 40 |

Table 12: HPLC conditions of racemic **113b** precursor

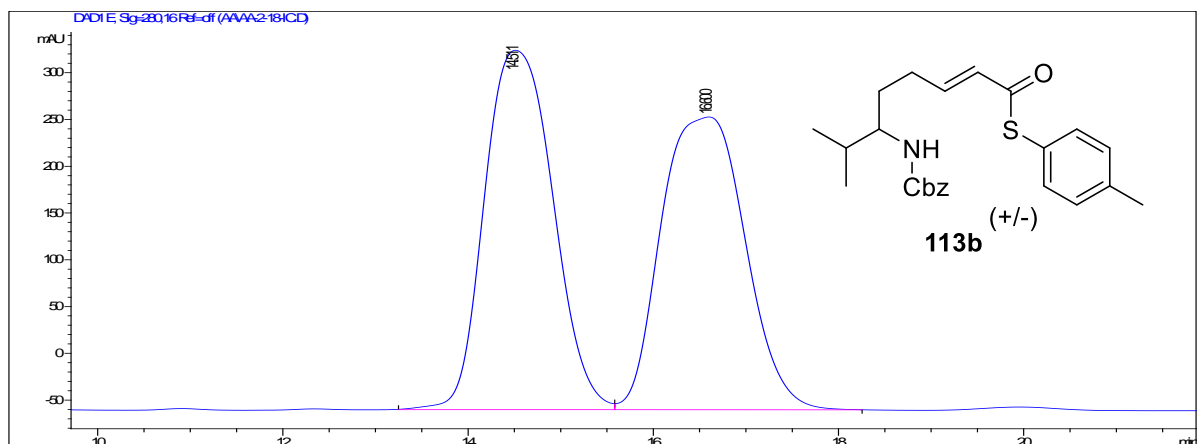
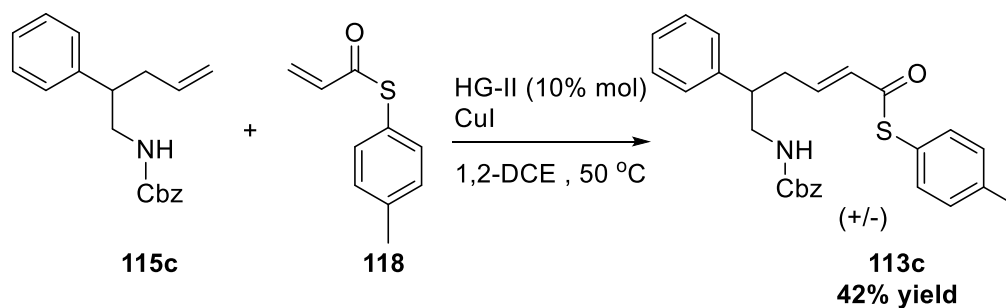


Figure 12: HPLC trace of **113b** precursor

| Racemic Substrate | Peak 1 (Retention time/ min) | Area% | Peak 2 (Retention time/ min) | Area% |
|-------------------|------------------------------|---------|------------------------------|---------|
| 113b | 14.511 | 33.5600 | 16.600 | 33.5070 |

Table 13: Retention times of **113b** precursor



Scheme 61: Cross metathesis reaction for **115c**

| Racemic Substrate | Column (CHIRALPAC) | Hexane:IPA | Flow rate (mL/min) | Temperature (°C) |
|-------------------|--------------------|------------|--------------------|------------------|
| 113c | IB | 80:20 | 1 | 40 |

Table 14: HPLC conditions of racemic **113c** precursor

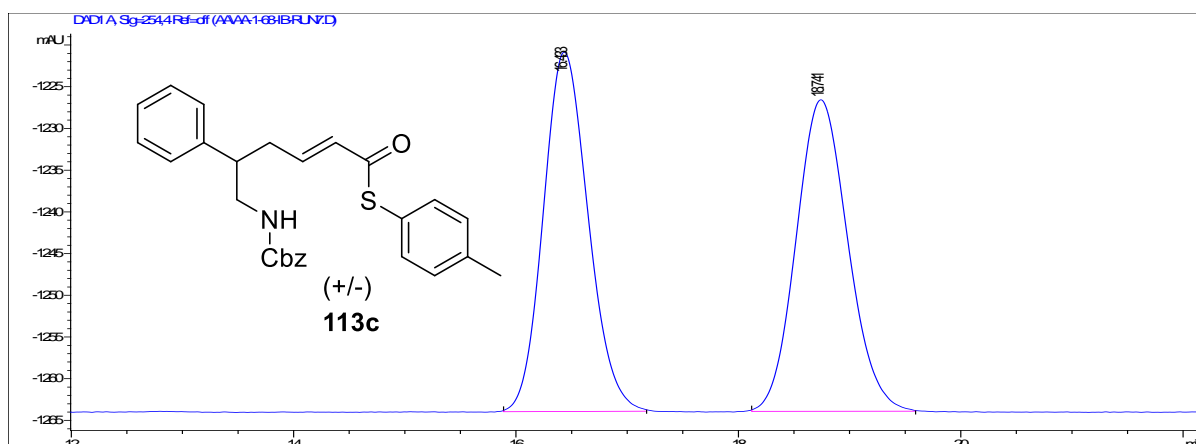


Figure 13: HPLC trace of **113c** precursor

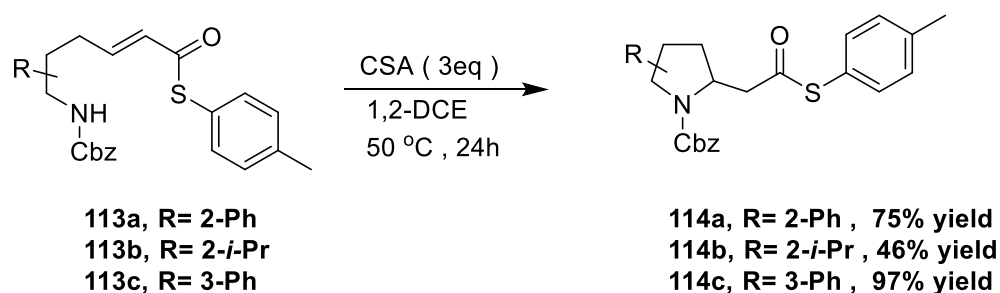
| Racemic Substrate | Peak 1 (Retention time/ min) | Area% | Peak 2 (Retention time/ min) | Area% |
|-------------------|------------------------------|---------|------------------------------|---------|
| 113c | 16.433 | 43.8099 | 18.741 | 43.7306 |

Table 15: Retention times of **113c** precursor

Following the encouraging results of the synthesis and analysis by chiral HPLC, the cyclisation precursors **113a-c** were subjected to cyclisation conditions under racemic and asymmetric conditions to study their enantioselectivities.

9.3 Brønsted Acid Catalyzed Cyclisation of Pyrrolidine Precursors

Based on previous projects within the Clarke group^{36,37}, the racemic cyclisation of the pyrrolidine precursors proceeded using camphorsulfonic acid (CSA) as the Brønsted acid. The protected amine nitrogen in the presence of a Brønsted acid proceeds to attack the β -position of the α,β -unsaturated thioester sidechain which forms the substituted pyrrolidines. The Brønsted acid catalysed cyclisation generates racemic products, which are used to form the substituted pyrrolidines used to screen chiral HPLC conditions. These are then used, to compare and measure the enantiomeric excess (% ee) of the pyrrolidines formed under asymmetric conditions using chiral Brønsted acid catalysts. The cyclisations of **113a-c** were attempted with an excess of 3 eq CSA using 1, 2-DCE as solvent and were carried out at 50 °C for 24h (Scheme 62).

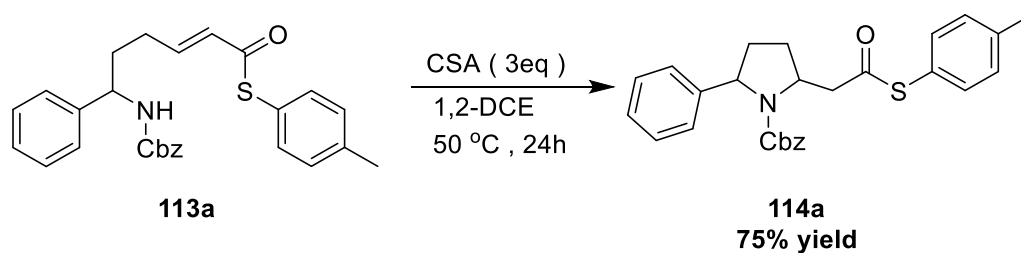


Scheme 62: Cyclisation of **113a-c** precursors using CSA

Following the synthesis of the substituted pyrrolidines **114a-c**, the racemic products were analyzed using chiral HPLC to resolve the enantiomers. Similar to resolving the enantiomers of their precursors, the pyrrolidines were subjected to various concentrations of the eluents (Hexane:IPA) and various chiral chromatography columns (CHIRALPAC IA/IB/IC/IG). The conditions used for each substituted pyrrolidine are summarized in the table and figures below. (Figure 14-16, Table 16-21).

The two enantiomers of the 2-phen-substituted pyrrolidine **114a** appear as two equal peaks with retention times at 10 and 12 minutes respectively and it confirms the previous observation that the 2-phen-precursor cyclized in the eluent solution (Figure 14). One more interesting observation was made upon trying to resolve the 3-phen-pyrrolidine **114c**. Looking at the HPLC trace, the second sharp peak at 8.7 minutes has a small 'shoulder' underneath and one smaller peak appears at approximately 11.5 minutes. This hints that perhaps the four peaks correspond to the

four diastereomers and they were showing up on the HPLC trace upon resolution, but this observation was not proven (Figure 16).



Scheme 63: Cyclisation of **113a** precursor using CSA

| Racemic Substrate | Column (CHIRALPAC) | Hexane:IPA | Flow rate (mL/min) | Temperature (°C) |
|-------------------|--------------------|------------|--------------------|------------------|
| 114a | IA | 80:20 | 1 | 40 |

Table 16: HPLC conditions of racemic **114a** pyrrolidine

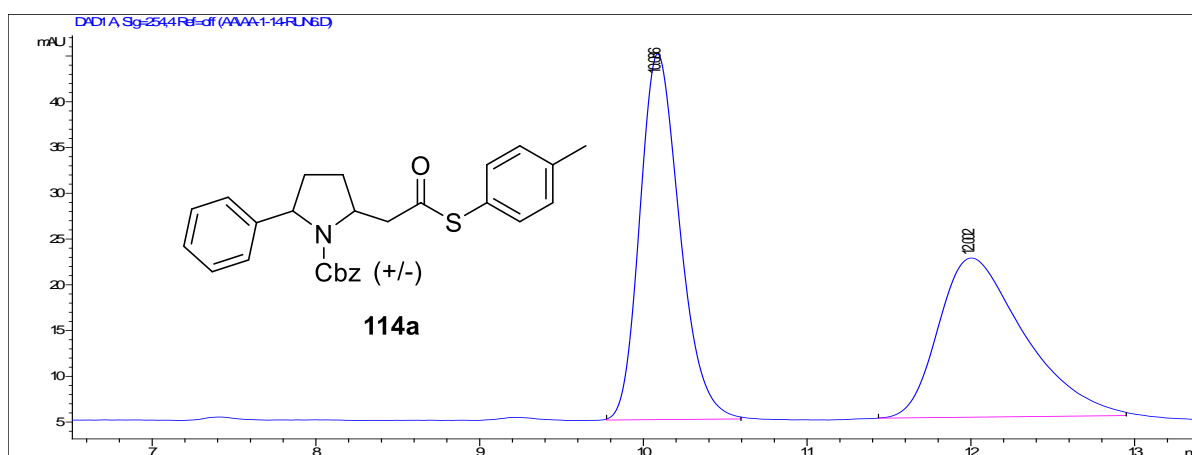
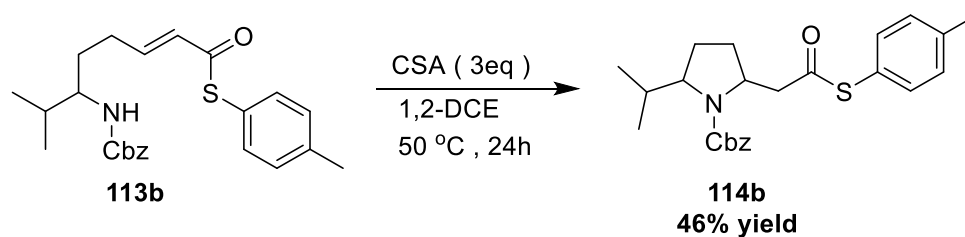


Figure 14: HPLC trace of racemic **114a** pyrrolidine

| Racemic Substrate | Peak 1 (Retention time/ min) | Area% | Peak 2 (Retention time/ min) | Area% |
|-------------------|------------------------------|---------|------------------------------|---------|
| 114a | 10.086 | 51.6233 | 12.002 | 48.3767 |

Table 17: HPLC retention times of racemic **114a** pyrrolidine



Scheme 64: Cyclisation of precursor **113b** using CSA

| Racemic Substrate | Column (CHIRALPAC) | Hexane:IPA | Flow rate (mL/min) | Temperature (°C) |
|-------------------|--------------------|------------|--------------------|------------------|
| 114b | IC | 80:20 | 1 | 40 |

Table 18: HPLC conditions of racemic **114b** pyrrolidine

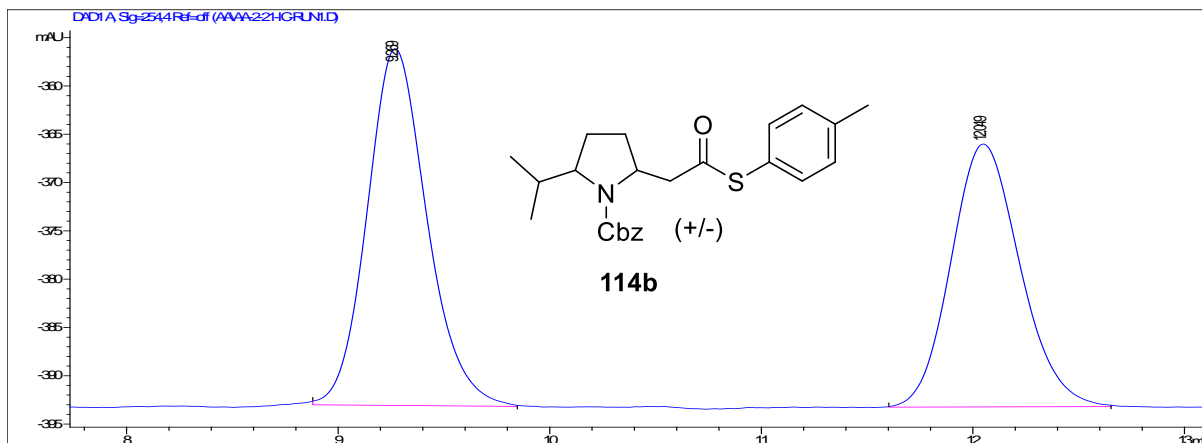
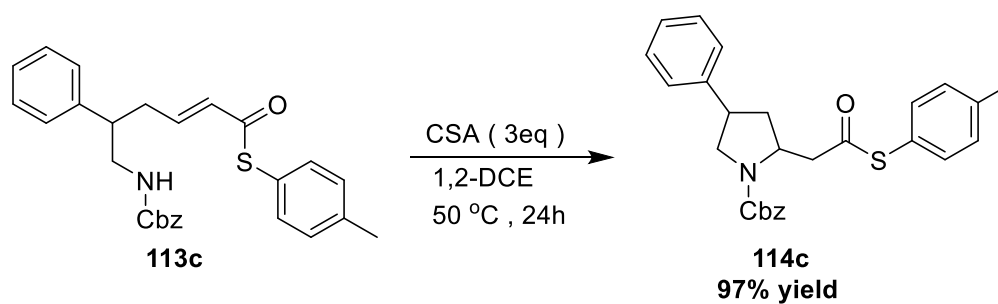


Figure 15: HPLC trace of racemic **114b** pyrrolidine

| Racemic Substrate | Peak 1 (Retention time/ min) | Area% | Peak 2(Retention time/ min) | Area% |
|-------------------|------------------------------|---------|-----------------------------|---------|
| 114b | 9.269 | 45.7837 | 12.048 | 38.8365 |

Table 19: HPLC retention times of racemic **114b** pyrrolidine



Scheme 65: Cyclisation of **113c** precursor using CSA

| Racemic Substrate | Column (CHIRALPAC) | Hexane:IPA | Flow rate (mL/min) | Temperature (°C) |
|-------------------|--------------------|------------|--------------------|------------------|
| 114c | IB | 80:20 | 1 | 40 |

Table 20: HPLC conditions of racemic **114c** pyrrolidine

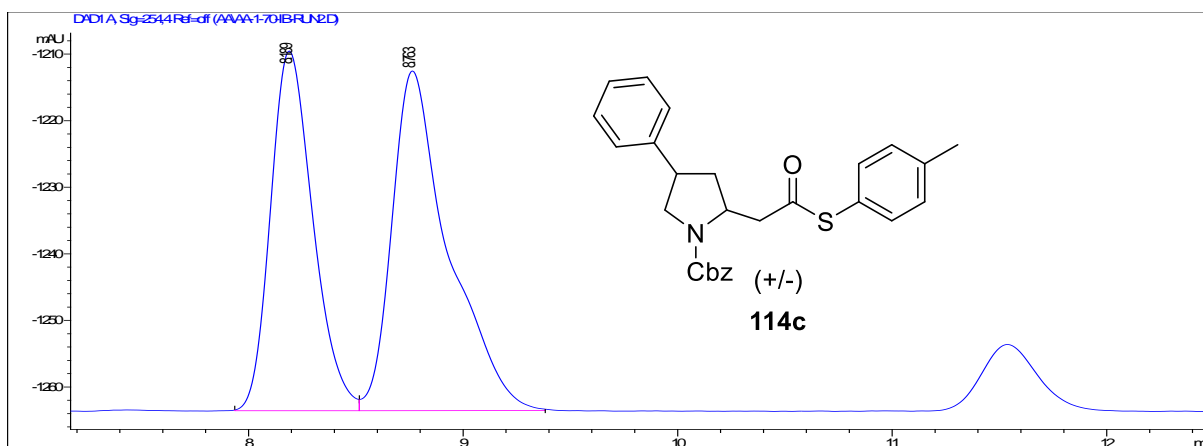


Figure 16: HPLC trace of racemic **114c** pyrrolidine

| Racemic Substrate | Peak 1 (Retention time/ min) | Area% | Peak 2 (Retention time/ min) | Area% |
|-------------------|------------------------------|---------|------------------------------|---------|
| 114c | 8.189 | 39.9611 | 8.763 | 50.2605 |

Table 21: HPLC retention times of racemic **114c** pyrrolidine

With the HPLC conditions for the three substituted **113a-c** precursors and their cyclized products **114a-c** set up, it was now possible to monitor the kinetic resolutions and observe the formation of the major enantiomer while the corresponding substrate enantiomer disappeared. Before subjecting the precursors to the asymmetric cyclisation conditions, HPLC samples that consisted of a mixture of **113a-c** precursor and cyclized product **114a-c** (1:1) were resolved. This provided the opportunity to visualize where each peak should be while monitoring the asymmetric reaction. In the asymmetric reaction catalyzed by a chiral phosphoric acid, starting material was being consumed while product was being formed as the reaction progresses over time. As a result, in an HPLC trace of an aliquot of the reaction four peaks should appear; the first two peaks correspond to the cyclisation product and the following two peaks are the enantiomers of precursors. The cyclisation precursors are more polar than the cyclisation products due to the N-H group in their structure that is capable of hydrogen bonding with the stationary phase of the HPLC column and that agrees with the longer retention times. The three following HPLC traces were in agreement with the separated HPLC traces of cyclisation precursors and cyclisation products and the retention times match for each one of them. As expected, two equal peaks that corresponded to the racemic cyclisation products followed by two equal peaks of the racemic cyclisation precursors appeared in each HPLC trace (Figure 17-19, Table 22-25).

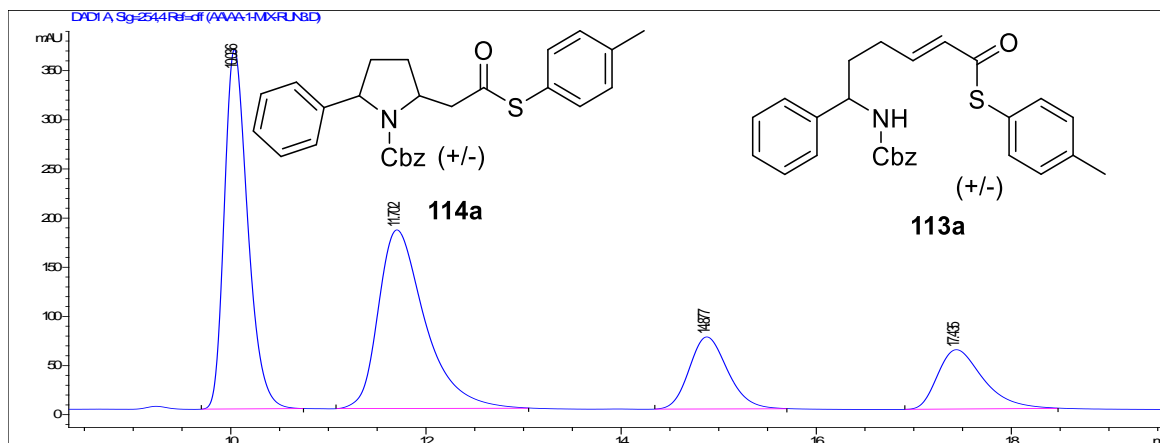


Figure 17: HPLC trace of racemic **113a** + racemic **114a**

| Racemic Substrate | Peak 1 (Retention time/ min) | Area% | Peak 2 (Retention time/ min) | Area% |
|-------------------|------------------------------|---------|------------------------------|---------|
| 114a | 10.036 | 37.7868 | 11.702 | 37.5270 |
| 113a | 14.887 | 12.4931 | 17.435 | 12.1930 |

Table 22: HPLC retention times of racemic **114a** pyrrolidine and racemic **113a** precursor

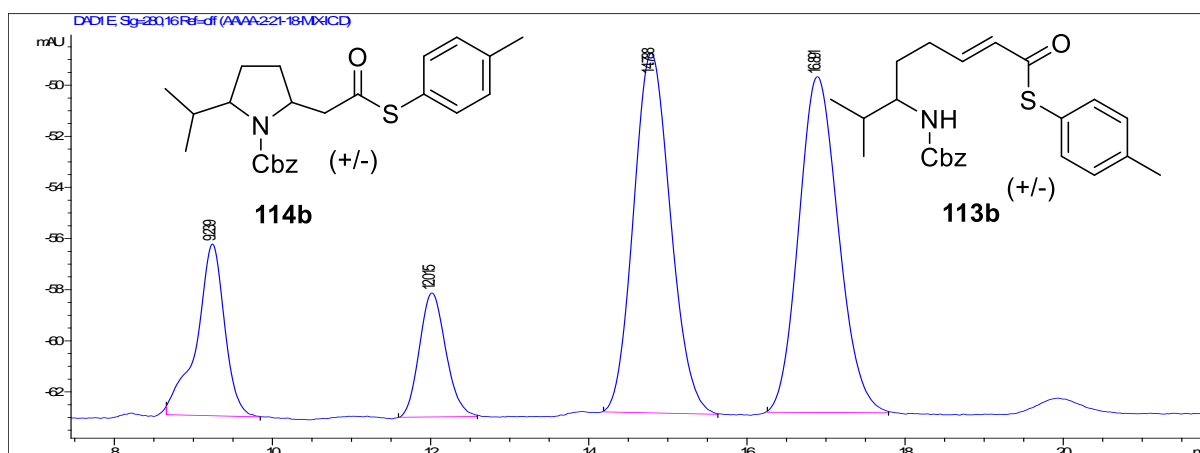


Figure 18: HPLC trace of racemic **113b** + racemic **114b**

| Racemic Substrate | Peak 1 (Retention time/ min) | Area% | Peak 2 (Retention time/ min) | Area% |
|-------------------|------------------------------|---------|------------------------------|---------|
| 114b | 9.230 | 3.4393 | 12.018 | 2.0902 |
| 113b | 14.765 | 16.1362 | 16.849 | 16.0152 |

Table 23: Table: HPLC retention times of racemic **114b** pyrrolidine and racemic **113b** precursor

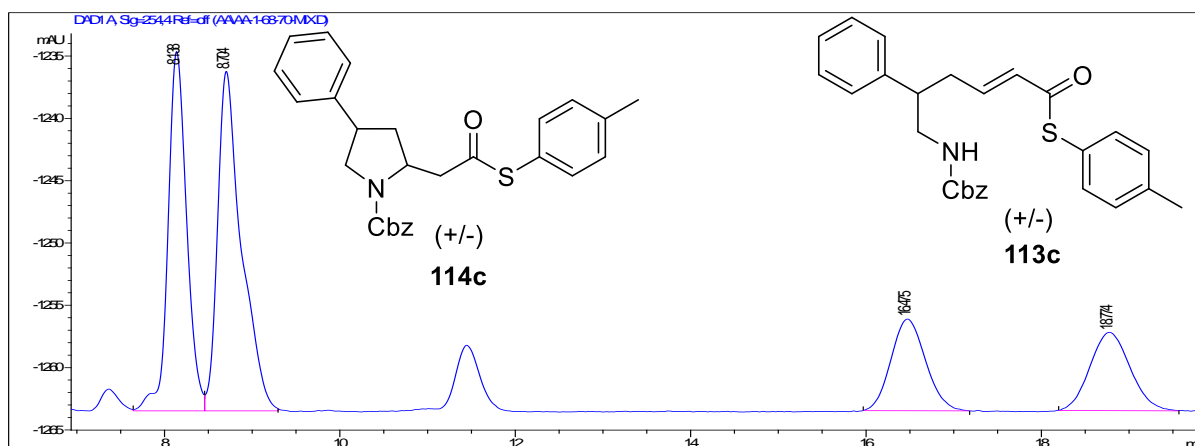


Figure 19: HPLC trace of racemic **113c** and racemic **114c**

| Racemic Substrate | Peak 1 (Retention time/ min) | Area% | Peak 2 (Retention time/ min) | Area% |
|-------------------|------------------------------|---------|------------------------------|---------|
| 114c | 8.138 | 30.0749 | 8.704 | 35.8024 |
| 113c | 16.475 | 17.0817 | 18.774 | 17.0411 |

Table 24: HPLC retention times of racemic **114c** pyrrolidine and racemic **113c** precursor

| Racemic Substrate | Column (CHIRALPAC) | Hexane:IPA | Flow rate (mL/min) | Temperature (°C) |
|--------------------|--------------------|------------|--------------------|------------------|
| 113a + 114a | IA | 80:20 | 1 | 40 |
| 113b + 114b | IC | 80:20 | 1 | 40 |
| 113c + 114c | IB | 80:20 | 1 | 40 |

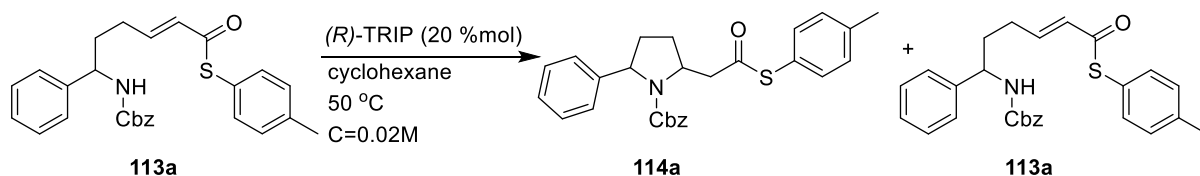
Table 25: HPLC conditions of racemic mixtures **113a-c**, **114a-c**

9.4 Kinetic Resolutions of the Pyrrolidine Precursors

The cyclisation **113a-c** precursors were subjected to asymmetric kinetic resolutions using chiral phosphoric acids (CPA) as the chiral Brønsted acid catalysts. For this purpose of study, (*R*)-TRIP was used as the catalyst and cyclohexane as the solvent based on studies upon pyrrolidine substrates within the Clarke group³⁷. It was found that (*R*)-TRIP and non-polar solvents like cyclohexane gave higher %ee's and %yields compared to polar solvents like 1,2-DCE. The concentration of all the asymmetric reactions was kept at 0.02M with a catalyst loading of 20 mol%. The conversion and %ee of the reaction were monitored at regular intervals using HPLC until conversion reached 50%. While following the evolution of the enantiomeric excess and the conversion, kinetic profiles for both the starting material and the product were built. During the asymmetric (*R*)-TRIP reactions, the same experimental procedure was followed: At regular

intervals, aliquots (0.1 – 0.2 mL) were obtained, quenched with a few drops of triethylamine and filtered through a microscale (pipette) column before being analysed by HPLC. These analyses allowed the monitoring of the formation of the products and the consumption of the starting materials through the time. Triple measurements analyzed by HPLC of each aliquot were taken and averaged. Once the reactions reached 50% conversion, they were quenched with triethylamine, and both enantioenriched product **114a-c** and recovered starting material **113a-c** were separated using flash column chromatography on silica and analysed by HPLC. The initial attempts of the kinetic resolutions were based on another kinetic resolutions' project in the Clarke group that involved asymmetric synthesis of tetrahydropyrans and tetrahydrofurans³⁶ using chiral Brønsted acid as catalysts; (*R*)-TRIP was used as catalyst in cyclohexane and the reaction was done at 50 °C. The investigation began using these set of conditions. The background work based on this project though, relates to enantioselective synthesis of spirocyclic pyrrolidines³⁷ and the asymmetric reactions were done in higher temperature, at 80 °C. For those reasons, the kinetic resolutions of our substrates were attempted at two different temperatures, 50 °C and 80 °C.

The study began with the **113a** precursor (28.0 mg) using (*R*)-TRIP (20 mol %), cyclohexane as solvent, at 50 °C and the concentration kept at 0.02M (Scheme 66, Table 26, Figure 20-21). The reaction's conversion and %ee were monitored by HPLC and aliquots were taken every 2 hours.



Scheme 66: Kinetic resolution of **113a** using 20 %mol (*R*)-TRIP at 50 °C

| T(h) | %Conversion | | %ee | |
|------|-------------|----------|----------|-----------|
| | %P | %SM | %P | %SM |
| 0 | 0 | 100 | 0 | 0 |
| 1 | 12.81709 | 87.18291 | 54.07733 | 13.228746 |
| 3 | 23.60179 | 76.39821 | 68.3402 | 32.470571 |
| 5 | 33.52804 | 66.47196 | 72.07738 | 52.617081 |
| 7 | 41.08277 | 58.91723 | 71.31912 | 70.716787 |
| 9 | 52.04752 | 47.95248 | 69.02735 | 79.478799 |

Table 26: Conversion and %ee of Starting Material **113a** and Product **114a**

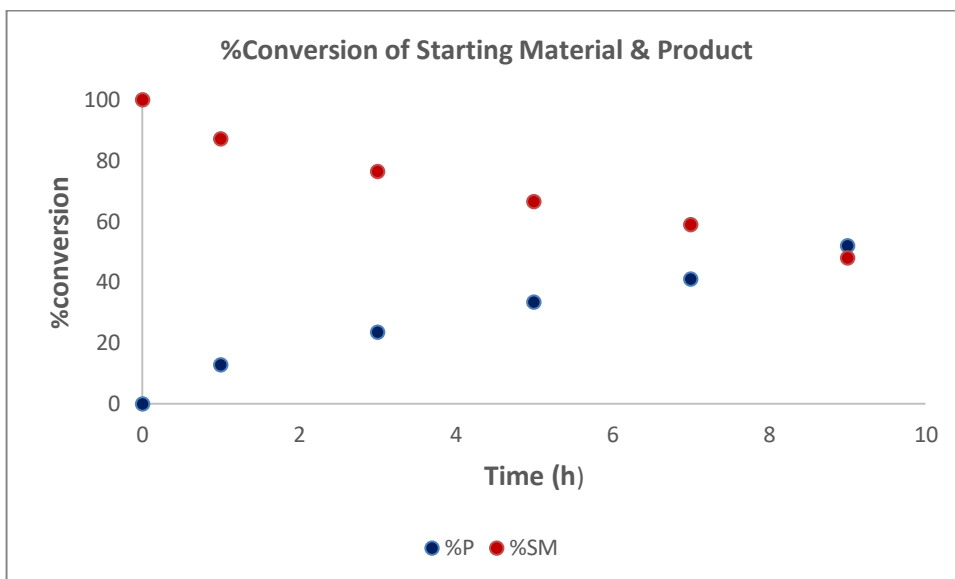


Figure 20: Conversion of Starting Material **113a** and Product **114a**

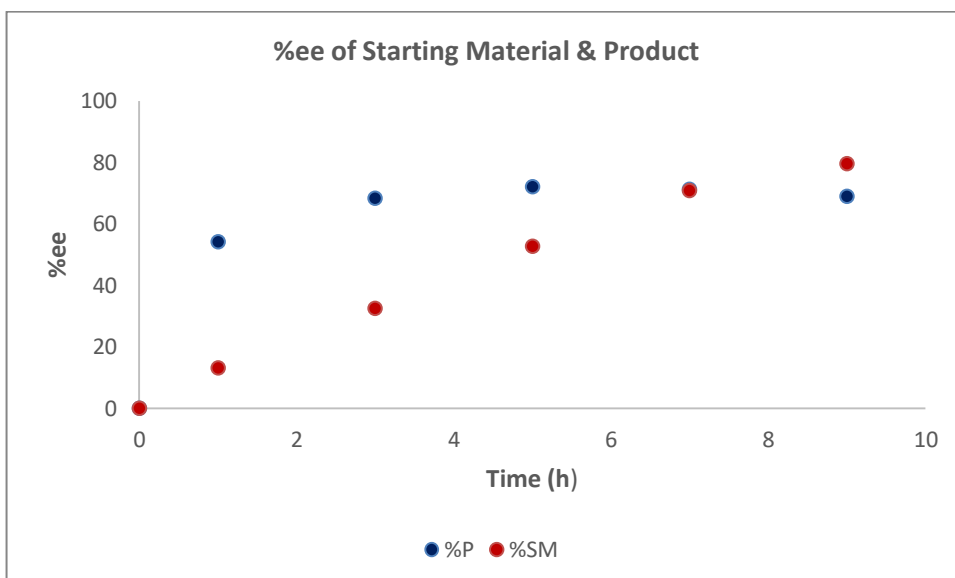
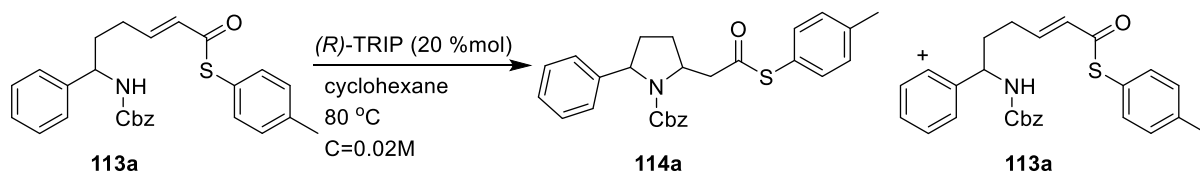


Figure 21: %ee of Starting Material **113a** and Product **114a**

The amount of starting material **113a** decreased gradually over a 9 hour period while products' increased smoothly. The reaction was quenched with trimethylamine upon both **113a** and **114a** were at ~50% conversion. Simultaneously, the starting material's enantioenrichment improved gradually to 80% after 9 h and the product's reached a maximum of 72% after 5 h but then began to decrease to 69%. This is due to the fact that the faster reacting enantiomer of the starting material is being consumed forming the desired product with high enantioselectivity; but when that is consumed, the slower reacting enantiomer starts interacting with the catalyst forming the other enantiomer of the product and that causes the enantioselectivity of the desired

enantioenriched product to drop. The quenched reaction mixture was purified with flash column chromatography and **113a** (5.8mg, 21% yield) and **114a** (3.8mg, 14% yield) were isolated. The %ee of the cyclized product should correspond to 69% and the starting material to 80%. To our delight, the ee of the **114a** (69%) and **113a** (81%) were within experimental error. The selectivity factor at 50% conversion of unreacted **113a** was calculated and resulted in a value of $s=32$.²⁸

Following the kinetic results on the **113a** precursor, the kinetic resolution was attempted at 80 °C using the same catalyst loading, solvent and concentration (30.0 mg of **113a**), and aliquots were taken every 30 minutes (Scheme 67).



Scheme 67: Kinetic resolution of **113a** using 20 %mol (R) -TRIP at 80 °C

| T(h) | %Conversion | | %ee | |
|------|-------------|----------|----------|----------|
| | %P | %SM | %P | %SM |
| 0 | 0 | 100 | 0 | 0 |
| 0.5 | 21.38624 | 78.61376 | 40.73134 | 23.26898 |
| 1 | 24.212 | 75.788 | 48.2298 | 26.97116 |
| 1.5 | 42.21684 | 57.78316 | 60.85804 | 58.66683 |
| 2 | 44.31505 | 55.68495 | 58.87981 | 74.86612 |
| 2.5 | 48.04446 | 51.95554 | 57.36853 | 83.99958 |
| 3 | 49.07859 | 50.92141 | 56.1521 | 87.44376 |
| 3.5 | 50.84661 | 49.15339 | 54.85008 | 91.65985 |

Table 27: Conversion and %ee of Starting Material **113a** and Product **114a**

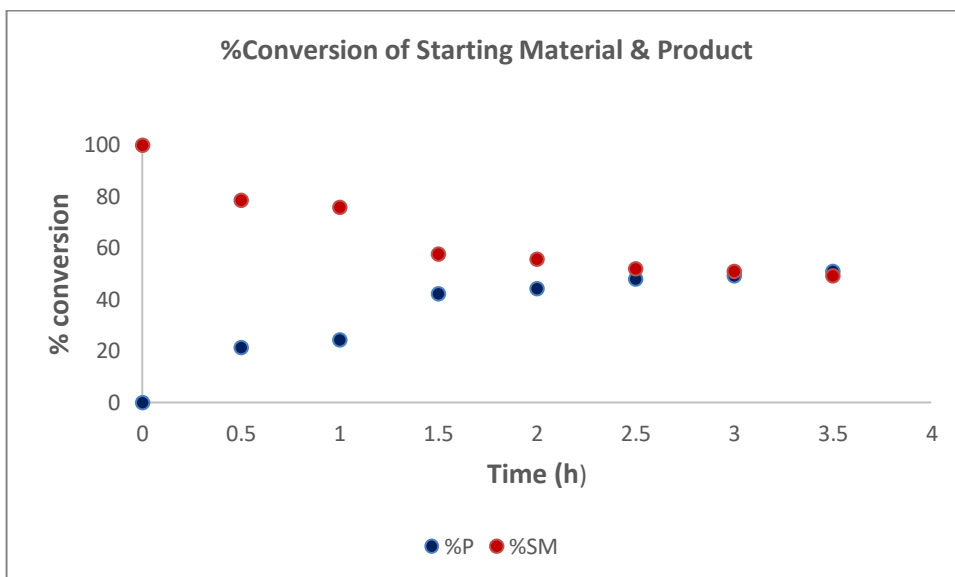


Figure 22: Conversion of Starting Material **113a** and Product **114a**

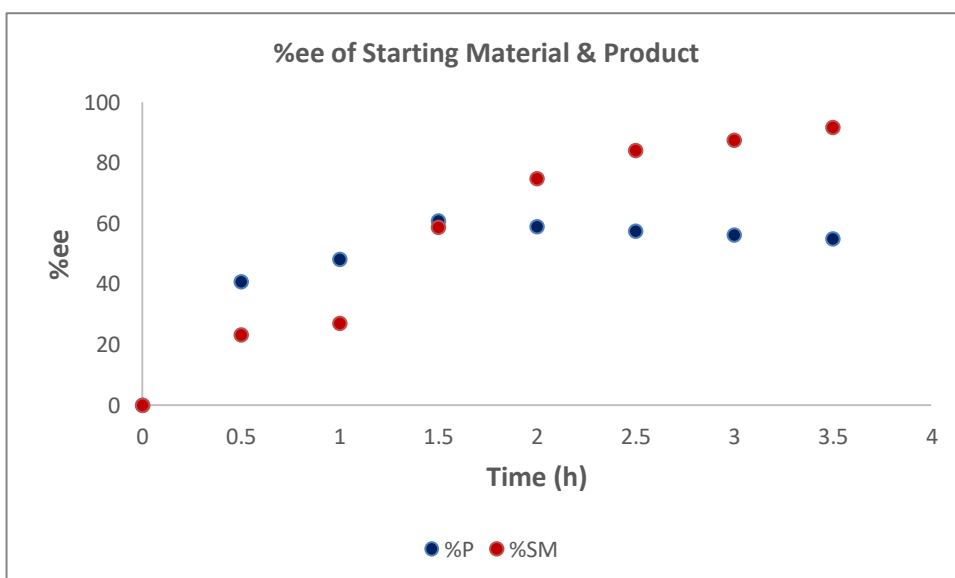


Figure 23: %ee of Starting Material **113a** and Product **114a**

A similar pattern of the initial reaction was observed, the amount of starting material decreased evenly to 49% and the reaction was then quenched. The **113a** decreased gradually over a 3 hour period while products' increased smoothly and the reaction was quenched upon both **113a** and **114a** were at 50% conversion. At the same it, the **113a** enantioenrichment reached 91% after 3.5 h and the product's reached 60% within 1.5 hours, but decreased to 54% upon 50% conversion as the slower reacting enantiomer started being formed. The quenched reaction mixture was purified with flash column chromatography and **113a** (5.6mg, 19% yield) and **114a** (4.9mg, 17% yield) were separated and analysed by HPLC with %ee's that corresponded to 91% and 51% respectively and these values were between experimental error (Figure 24-25). The HPLC traces

were compared to the corresponding racemic products from both starting material and product. The major product enantiomer peak appeared at 11 min, while the starting material's major enantiomer appeared at 16 min. The selectivity factor at 50% conversion of unreacted **113a** was $s=122$.

| Enantioenriched Substrate | Column (CHIRALPAC) | Hexane:IPA | Flow rate (mL/min) | Temperature (°C) |
|---------------------------|--------------------|------------|--------------------|------------------|
| 113a+114a | IA | 80:20 | 1 | 40 |

Table 28: HPLC conditions of enantioenriched **113a+114a**

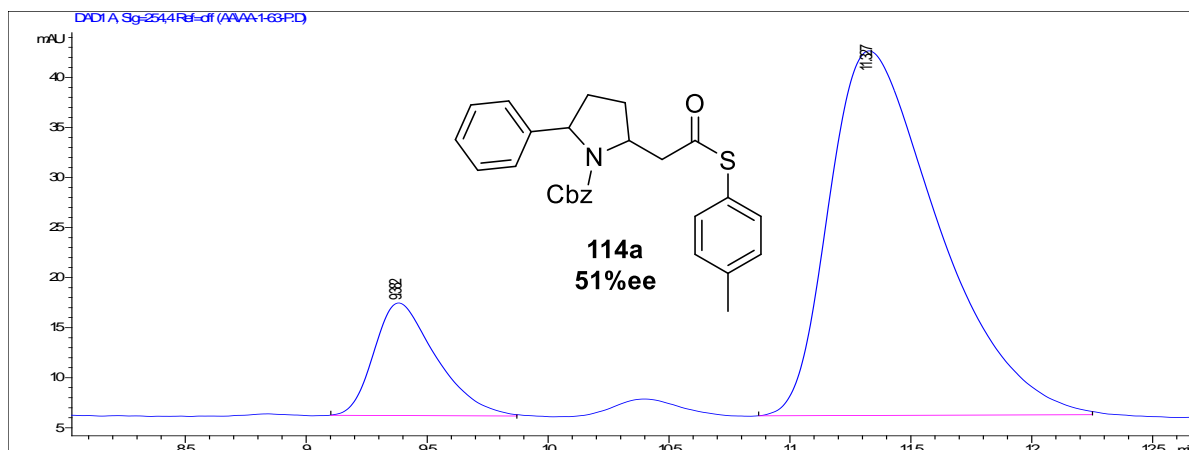


Figure 24: HPLC trace of enantioenriched **114a**

| Enantioenriched Substrate | Minor Peak (Retention time/min) | Area% | Major Peak (Retention time/min) | Area% |
|---------------------------|---------------------------------|---------|---------------------------------|---------|
| 114a | 9.382 | 13.7030 | 11.327 | 77.8590 |

Table 29: HPLC retention times of enantioenriched **114a**

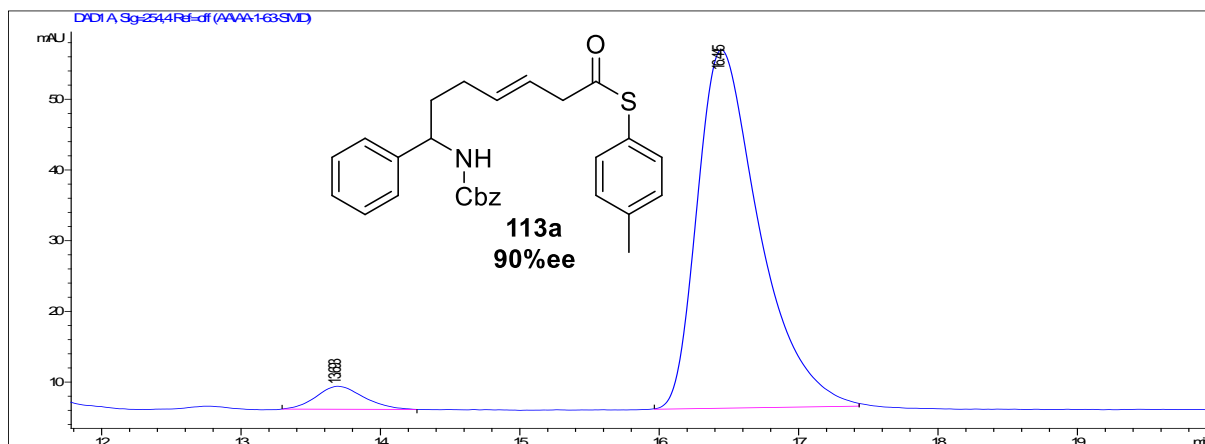
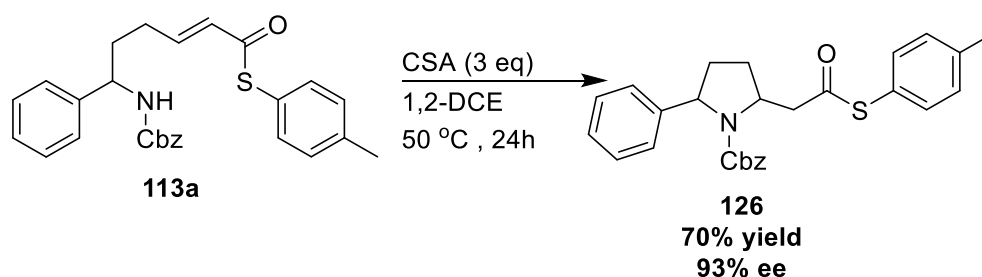


Figure 25: HPLC trace of enantioenriched **113a**

| Enantioenriched Substrate | Minor Peak (Retention time/min) | Area% | Major Peak (Retention time/min) | Area% |
|---------------------------|---------------------------------|--------|---------------------------------|---------|
| 113a | 13.693 | 3.3976 | 16.445 | 68.4589 |

Table 30: HPLC retention times of enantioenriched **113a**

Subsequently, the enantioenriched **113a** was further cyclised to give the opposite enantiomer *via* the Brønsted acid catalyzed cyclisation, using camphorsulfonic acid as the Brønsted acid (Scheme 68). The recovered **113a** was reacted with 3 eq of camphorsulfonic acid, in 1,2-dichloroethane and the reaction was heated at 50 °C. After 24 h, the reaction was quenched with sodium bicarbonate solution, followed by purification with flash column chromatography and analysis with HPLC. The opposite enantiomer (6.0 mg) from that formed in the kinetic resolution reaction appeared at 9min and was obtained in good yield and in higher enantioselectivity (93%ee). The enantioselectivity of the opposite enantiomer **126** was comparable to the enantioselectivity of the recovered **113a** and no racemization of the stereocentre of **113a** appeared (Figure 26, Table 31-32).



Scheme 68: Cyclisation of enantioenriched **113a** using CSA

| Enantioenriched Substrate | Column (CHIRALPAC) | Hexane:IPA | Flow rate (mL/min) | Temperature (°C) |
|---------------------------|--------------------|------------|--------------------|------------------|
| 126 | IA | 80:20 | 1 | 40 |

Table 31: HPLC conditions of enantioenriched **126**

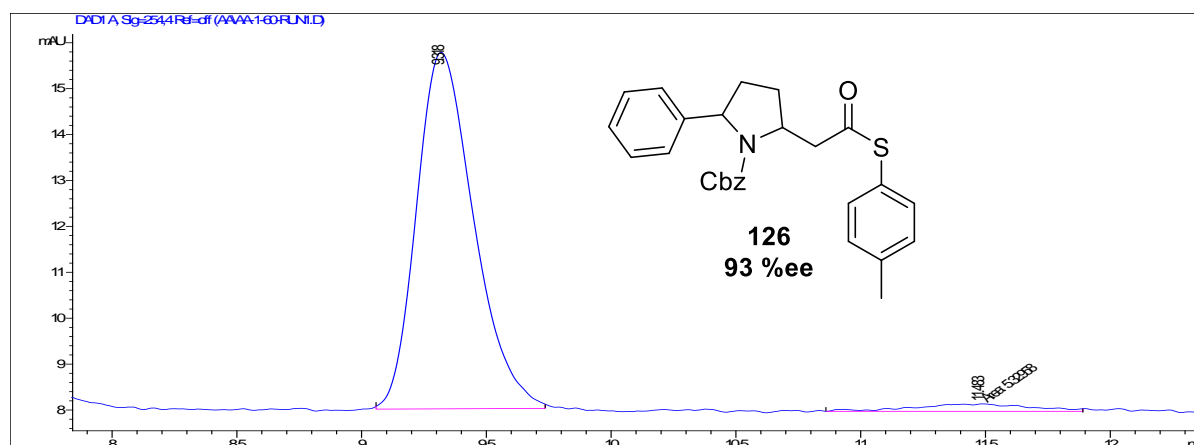


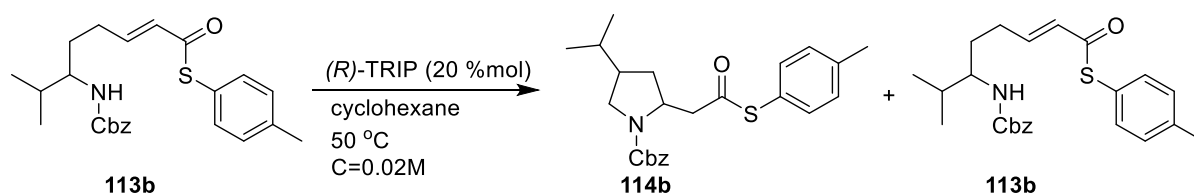
Figure 26: HPLC trace of enantioenriched **126**

| Enantioenriched Substrate | Major Peak (Retention time/min) | Area% | Minor Peak (Retention time/min) | Area% |
|---------------------------|---------------------------------|---------|---------------------------------|--------|
| 126 | 9.318 | 86.6953 | 11.483 | 2.9274 |

Table 32: HPLC retention times of enantioenriched **126**

Next, the kinetic resolution of 2-isopropyl-substituted **113b** precursor was attempted using (*R*)-TRIP at 50 °C and at 80 °C. The same experimental procedure was followed and reactions' conversion and %ee were monitored by HPLC (Scheme 69-70).

Starting with the asymmetric reaction at 50 °C, aliquots were taken every hour and some interesting observations were made. The amount of **113b** decreased gradually to 48% over a 7 h period while product's increased to reach 51% and the reaction was quenched with triethylamine. Quick enantioenrichment of **114b** was observed after 2 h, from 0 to 86%, yet it started decreasing as the reaction proceeded as the slower reacting enantiomer of starting material was also consumed. Upon 50% conversion, **114b** %ee reached 74% while **113b** enantioenrichment reached 61%. The quenched reaction mixture was purified with flash column chromatography and starting material and product were separated and analyzed by HPLC (Figure 27-28, Table 33). The calculated s-factor for unreacted **113b** at 50% conversion was s=8.



Scheme 69: Kinetic resolution of **113b** using 20 %mol (*R*)-TRIP at 50 °C

| T(h) | %Conversion | | %ee | |
|----------|-------------|----------|----------|----------|
| | %P | %SM | %P | %SM |
| 0 | 0 | 100 | 0 | 0 |
| 1 | 9.615817 | 90.38418 | 85.65735 | 8.73545 |
| 2 | 16.00781 | 83.99219 | 86.4917 | 16.44936 |
| 3 | 22.98422 | 77.01578 | 83.51349 | 26.60197 |
| 4 | 30.10243 | 69.89757 | 80.85213 | 36.43961 |
| 5 | 32.62789 | 67.37211 | 79.14571 | 45.24952 |
| 6 | 37.02069 | 62.97931 | 77.08291 | 54.17577 |
| 7 | 51.1251 | 48.8749 | 74.61255 | 61.10019 |

Table 33: Conversion and %ee of Starting Material **113b** and Product **114b**

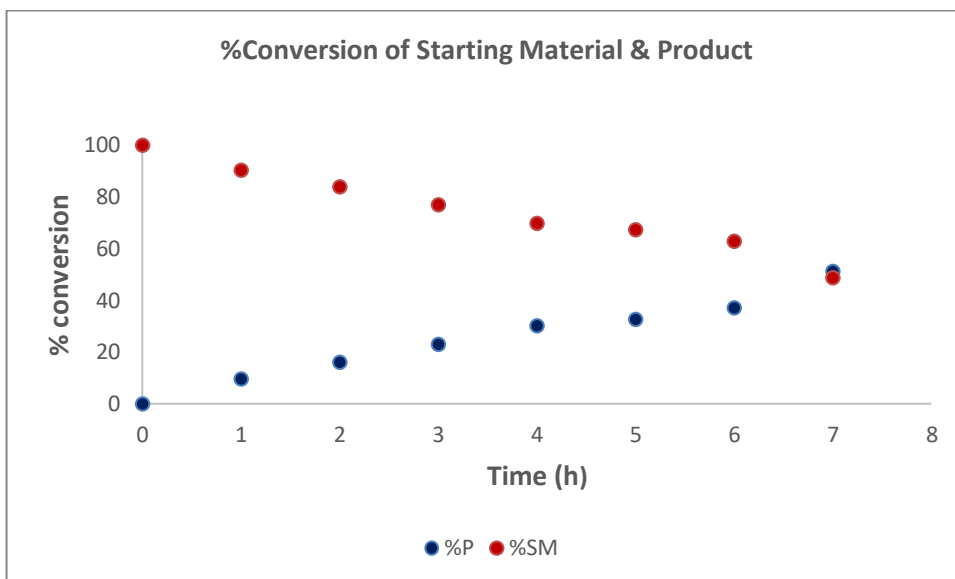


Figure 27: Conversion of Starting Material **113b** and Product **114b**

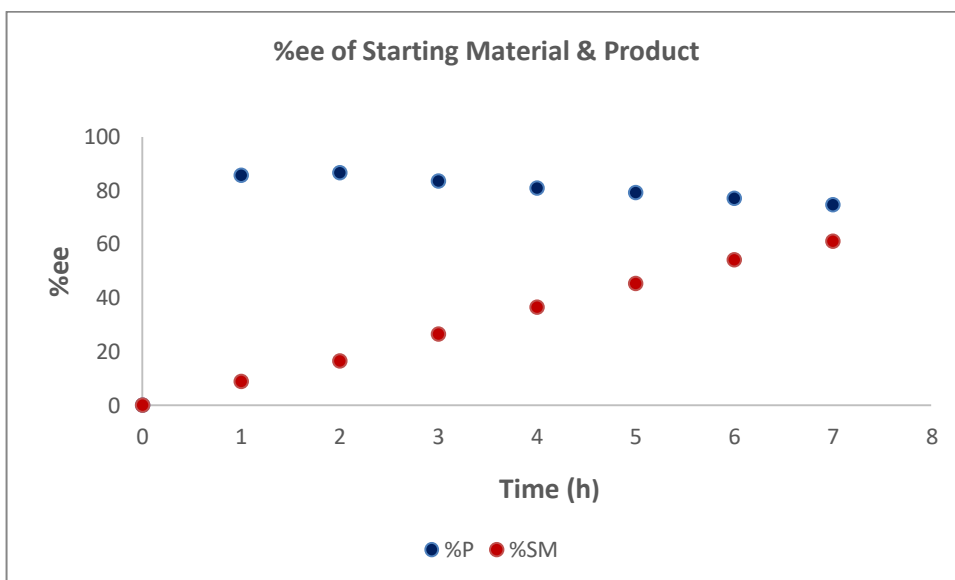
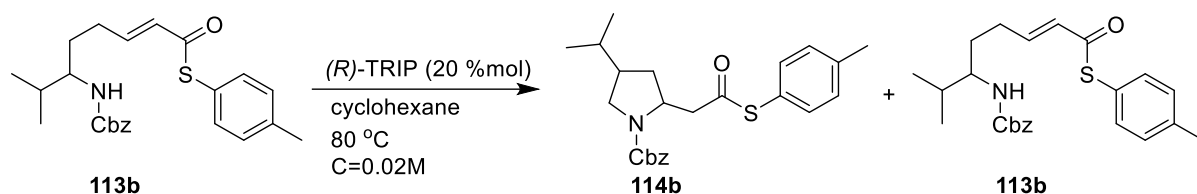


Figure 28: %ee of Starting Material **113b** and Product **114b**

For the asymmetric reaction of **113b** at 80 °C, aliquots were taken every 30 minutes and a similar pattern was observed. The amount of conversion of starting material decreased steadily to 51% within 3 hours and the reaction was quenched with triethylamine. The enantioenrichment of **114b** rapidly jumped from 0 to 90% within 30 minutes, but it reached 65% as the reaction proceeded to 50% conversion and enantioenrichment of **113b** was 70%. The quenched reaction mixture was purified with flash column chromatography and **113b** (23.0 mg, 35% yield) and **114b** (39.0 mg, 60% yield) were separated and analyzed by HPLC. The enantioenrichment of starting material and product corresponded to 74% and 63% respectively and the values were between

experimental errors. The HPLC traces were compared to the corresponding racemic products from both **113b** and **114b**. The major product enantiomer peak appeared at 9 min, while the starting material's major enantiomer appeared at 15 min (Figures 29-32, Table 34-36). The selectivity of unreacted **113b** at 50% conversion was $s=9$.



Scheme 70: Kinetic resolution of **113b** using 20 %mol (*R*)-TRIP at 80 °C

| T(h) | %Conversion | | %ee | |
|------|-------------|----------|----------|----------|
| | %P | %SM | %P | %SM |
| 0 | 0 | 100 | 0 | 0 |
| 0.5 | 12.08216 | 87.91784 | 90.38418 | 12.21585 |
| 1 | 25.58742 | 74.41258 | 77.76875 | 29.98132 |
| 1.5 | 31.68066 | 68.31934 | 76.65931 | 41.77613 |
| 2 | 36.73414 | 63.26586 | 74.07198 | 51.34859 |
| 2.5 | 47.33961 | 52.66039 | 70.98555 | 60.2819 |
| 3 | 48.04921 | 51.95079 | 65.06756 | 70.00516 |

Table 34: Conversion and %ee of Starting Material **113b** and Product **114b**

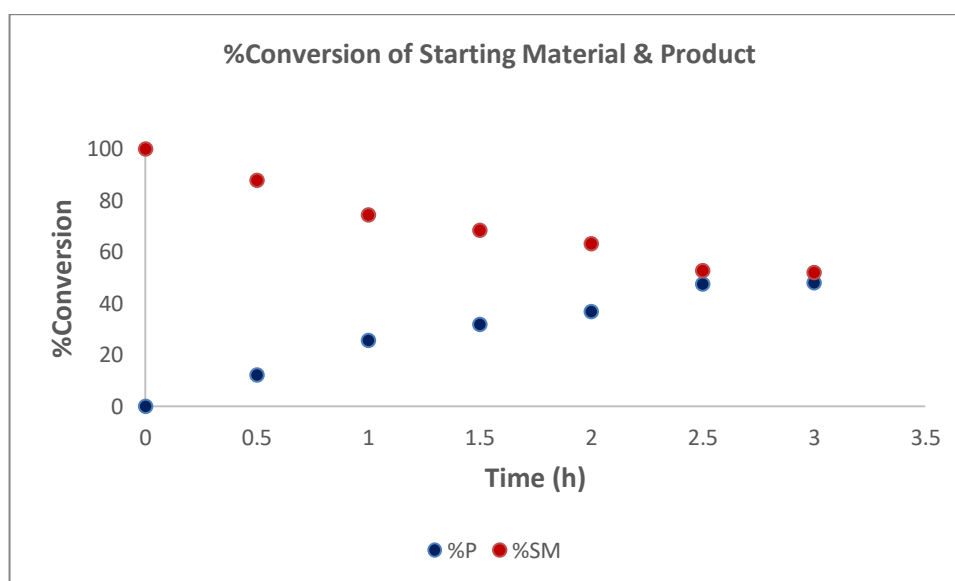


Figure 29: Conversion of Starting Material **113b** and Product **114b**

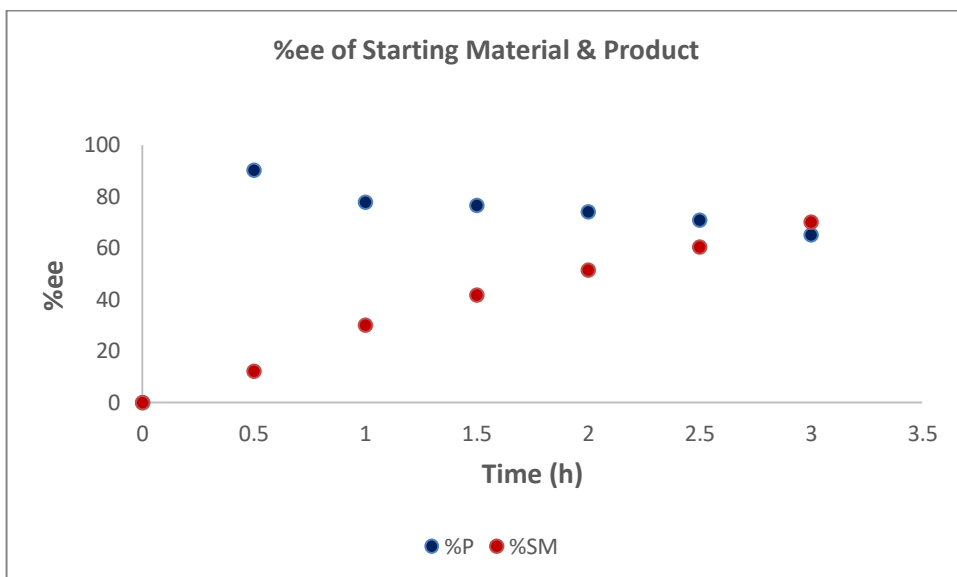


Figure 30: %ee of Starting Material **113b** and Product **113b**

| Enantioenriched Substrate | Column (CHIRALPAC) | Hexane:IPA | Flow rate (mL/min) | Temperature (°C) |
|---------------------------|--------------------|------------|--------------------|------------------|
| 113b + 114b | IC | 80:20 | 1 | 40 |

Table 35: HPLC conditions of enantioenriched **113b+114b**

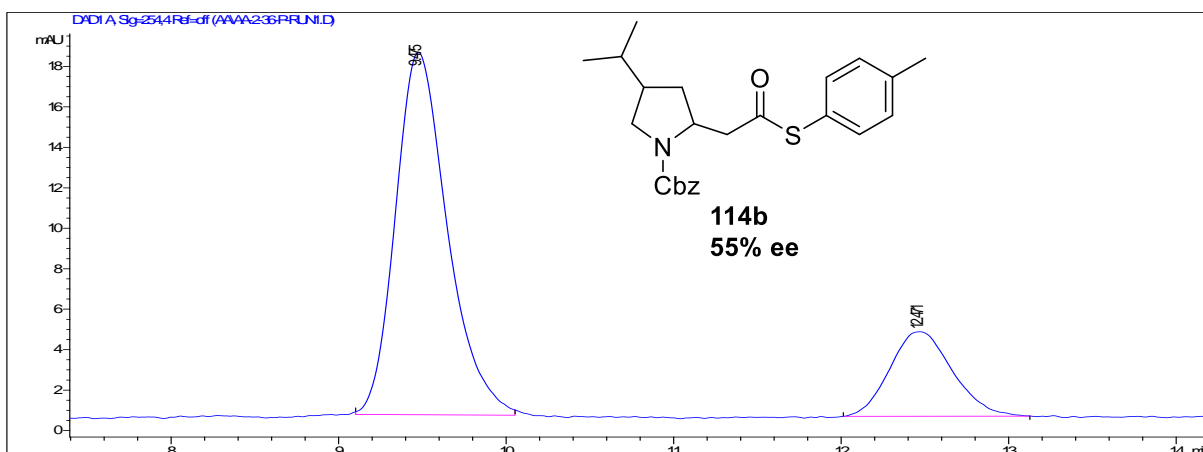


Figure 31: HPLC trace of enantioenriched **114b**

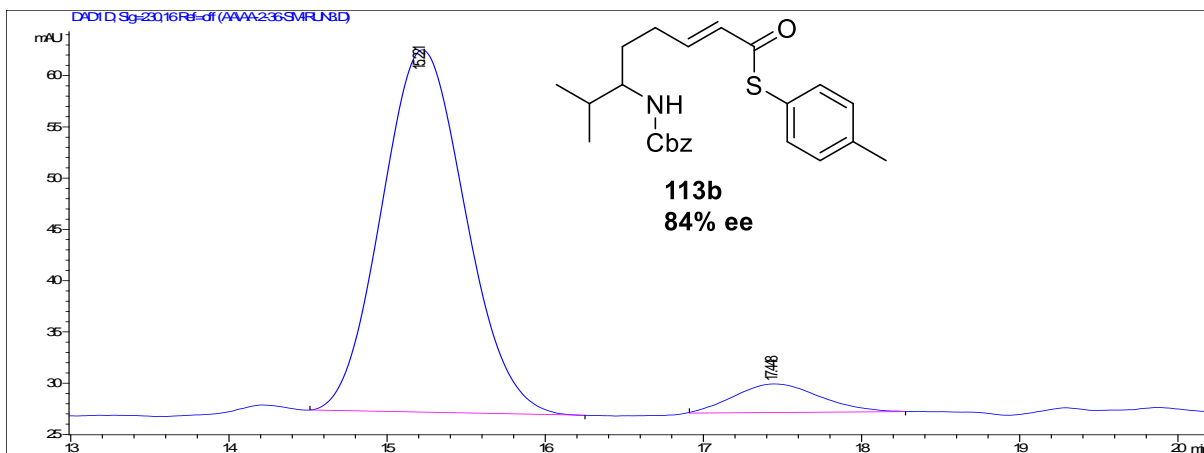


Figure 32: HPLC trace of enantioenriched **113b**

| Enantioenriched Substrate | Major Peak (Retention time/ min) | Area% | Minor Peak (Retention time/ min) | Area% |
|---------------------------|----------------------------------|---------|----------------------------------|---------|
| 114b | 9.475 | 45.0795 | 12.471 | 12.8108 |
| 113b | 15.221 | 80.0310 | 17.448 | 6.7495 |

Table 36: HPLC retention times of enantioenriched **113b+114b**

Furthermore, the opposite enantiomer was obtained in moderate yield and %ee. The enantioenriched **113b** was cyclised *via* the Brønsted acid catalyzed cyclisation, with 3 equivalents of camphorsulfonic acid in 1,2-dichloroethane at 50 °C (Scheme 71). After 24 h, the reaction was quenched with sodium bicarbonate solution, purified with flash column chromatography followed by analysis with HPLC. The opposite enantiomer **127** (8.0 mg) appeared at 12 min and was obtained in moderate yield and enantioselectivity (61% ee). In comparison with the enantiomer formed in the asymmetric kinetic reaction, the enantioselectivities of the opposite enantiomers are almost identical (63% ee for **114b**, 61% ee for **127**). A slight racemization of the enantioenriched recovered **113b** (74% ee) occurred that led to 61% ee of the product formed (Figure 33, Table 37-38).



Scheme 71: Cyclisation of enantioenriched **113b** using CSA

| Enantioenriched Substrate | Column (CHIRALPAC) | Hexane:IPA | Flow rate (mL/min) | Temperature (°C) |
|---------------------------|--------------------|------------|--------------------|------------------|
| 127 | IC | 80:20 | 1 | 40 |

Table 37: HPLC conditions of enantioenriched **127**

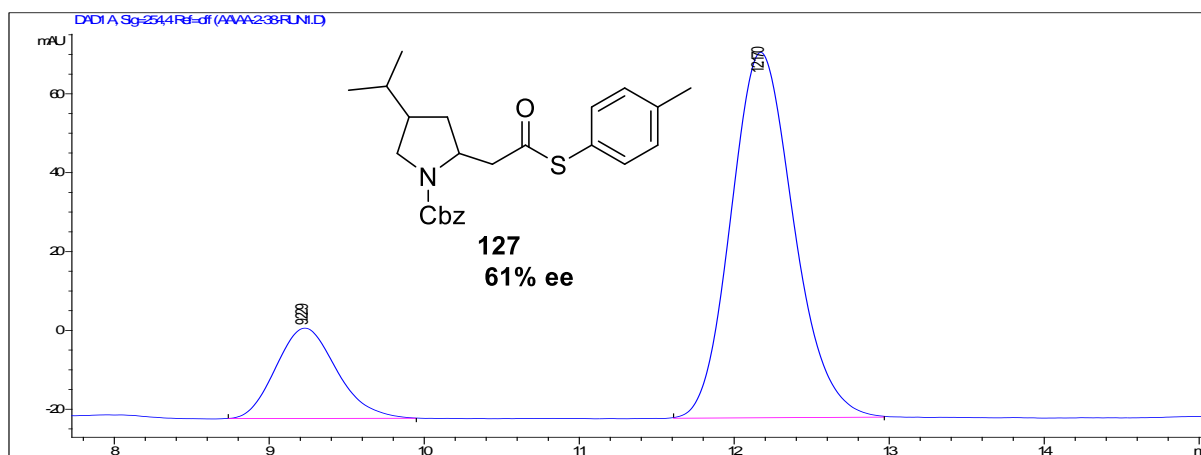
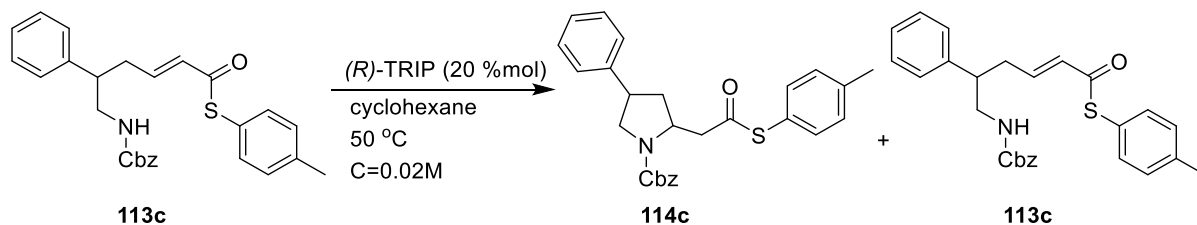


Figure 33: HPLC trace of enantioenriched **127**

| Enantioenriched Substrate | Minor Peak (Retention time/ min) | Area% | Major Peak (Retention time/ min) | Area% |
|---------------------------|----------------------------------|---------|----------------------------------|---------|
| 127 | 9.229 | 18.2519 | 12.170 | 75.7477 |

Table 38: HPLC retention times of enantioenriched **127**

The last set of kinetic resolutions was performed on the 3-phenyl substituted precursor **113c** (26mg). Similarly to the other substrates, (*R*)-TRIP and cyclohexane were used in different temperatures (50 °C and 80 °C) to study the enantioselectivity of the asymmetric reactions. However, when the temperature was set at 80 °C, the reaction proceeded too quickly for us to monitor. The conversion of **113c** dropped below 50% within the first hour of the reaction, making it difficult for us to monitor it. Following that, the asymmetric reaction was conducted at 50 °C; aliquots were taken every 30 minutes and analyzed by HPLC (Scheme 72, Figures 34-35, Table 39). The reaction was quenched with triethylamine after 5 hours, when 43% of **113c** was left. The enantioselectivity of product increased to 67% within the first hour, but decreased to 40% upon 56% conversion, while starting material was recovered with 83% ee. The reaction mixture was separated with flash column chromatography and both **113c** (11.0 mg, 42%yield) and **114c** (14.0 mg, 54% yield) were analyzed by HPLC (Figures 36-37, Table 40-41). The enantioenrichment of starting material and product corresponded to 85% and 32% respectively and the values were between experimental errors. The HPLC traces were compared to the corresponding racemic products from both **113c** and **114c**. The major product enantiomer peak appeared at 7 min, while the starting material's major enantiomer appeared at 12 min. The *s*-factor for **113c** at 50% conversion was calculated at *s*=55.



Scheme 72: Kinetic resolution of **113c** using 20 %mol (*R*)-TRIP at 50 °C

| T(h) | %Conversion | | %ee | |
|------|-------------|----------|----------|----------|
| | %P | %SM | %P | %SM |
| 0 | 0 | 100 | 0 | 0 |
| 1 | 12.40826 | 87.59174 | 67.42561 | 16.87628 |
| 2 | 25.299 | 74.701 | 59.12057 | 37.87456 |
| 3 | 43.37921 | 56.62079 | 55.28492 | 56.59632 |
| 4 | 49.99723 | 50.00277 | 46.50439 | 71.40204 |
| 5 | 56.84682 | 43.15318 | 40.9017 | 83.64721 |

Table 39: Conversion and %ee of Starting Material **113c** and Product **114c**

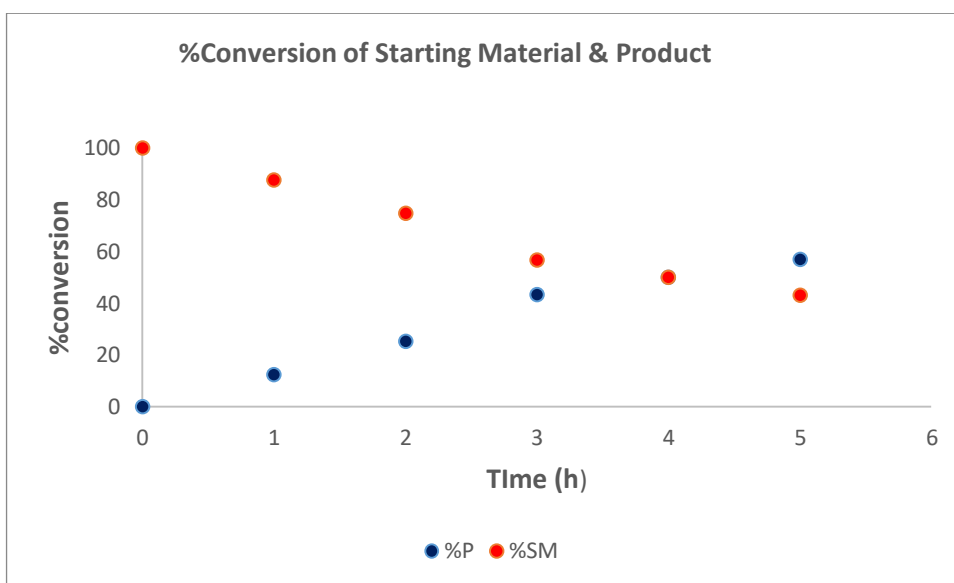


Figure 34: Conversion of Starting Material **113c** and Product **114c**

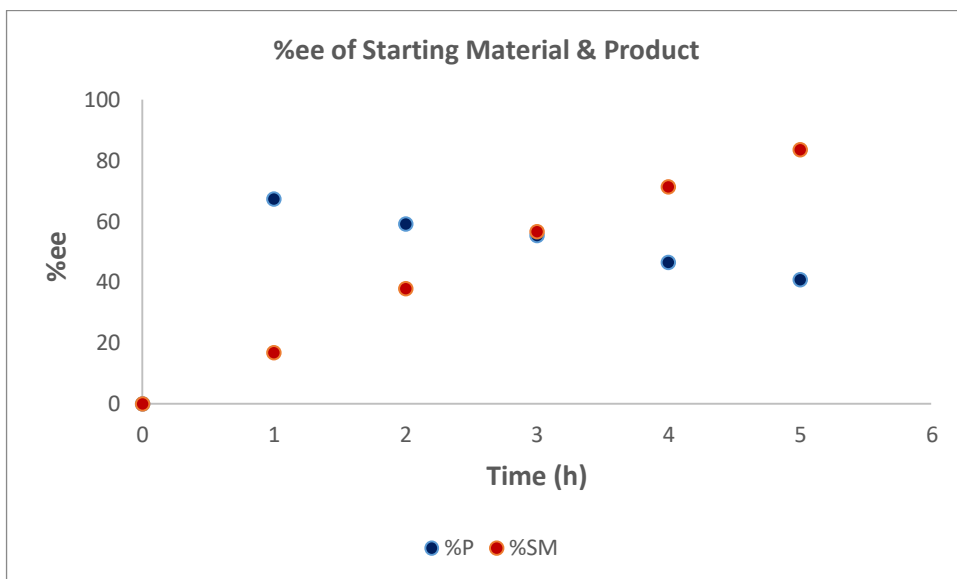


Figure 35: %ee of Starting Material **113c** and Product **114c**

| Enantioenriched Substrate | Column (CHIRALPAC) | Hexane:IPA | Flow rate (mL/min) | Temperature (°C) |
|---------------------------|--------------------|------------|--------------------|------------------|
| 113c+114c | IB | 80:20 | 1 | 40 |

Table 40: HPLC conditions of enantioenriched **113c+114c**

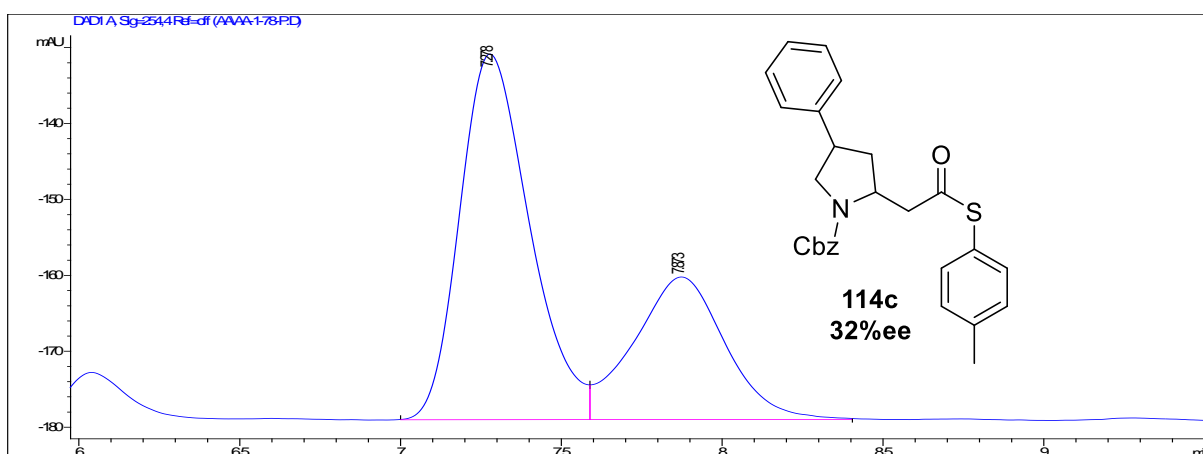


Figure 36: HPLC trace of enantioenriched **114c**

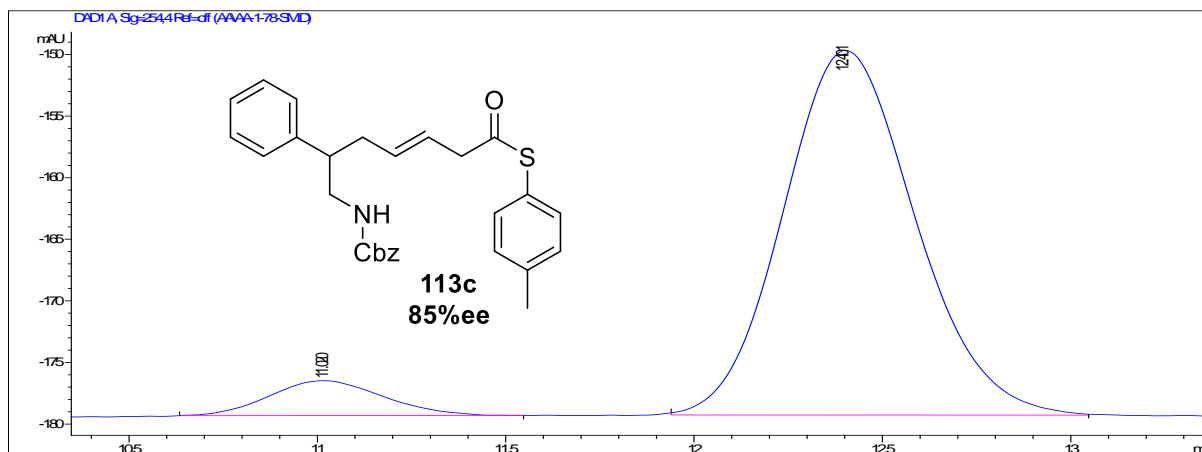
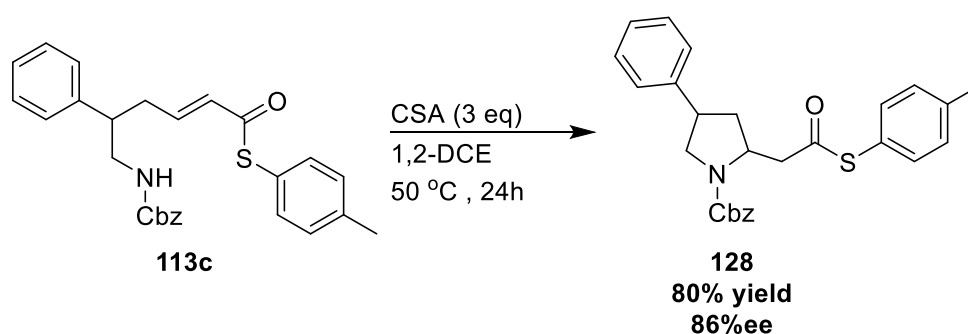


Figure 37: HPLC trace of enantioenriched **113c**

| Enantioenriched Substrate | Minor Peak (Retention time/ min) | Area% | Major Peak (Retention time/ min) | Area% |
|---------------------------|----------------------------------|---------|----------------------------------|---------|
| 114c | 7.278 | 51.9636 | 7.873 | 26.4718 |
| 113c | 11.020 | 6.8418 | 12.401 | 82.8710 |

Table 41: HPLC retention times of enantioenriched **113c+114c**

Furthermore, the opposite enantiomer was obtained in good yield and %ee (Scheme 70). The enantioenriched **113c** was further cyclised *via* the Brønsted acid catalyzed cyclisation, with 3 equivalents of camphorsulfonic acid in 1, 2-dichloroethane and the reaction was heated at 50 °C. After a period of 24 h, the reaction was quenched with sodium bicarbonate solution, purified with flash column chromatography and the product **128** (7.0 mg , 80% yield) was analyzed by HPLC (Figure 38, Table 42-43). The opposite enantiomer from that formed in the kinetic resolution reaction appeared at 8 min in higher enantioselectivity (86% ee) than the other enantiomer (32% ee). No racemization of the enantioenriched recovered **113c** (85% ee) occurred.



Scheme 73: Cyclisation of enantioenriched starting material **113c** using CSA

| Enantioenriched Substrate | Column (CHIRALPAC) | Hexane:IPA | Flow rate (mL/min) | Temperature (°C) |
|---------------------------|--------------------|------------|--------------------|------------------|
| 128 | IB | 80:20 | 1 | 40 |

Table 42: HPLC conditions of enantioenriched product **128**

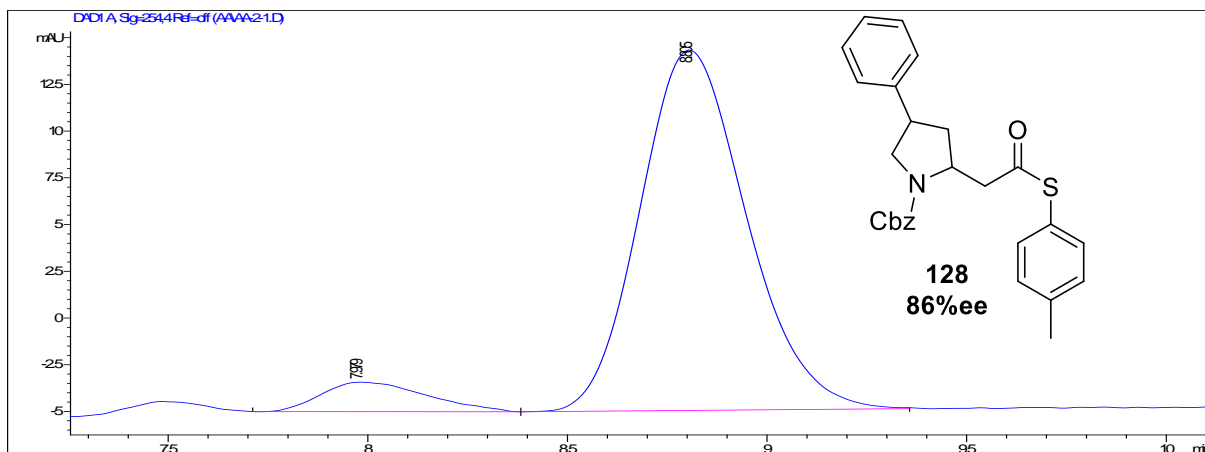


Figure 38: HPLC trace of enantioenriched **128**

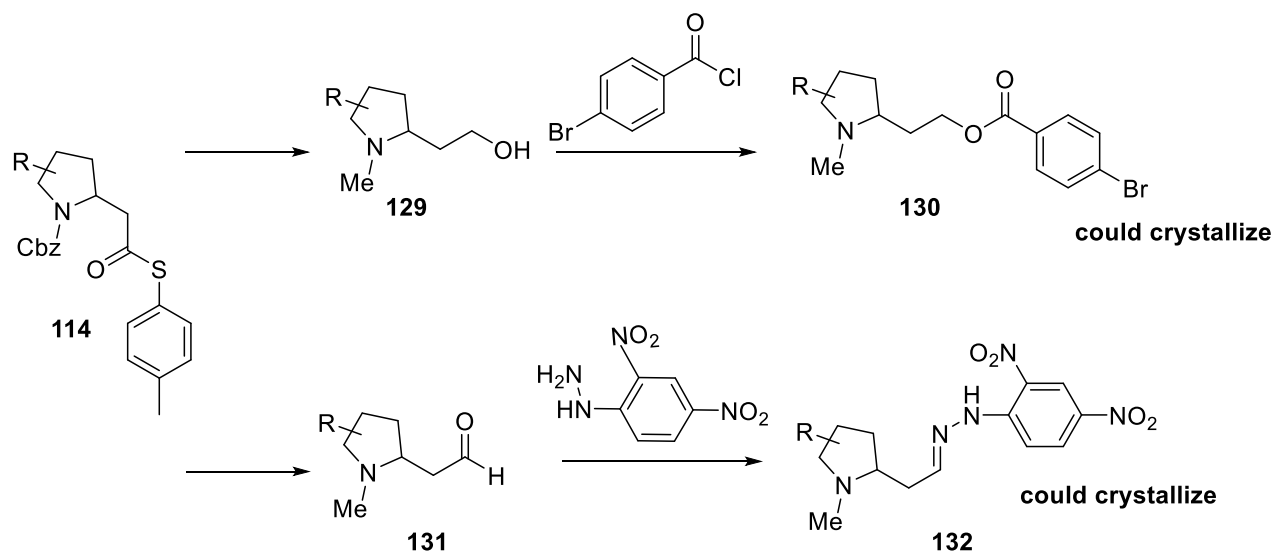
| Enantioenriched Substrate | Minor Peak (Retention time/ min) | Area% | Major Peak (Retention time/ min) | Area% |
|---------------------------|----------------------------------|--------|----------------------------------|---------|
| 128 | 7.979 | 5.8409 | 8.805 | 72.0642 |

Table 43: HPLC retention time of enantioenriched **128**

In conclusion, the asymmetric synthesis *via* kinetic resolutions of substituted pyrrolidines using the chiral phosphoric acid (*R*)-TRIP was successfully studied. The kinetic studies for all the three different substrates were conducted in two different temperatures (50 °C and 80 °C), but in the same solvent (cyclohexane) and same catalyst loading ((*R*)-TRIP 20 %mol) while the concentration was kept at 0.02M. Enantioenriched product and recovered starting material were obtained in good and moderate enantioselectivities as well as the opposite enantiomer of the product.

9.5 Determination of stereochemistry

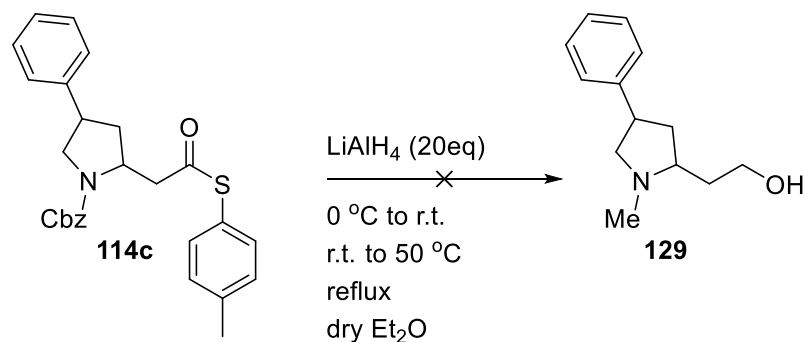
It was hoped that the absolute stereochemistry could be determined by X-ray crystallography (Scheme 74). The thioester functionality is essential for the cyclisation step and it is also a versatile handle for further transformations. Thioesters can be converted directly to alcohols, aldehydes, amides, esters and ketones under very mild conditions.⁴⁷ In the scheme below, are shown the potential routes we could follow to get a crystalline compound.



Scheme 74: Plan of determination of absolute stereochemistry

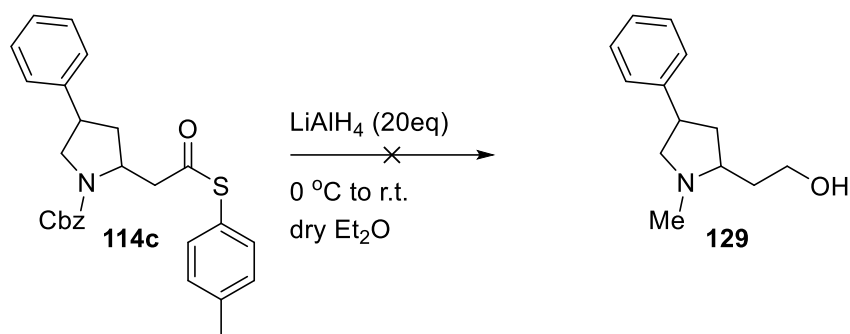
The first plan was to reduce the thioester group using a reducing agent, such as lithium aluminium hydride (LiAlH_4)⁴⁸ and reacting the formed alcohol **129** with 4-bromobenzoyl chloride to form the ester **130**. Another possible route, was to convert the thioester group to an aldehyde or a ketone and trap the carbonyl group $\text{C}=\text{O}$ with a hydrazine such as 2,4-dinitrophenylhydrazine and crystallize the formed **132**. By incorporating a heavy atom such as bromo- or nitro- groups crystals could be isolated for X-ray crystallographic analysis, permitting the determination of the absolute stereochemistry of **114**.

An initial attempt involved treating **114c** with LiAlH_4 to reduce the thioester group to the corresponding alcohol **129** (Scheme 75). Approximately, 20 eq of LiAlH_4 were added to a solution of **114c** in dry diethyl ether and the reaction was cooled down to 0°C . After stirring for 30 min in that temperature, the reaction was warmed to room temperature and was heated with reflux conditions overnight. The Fieser workup⁴² was followed to quench and workup the reaction mixture. Unfortunately, analysis of the crude reaction mixture by ^1H NMR and Mass spectroscopy resulted in complexes spectrums with no evidence for the formation of **129**.



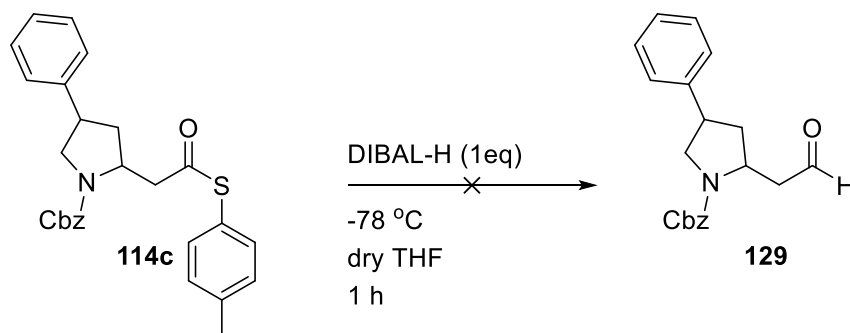
Scheme 75: Attempted synthesis of alcohol **129**

Next, the reduction of the thioester to the alcohol **129** reaction was repeated, but we envisaged leaving the reaction stirring in room temperature instead of heating under reflux (Scheme 76). Similar experimental procedure was followed, 20 eq of LiAlH_4 were added to a solution of **114c** in dry diethyl ether and the reaction was cooled down to $0\text{ }^\circ\text{C}$. After stirring for 30 min in that temperature, the reaction was warmed to room temperature and left stirring overnight. The reaction mixture was monitored by thin layer chromatography (TLC) until the **114c** was consumed and the TLC analysis indicated the presence of several different products. The Fieser workup was followed to quench and workup the crude reaction mixture, which was then analysed by ^1H NMR and Mass spectroscopy. However, the complex spectrums showed no evidence of alcohol **129**.



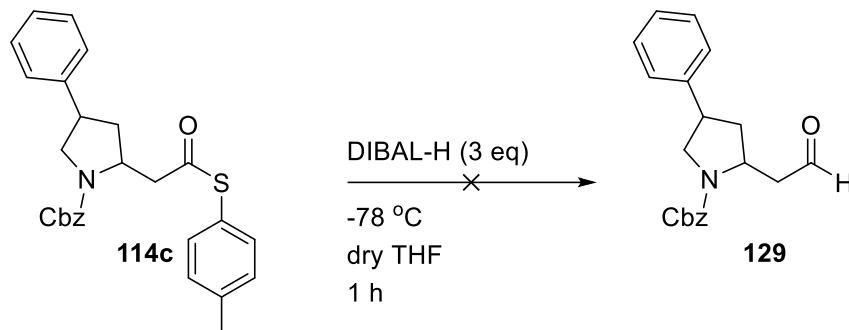
Scheme 76: Attempted synthesis of alcohol **129**

Due to the failed reduction reactions, alternative routes were tried to reduce the thioester group to aldehyde **131** by using the bulky reducing agent, di-isobutyl aluminum hydride (DIBAL-H) (Scheme 77). In a solution of **114c** in dry tetrahydrofuran in $-78\text{ }^\circ\text{C}$, was added 1 eq of DIBAL-H and the reaction was stirred for 1 h in that temperature. The reaction progression was followed by TLC until full conversion of **114c**. Analysis of the crude reaction mixture by ^1H NMR spectroscopy and mass spectrometry resulted in complex mixtures and no aldehyde peak was observed in the ^1H NMR.



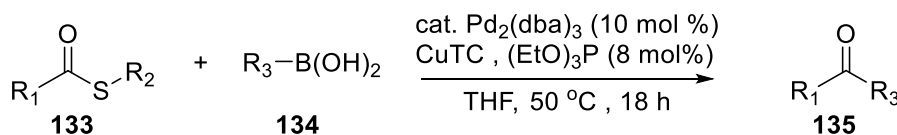
Scheme 77: Attempted synthesis of aldehyde **129**

It was decided to repeat the reaction to form the **129** but using 3 eq of the reducing agent DIBAL-H, instead of 1 eq (Scheme 78). In a solution of **114c** in dry tetrahydrofuran in $-78\text{ }^{\circ}\text{C}$, was added 1 eq of DIBAL-H and the reaction was stirred for 1 h in that temperature. When TLC monitoring showed full conversion of **114c** the crude mixture was analysed by ^1H NMR and mass spectroscopy. Disappointingly, no aldehyde peak was observed.



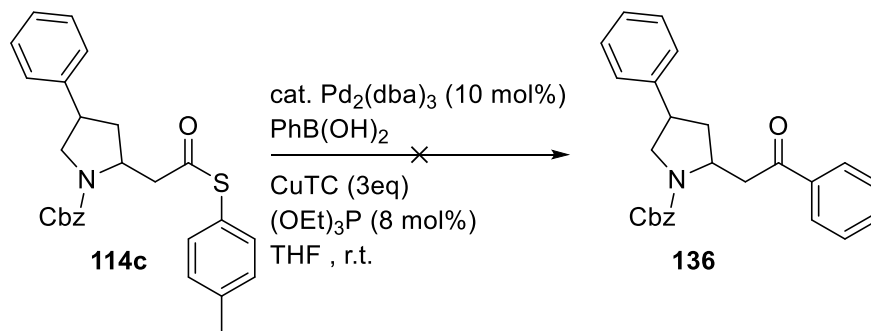
Scheme 78: Attempted synthesis of aldehyde **129**

The final reaction of the thioester group to a ketone was attempted, using a Pd(0) catalyst for a Liebeskind–Srogl type coupling reaction.⁴⁹ Liebeskind–Srogl proposed a new reaction for the synthesis of ketones, as shown in the scheme below. The palladium-catalysed cross-coupling reaction between a thioesters **133** and boronic acids **134** proceeded in the presence of a copper co-catalyst to generate the corresponding ketones **135**(Scheme 79).



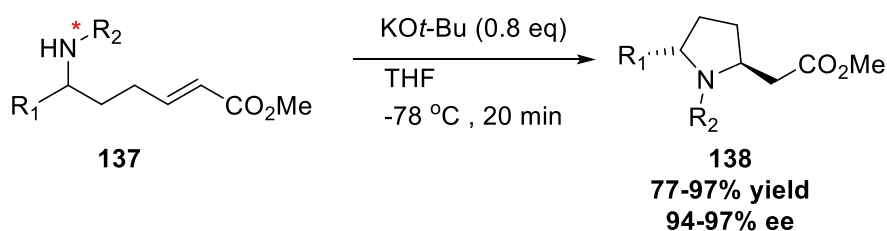
Scheme 79: Liebeskind–Srogl coupling reaction

In this case, a preparation previously developed in the Clarke group for the synthesis of Diospongin A was followed.⁵⁰ The palladium pre-catalyst which we used was $\text{Pd}_2(\text{dba})_3$ with a 10 mol % catalyst loading. The rest of the reagents and conditions used were 3 eq of copper(I)-thiophene-2-carboxylate (CuTC), 8 mol % of triethyl phosphite $(\text{EtO})_3\text{P}$ and 3 eq of phenylboronic acid (PhB(OH)_2) (3.0 eqv) in dry tetrahydrofuran. The reaction was stirred at room temperature stirred for 18 h. Unfortunately, these conditions resulted in the formation of many unknown products but were unsuccessful at generating the desired product (Scheme 80).



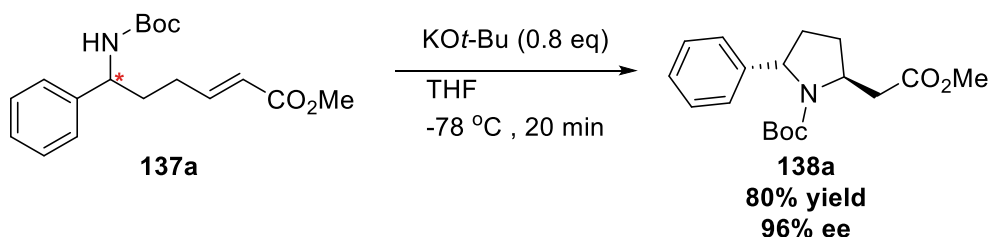
Scheme 80: Liebeskind–Srogl coupling reaction between phenylboronic acid and **114c**

In a publication by Farwick²⁶ reported syntheses of various pyrrolidine derivatives through a domino hydroformylation/Wittig olefination, followed by an aza-Michael addition (Scheme 81). They, also, reported that the *trans*-configuration of 2,5-substituted pyrrolidines **138** was generally preferred at a reaction temperature of $-78\text{ }^{\circ}\text{C}$ upon use of potassium *tert*-butoxide (*t*-BuOK) as base. The aza-Michael reactions yielded the **138** with KO-*t*-Bu (0.8 equiv.) at $-78\text{ }^{\circ}\text{C}$ in tetrahydrofuran as solvent and the reactions were stirred for 20 min. The *trans*-diastereoisomers were obtained in good to excellent yields (77–97%), with high enantiomeric excess (94–97%).



Scheme 81: Intramolecular aza-Michael reaction

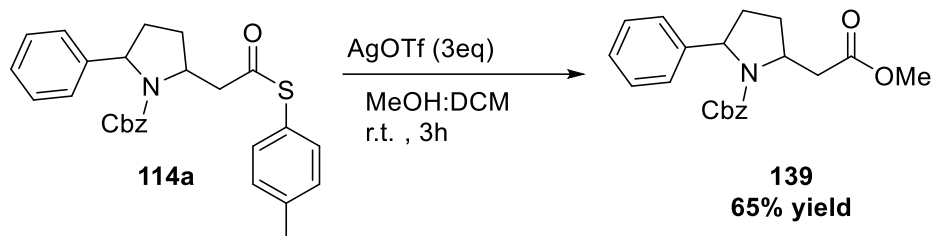
One of the 2,5-disubstituted pyrrolidine products that they reported was similar to one of pyrrolidine products that was synthesised, the **114a**, as shown in the scheme below (Scheme 82). The Boc-protected pyrrolidine ring has *trans*-diastereoselectivity; it was envisaged that the stereochemistry could be determined by a ^1H NMR comparison between the pyrrolidine **114a** product and the pyrrolidine **138a** from literature.



Scheme 82: Intramolecular aza-Michael reaction

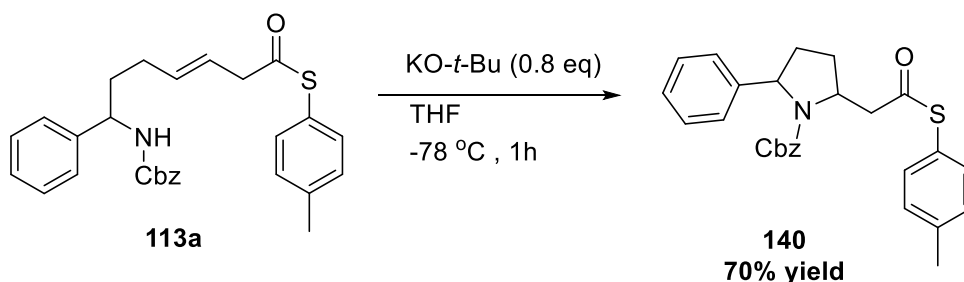
In order to directly compare the stereochemistry of the compounds against **138a** the thioester needed to be converted in a methyl ester. . A report by Hanessian³⁸ used a method with silver

trifluoromethanesulfonate (AgOTf) in methanol:dichloromethane (MeOH/CH₂Cl₂) to convert a thiophenyl ester into a methyl ester. Using this procedure the methyl ester was generated in moderate yield (Scheme 83). To a solution of **114a** in 1:1 MeOH:CH₂Cl₂ were added 3 eq of AgOTf and the reaction was stirred for 3 h in room temperature, followed by purification with flash column chromatography.



Scheme 83: Methyl ester **139** synthesis

In addition, the aza-Michael cyclisation reaction conditions by Farwick were followed to synthesise the 2,5- disubstituted pyrrolidine **140**, using the 2-phen precursor **113a** (Scheme 84). A solution of **113a** in dry tetrahydrofuran was cooled to -78 °C and 0.8 eq of KO-*t*-Bu was added and the mixture stirred for 1 h, when thin layer chromatography (TLC) showed full conversion. The reaction was then quenched with saturated aqueous ammonium chloride solution and was purified by flash column chromatography to yield the **140** (70% yield).



Scheme 84: Intramolecular aza-Michael cyclisation reaction

Synthesizing the pyrrolidine **140** using the *t*-BuOK cyclisation procedure provide the opportunity to compare the **140** and the **114a** pyrrolidine from the chiral phosphoric acid cyclisation and see whether the data matches or not. Looking at the ¹H NMR spectra, the data between the two different products were consistent (Figure 39-42).

The "quartet" at 5.17 ppm, are actually 2 doublets at 5.17 ppm (*J*=16 Hz) and 5.13 ppm (*J*=16 Hz) were from the one rotamer of Cbz group (H-17). The other rotamer of the Cbz group was the two doublets at 5.01 ppm (*J*=12 Hz) and 4.87 ppm (*J*=12 Hz). The resonance for H-11 was at also at 5.01 ppm overlapping one half of the Cbz-doublet and this signal is a multiplet. The H-8 proton was assigned as the multiplet at 4.65-4.55ppm (Figure 39-40).

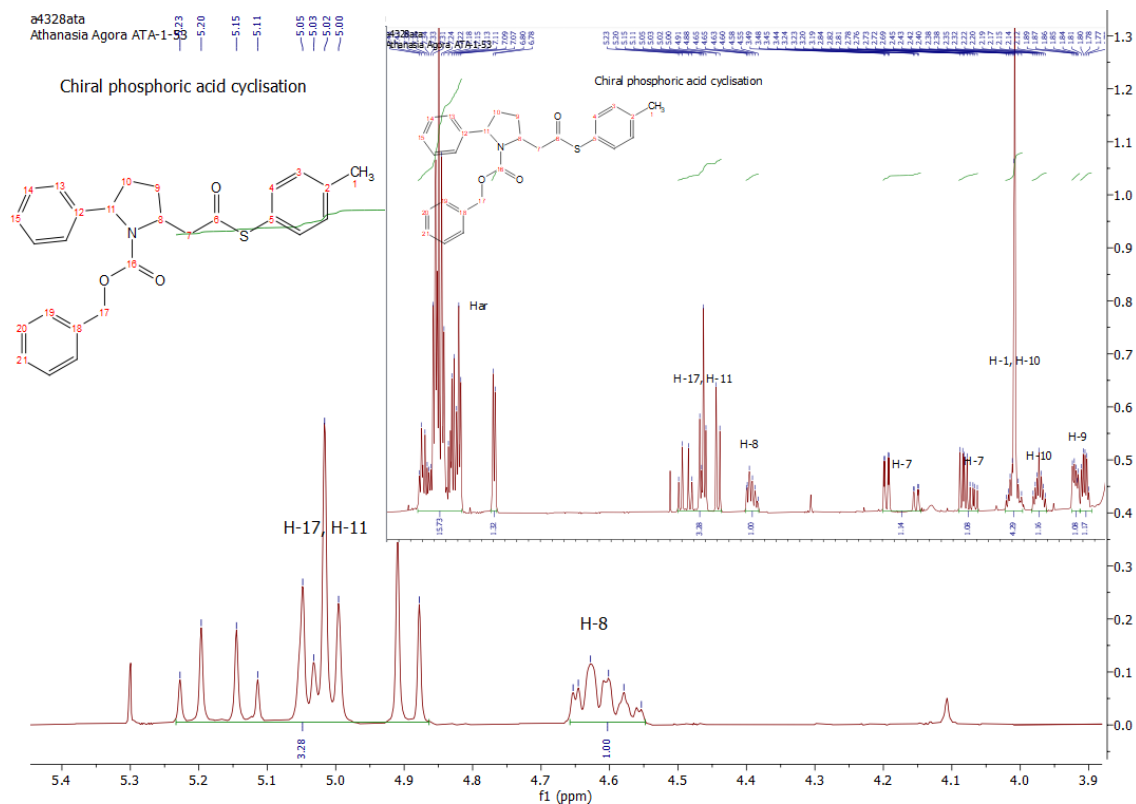


Figure 39: ^1H NMR (CDCl_3) spectrum of **114a**

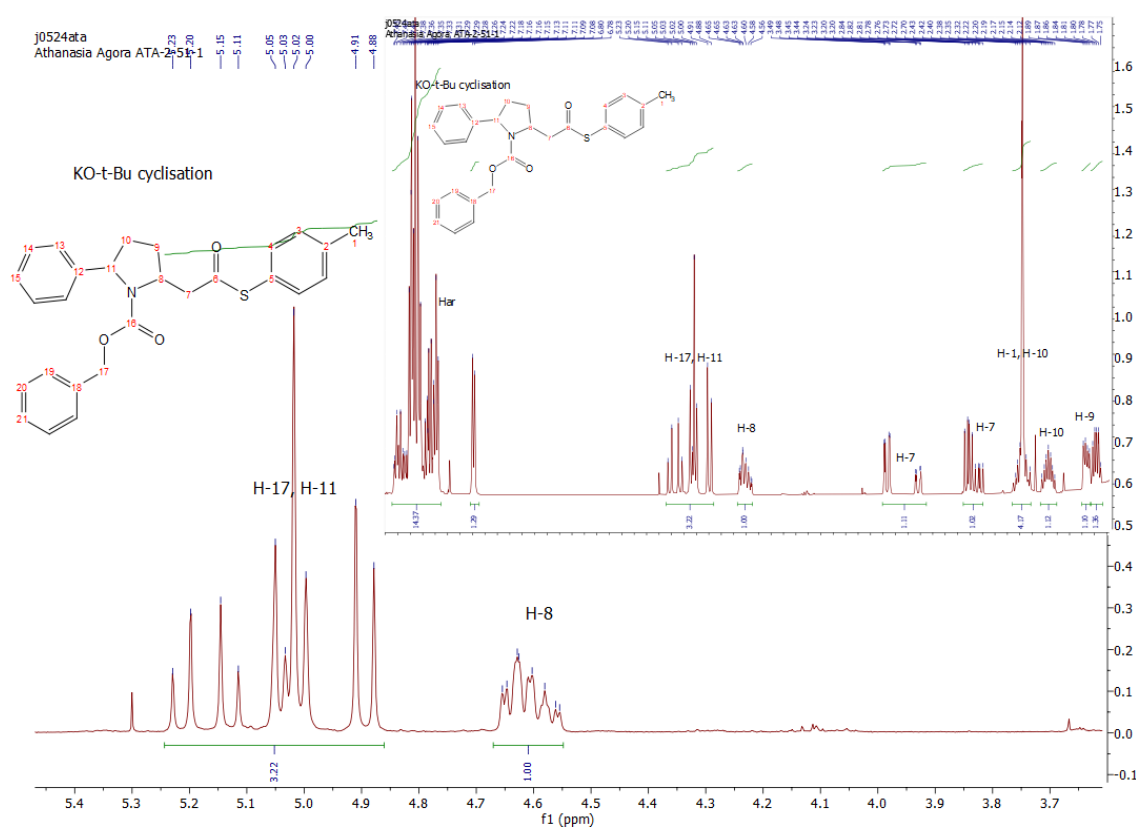


Figure 40: ^1H NMR (CDCl_3) spectrum of **140**

The two doublets at 3.49 ppm and 3.45 ppm and the two doublets at 3.24 ppm and 3.20 ppm with a coupling constant of $J=3$ Hz were assigned as one H-7 proton. The second H-7 proton was assigned as the multiplet at 2.84-2.70 ppm. One H-10 proton overlapped with the three H-1 protons as the multiplet at 2.46-2.32 ppm; the second H-10 proton was assigned as the multiplet at 2.22-2.12 ppm. The two H-9 protons were assigned as the two multiplets at 1.86 ppm and 1.78 ppm respectively (Figure 41-42).

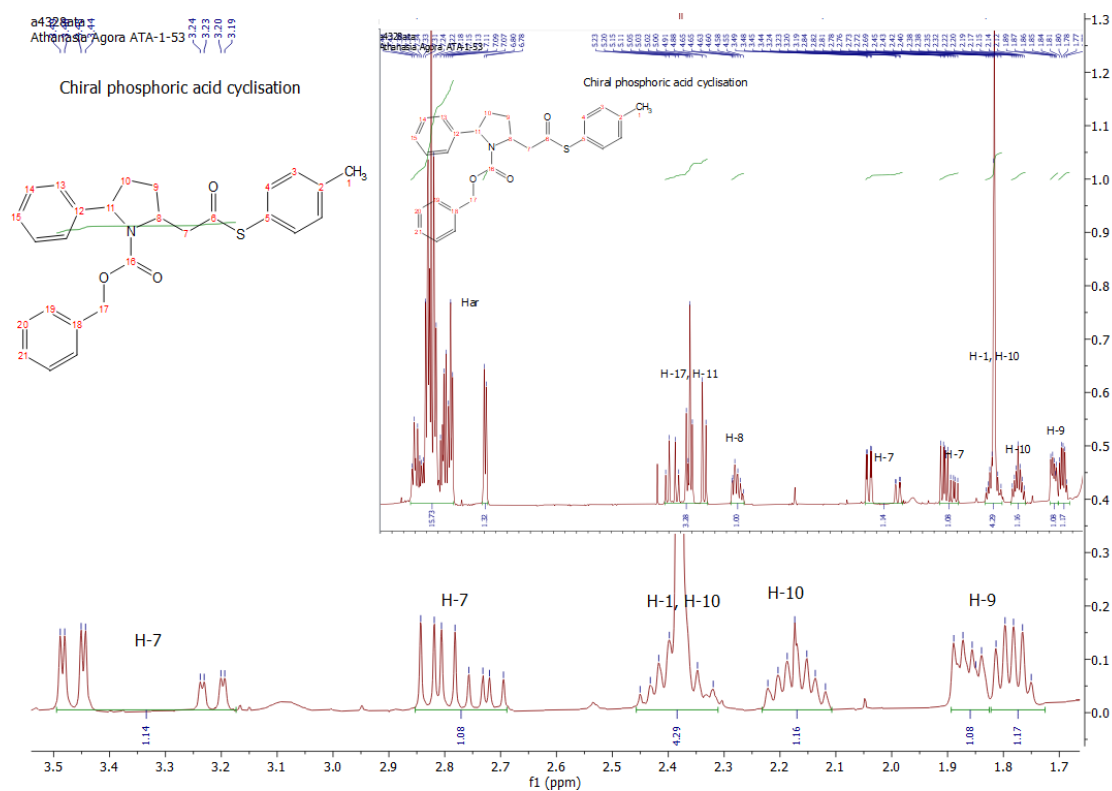


Figure 41: ^1H NMR (CDCl_3) spectrum of **114a**

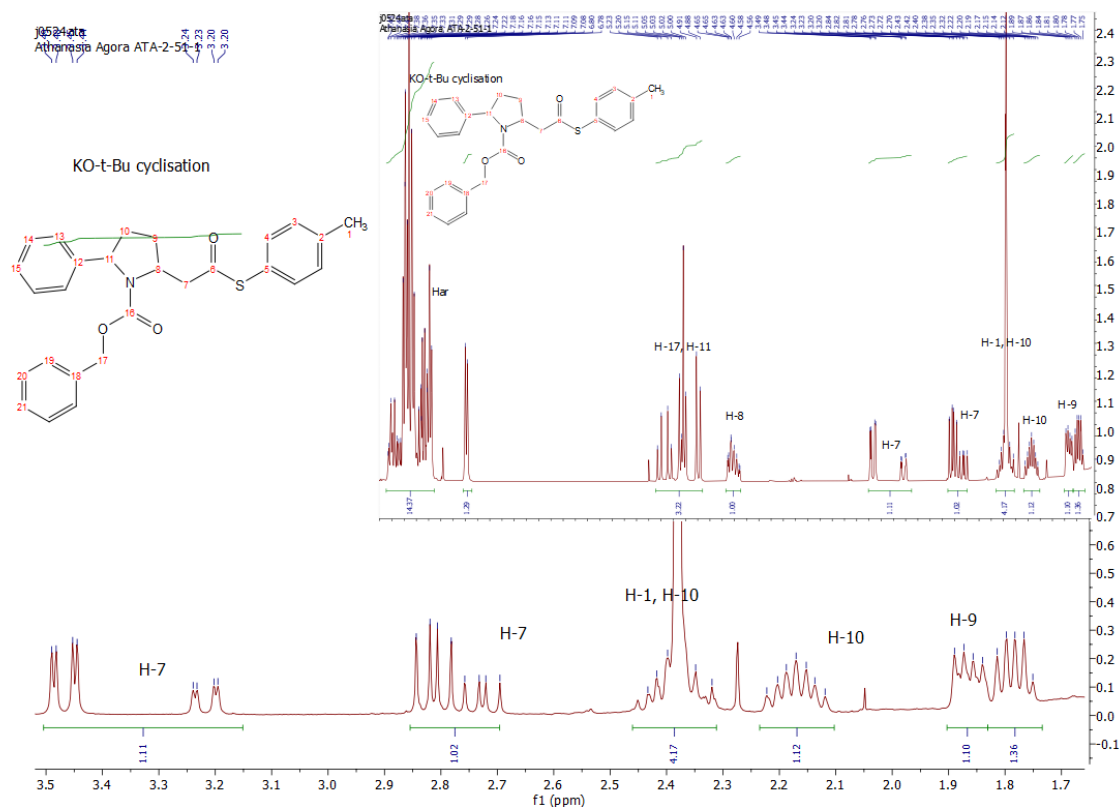
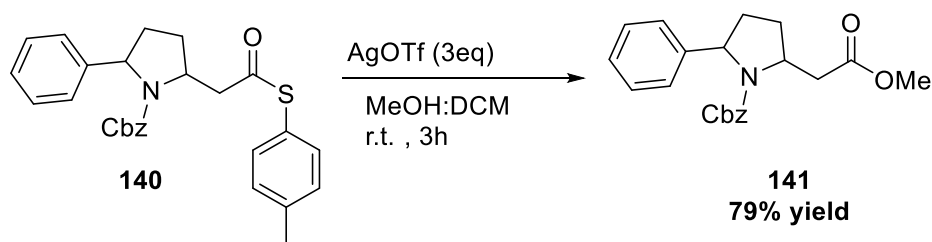


Figure 42: ^1H NMR (CDCl_3) spectrum of **140**

Following the data comparison of the two pyrrolidine rings, the next step was the conversion of the thioester group of **140** to its' methyl ester (Scheme 85). To a solution of **140** in 1:1 MeOH: CH_2Cl_2 were added 3 eq of AgOTf and the reaction was stirred for 3 h in room temperature, followed by purification with flash column chromatography to yield the **141**.



Scheme 85: Methyl ester **141** synthesis

Synthesizing the pyrrolidine **141** provided the opportunity to compare the **141** from the *t*-BuOK cyclisation procedure and the **114a** pyrrolidine from the chiral phosphoric acid cyclisation and see whether the data matches or not. Once again, the ^1H NMR data between the two different procedures was consistent (Figure 43-46).

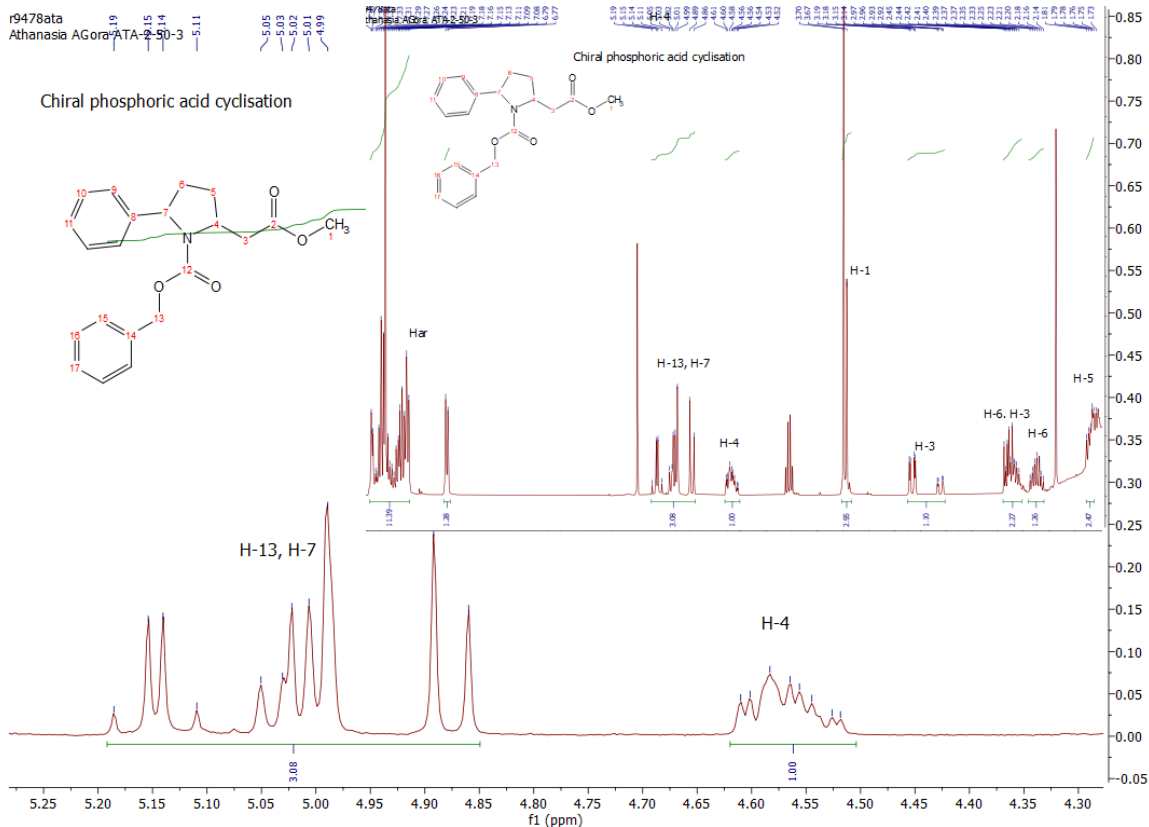


Figure 43: ^1H NMR (CDCl_3) spectrum of **139**

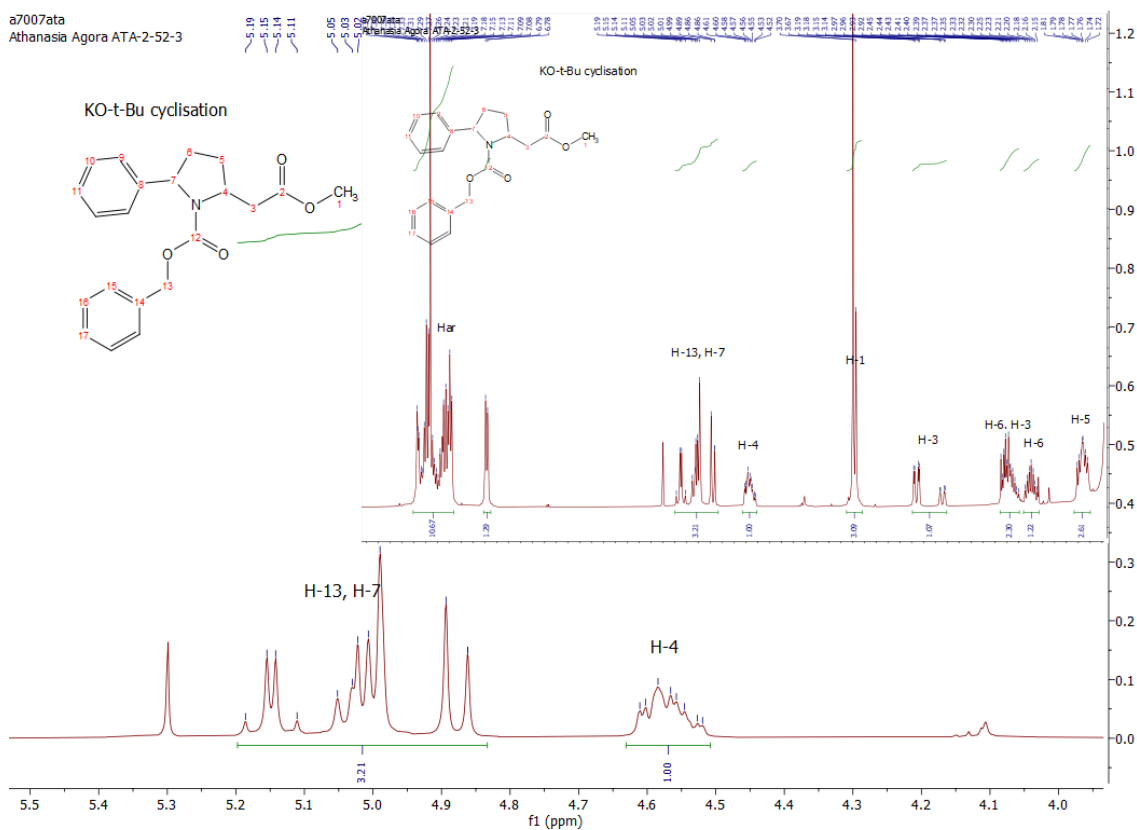


Figure 44: ^1H NMR (CDCl_3) spectrum of **141**

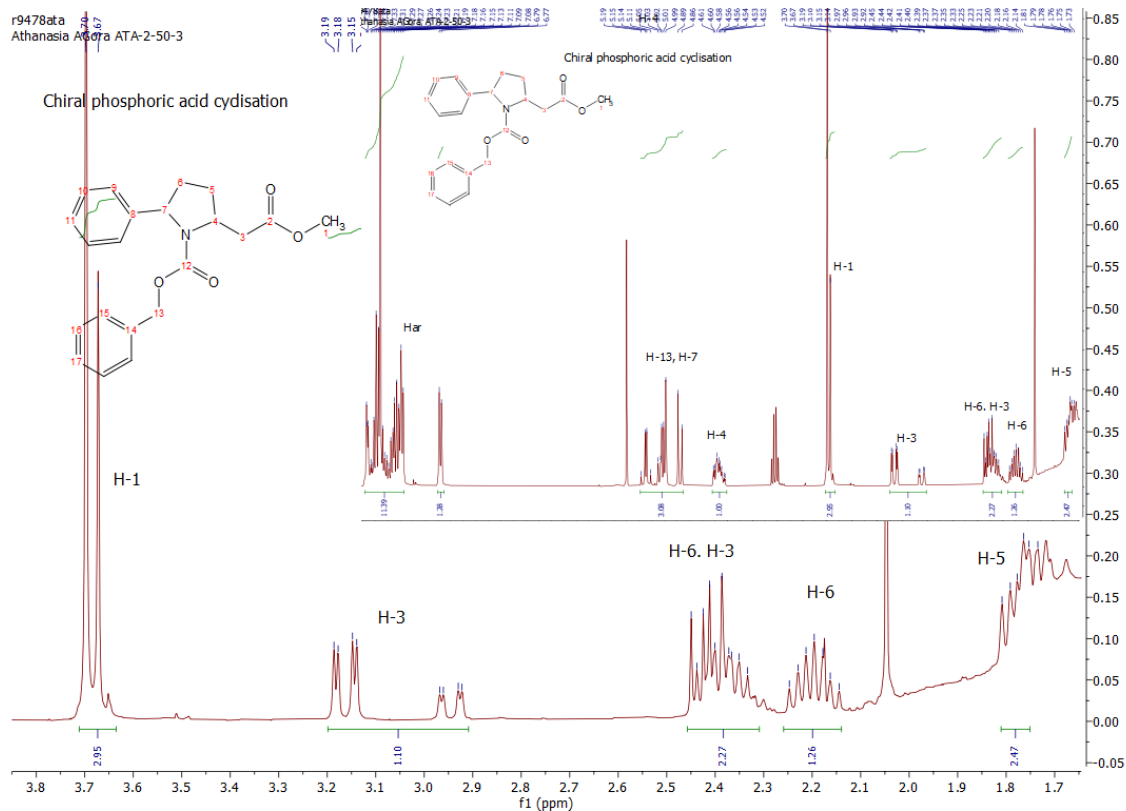


Figure 45: ^1H NMR (CDCl_3) spectrum of **139**

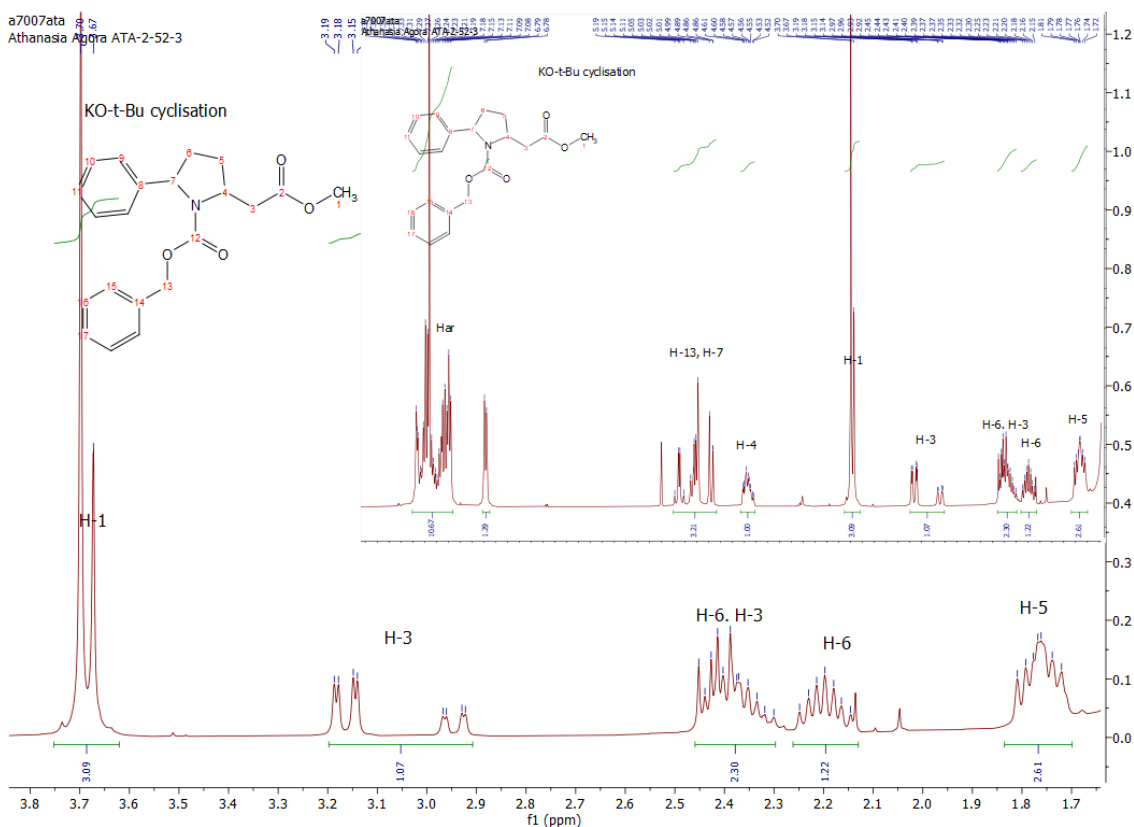


Figure 46: ^1H NMR spectrum of **141**

Looking at the ^1H NMR spectra, the peaks at 7.37-6.78 ppm were assigned as the aromatic protons. The "quartet" at 5.17 ppm, which were actually 2 doublets at 5.17 ppm ($J=16$ Hz) and

5.13 ppm ($J=16$ Hz) were from the one rotamer of Cbz group (H-13). The other rotamer of the Cbz groups was the two doublets at 5.01 ppm ($J=12$ Hz) and 4.87 ppm ($J=12$ Hz). The H-13 was also at 5.01 ppm overlapping one half of the Cbz-doublet and this signal is a multiplet. The H-4 proton was assigned as the multiplet in 4.65-4.55 ppm. The three H-1 were assigned as two singlets at 3.70 ppm and 3.67 ppm. The two doublets at 3.18 ppm and 3.14 ppm correspond to the major and the minor rotamer respectively and the two doublets at 2.96 ppm and 2.93 ppm with a coupling constant of 3 Hz were assigned as one H-3 proton. One H-6 proton overlapped with the other H-3 proton as the multiplet at 2.46-2.30 ppm; the second H-6 proton was assigned as the multiplet at 2.22-2.12 ppm. The two H-5 protons were assigned as the multiplet at 1.82-1.70 ppm.

In the literature procedure, the NMR (^1H , ^{13}C) analysis of compounds was conducted in 500 MHz at 90 °C and in toluene- d_8 as the solvent. However, due to laboratory facilities shut down by the COVID-19 pandemic definitive proof could not be obtained. It can be assumed that the absolute stereochemistry is *trans*- for the 2-phenyl and 2-isopropyl substituted pyrrolidine rings as the data is consistent upon ^1H NMR analysis (400 MHz, CDCl_3).

9.6 Conclusions and future work

The synthesis of the racemic pyrrolidine cyclisation precursors **113a-c** was achieved in good yields *via* a Hoveyda-Grubbs catalyzed metathesis reaction; the unsaturated Cbz-protected (**115a-c**) amines were 'clipped' with the thioacrylate **118**. The Brønsted acid catalyzed cyclisation using CSA was carried out and generated the racemic substituted pyrrolidines **114a-c** in good yields. The racemic pyrrolidine precursors and the corresponding cyclisation products were successfully screened under chiral HPLC conditions.

The kinetic resolution studies of the pyrrolidine cyclisation precursors **113a-c** using the chiral phosphoric acid (*R*)-TRIP were successful and was achieved with good to moderate selectivity. Both recovered enantioenriched starting material and product were isolated with good to moderate enantioselectivities; enantioenriched starting material was further cyclised under CSA conditions to yield the opposite enantiomer. It was found that the increase in temperature had an accelerating effect on the asymmetric cyclisation reactions, reaching the desirable 50% conversion within a few hours.

The resolution process of the 2-phenyl pyrrolidine **113a** precursor yielded in high enantioselectivity for the unreacted **113a** (90% ee) and in high selectivity (*s*-factor= 122). The pyrrolidine **114a** was afforded in low enantiomeric excess (51% ee) upon 50% conversion after 3.5

hours at 80 °C. The 3-phenylprecursor **113c** was resolved in lower selectivity (*s*-factor=55); the enantiomerically enriched **113c** was obtained with 85%ee and the corresponding pyrrolidine **114c** in 32% ee. The asymmetric reaction reached 50% conversion within 5 hours and the temperature was kept at 50 °C. The opposite enantiomers **126** and **128** were generated in good enantioselectivities under further CSA cyclisation conditions. The recovered **113a** and **113c** were further cyclized under CSA conditions to generate the corresponding opposite **126** and **128** enantiomers and no racemization of the **113a** and **113c** occurred. The 2-isopropyl precursor **113b** underwent a less effective kinetic resolution (*s*-factor=9) with moderate enantiomeric excesses for the recovered **113b** (74% ee) and the corresponding pyrrolidine **114b** (63% ee) upon reaching 50% conversion after 3 hours.

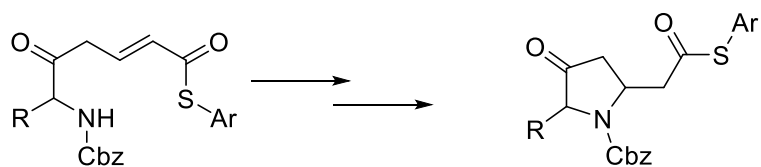
The determination of the absolute stereochemistry was carried out by a ¹H NMR comparison between our 2-phenyl pyrrolidine product (**114a**) and the 2-phenyl pyrrolidine (**138a**) from literature. In the publication it was reported that the *trans*-configuration of 2, 5-disubstituted pyrrolidines was preferred upon optimized cyclisation conditions. Using the optimized conditions from the literature (KO-*t*-Bu as a base, in – 78 °C) the 2-phenyl pyrrolidine **139** was synthesised in good yield (70% yield). In order to directly compare the stereochemistry of **114a** **140**, the thioester groups were converted into the methyl ester groups (**139**, **141**) Finally, the data from ¹H NMR in CDCl₃ analysis between the pyrrolidines **114a** and **139** from the chiral phosphoric acid cyclisation and the pyrrolidines **140** and **141** from the KO-*t*-Bu cyclisation was consistent.

It can be assumed that the 'Clip-Cycle' methodology proceeds with *trans*-configuration for the 2,5-disubstituted pyrrolidines (**11a**, **114b**). Definitive proof was not obtained, due to Spring 2020 COVID-19 shutdown of laboratory facilities.

In conclusion, 'Clip-Cycle' methodology can be used to generate enantiomerically pure substituted pyrrolidine rings with moderate to good yields and %ee's *via* a kinetic resolution reaction. Both enantiomers of can be obtained; one from the asymmetric chiral phosphoric acid cyclisation, the opposite one from the Brønsted acid catalyzed cyclisation of the recovered pyrrolidine precursor.

Future work would include kinetic resolutions of a broader pyrrolidine precursor scope using the 'Clip-Cycle' methodology. The absolute stereochemistry of the enantioenriched 2- and 3-substituted products would need to be determined with X-ray crystallography.

Additionally, the scope could be further extended by studying a dynamic kinetic resolution on substituted pyrrolidines.



Scheme 86: A dynamic kinetic resolution

A dynamic kinetic resolution overcomes the drawback of the classical resolution and it is theoretically possible to obtain 100% yield of the desired enantiomers. The substrate is continuously isomerized during the resolution process and in this way the non-reacting enantiomer is transformed into the reacting one. It would be an interesting yet challenging scope to explore.⁵¹

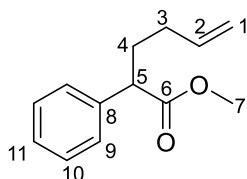
10. Experimental

10.1 General Experimental

Unless otherwise noted all compounds were bought from commercial suppliers and used without further purification. Nuclear magnetic resonance spectra were recorded on a Jeol ECS-400 spectrometer at ambient temperature and spectra were processed using MestreNova. Chemical shifts are quoted in parts per million (ppm) and were referenced as follows: chloroform-d, 7.26 ppm for ^1H NMR; chloroform-d, 77.0 ppm for ^{13}C NMR. Coupling constants (J) are quoted in Hertz. Infra-red spectra were recorded on an ATI Mattson Genesis FT-IR spectrometer. Mass spectrometry was performed by the University of York mass spectrometry service using electron spray ionisation (ESI) technique. Thin layer chromatography was performed on aluminium sheets coated with Merck Silica gel 60 F₂₅₄. The plates were developed using ultraviolet light, acidic aqueous ceric ammonium molybdate or basic aqueous potassium permanganate. Liquid chromatography was performed using forced flow (flash column) with the solvent systems indicated. The stationary phase was silica gel 60 (220–240 mesh) supplied by Sigma-Aldrich. Dry solvents were acquired from PureSolv alumina columns from Innovative Technologies. High Performance Liquid Chromatography (HPLC) was performed using an Agilent 1200 series instrument using the chiral columns indicated and a range of wavelengths from 210-280 nm for detection. All other solvents and reagents were used as received from commercial suppliers. All numbering on the structures below is for the benefit of characterisation and does not necessarily conform to IUPAC rules. For a few compounds, full characterisation was not obtained due to the Spring 2020 COVID-19 shutdown of laboratory facilities.

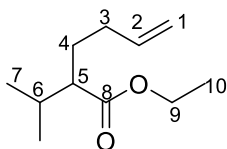
10.2 Experimental procedures

Methyl 2-phenylhex-5-enoate (**117a**)



To a solution of diisopropylamine (1.51 ml, 10.78 mmol) in dry THF (5 ml) at $-78\text{ }^{\circ}\text{C}$ under N_2 was added n-BuLi (1.42M, 7.60 mL) and the solution was stirred for 45 mins. A solution of methyl 2-phenylacetate (1.41 mL, 10.00 mmol) in dry THF (5 ml) was added over 2 minutes at $-78\text{ }^{\circ}\text{C}$ and the reaction was stirred for 45 mins. 4-bromo-1-butene (2 ml, 20 mmol) was added over 1 min at $-78\text{ }^{\circ}\text{C}$ and the reaction warmed to room temperature. The reaction was stirred overnight and quenched with 1 M aq. HCl (10 ml). The reaction was extracted with diethyl ether (3 x 30 mL), the organic fractions were combined, washed with saturated brine solution (30 ml), dried with MgSO_4 , filtered and *in vacuo*. The crude residue was purified by flash column chromatography (1% EtOAc/hexane) to afford **117a** as colorless oil (1.21 g, 5.92 mmol, 59% yield). $^1\text{H NMR}$ (400 MHz, Chloroform-*d*): δ 7.29 – 7.17 (5H, m, H-Ar), 5.74 (1H, dddd, $J = 16.8, 12.7, 6.5, 2.1$ Hz, H-2), 5.01 – 4.92 (2H, m, H-1), 3.57 (3H, s, H-7), 3.53 (1H, dd, $J = 7.5$ Hz, 2.1 Hz, H-5), 2.21 – 2.09 (1H, m, H-4), 2.00 – 1.94 (2H, m, H-3), 1.90 – 1.80 (1H, m, H-4) ppm; $^{13}\text{C NMR}$ (101 MHz, Chloroform-*d*): δ 174.41 (C-6), 139.12 (C-8), 137.66 (C-2), 128.78 (C-10), 128.11 (C-9), 127.40 (C-11), 115.56 (C-1), 51.96 (C-7), 50.83 (C-5), 32.68 (C-4), 31.64 (C-3) ppm; **HRMS (ESI)**: 205.121550 ($\text{M}^+ \text{H}^+$, $\text{C}_{13}\text{H}_{17}\text{O}_2$ requires 205.122306). IR (ATR) characterisation was not obtained due to the Spring 2020 COVID-19 shutdown of laboratory facilities.

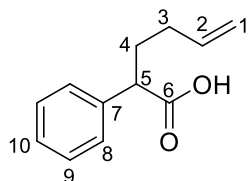
Ethyl 2-isopropylhex-5-enoate (**117b**)



Compound **117b** was synthesised using the same procedure as **117a** with diisopropylamine (1.54 mL, 10.98 mmol), n-BuLi (1.98 M, 5.56 mmol), ethyl isovalerate (1.50 ml, 9.96 mmol) and 4-bromo-1-butene (2 ml, 20 mmol). **117b** yielded as colorless oil (416.48 mg, 2.26 mmol, 23% yield). $^1\text{H NMR}$ (400 MHz, Chloroform-*d*): δ 5.78 (1H, dddd, $J = 17.0$ Hz, 10.2 Hz, 6.8 Hz, 6.8 Hz Hz, H-2), 4.93 (1H, ddd, $J = 16.8$ Hz, 1.2 Hz, 1.2 Hz, H-1), 4.87 (1H, bd, $J = 10.3$ Hz), 4.07 (2H, q, $J = 7.1$ Hz, H-9), 2.06 (1H, ddd, $J = 14.0$ Hz, 7.4 Hz, 3.8 Hz, H-5), 2.01 – 1.93 (1H, m, H-3), 1.92 – 1.83 (1H,

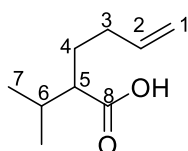
m, H-3), 1.78 (1H, apparent dq, $J = 13.8$ Hz, 6.9 Hz, H-6), 1.70 – 1.58 (1H, m, H-4), 1.55 – 1.44 (1H, m, H-4), 1.19 (3H, t, $J = 7.0$ Hz, H-10), 0.86 (3H, d, $J = 8.4$ Hz), 0.84 (3H, d, $J = 8.4$ Hz); $^{13}\text{C NMR}$ (101 MHz, Chloroform-*d*): δ 175.69 (C-8), 138.23 (C-2), 115.04 (C-1), 60.00 (C-9), 52.19 (C-5), 32.07 (C-3), 30.75 (C-6), 28.96 (C-4), 20.55 - 20.30 (C-7), 14.48 (C-10) ppm; **IR (ATR)**: ν_{max} 2960, 1731, 1641, 1459, 1373, 1176, 1033, 911; **HRMS (ESI)**: 185.153103 ($\text{M}^+ \text{H}^+$, $\text{C}_{11}\text{H}_{21}\text{O}_2$ requires 185.153606)

2-phenylhex-5-enoic acid (**116a**)



To a solution of ester **117a** (0.29 g, 1.44 mmol) in MeOH (10 ml) was added NaOH (20% w/w, 2.5 ml) and reaction was heated to reflux while stirring for 24 hours. Reaction was then cooled to room temperature and diluted with H_2O (10 ml) and extracted with diethyl ether (20 ml). The aqueous layer was acidified to pH 1 with 2M aq. HCl (10 ml), extracted with diethyl ether (3 x 20 ml). The combined organics were dried with MgSO_4 , filtered and concentrated *in vacuo* to give **116a** as a colourless oil (0.23 g, 1.18 mmol, 82% yield). $^1\text{H NMR}$ (400 MHz, Chloroform-*d*): δ 10.77 (1H, s, COOH), 7.37 – 7.23 (5H, m, Ar-H), 5.75 (1H, dddd, $J = 17.0, 10.2, 6.4, 6.4$ Hz, H-2), 5.04 – 4.96 (2H, m, H-1), 3.59 (1H, dd, $J = 7.6$ Hz, 7.6 Hz H-5), 2.23 – 2.12 (1H, m, H-4), 2.06 – 1.99 (2H, m, H-3), 1.94 – 1.83 (1H, m, H-4) ppm; $^{13}\text{C NMR}$ (101 MHz, Chloroform-*d*): δ 179.13 (C-6), 138.79 (C-7), 137.33 (C-2), 128.78 (C-10), 128.11 (C-9), 127.41 (C-11), 115.60 (C-1), 51.06 (C-5), 31.97 (C-4), 31.31 (C-3) ppm. IR (ATR) and HRMS (ESI) characterisation was not obtained due to the Spring 2020 COVID-19 shutdown of laboratory facilities.

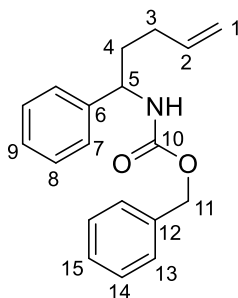
2-isopropylhex-5-enoic acid (**116b**)



Compound **116b** was synthesised using the same procedure as **116a** with ester 1b (416.47 mg, 2.26 mmol). **116b** yielded as a colourless oil (251.53 mg, 1.61 mmol, 71% yield). $^1\text{H NMR}$ (400 MHz, Chloroform-*d*): δ 11.66 (1H, s, COOH), 5.79 (1H, dddd, $J = 17.1$ Hz, 10.2 Hz, 6.8 Hz, 6.8 Hz, H-2), 5.03 (1H, dt, $J = 17.6$ Hz, 1.9 Hz, H-1), 4.97 (1H, bd, $J = 10.4$ Hz, H-1), 2.21 – 2.08 (2H, m, H-3, H-5), 2.07 – 1.96 (1H, m, H-3), 1.90 (1H, dq, $J = 13.6$ Hz, 6.8 Hz Hz, H-6), 1.77 – 1.67 (1H, m, H-4), 1.63

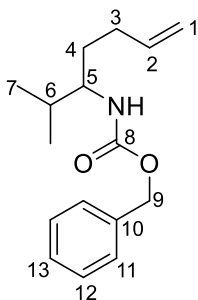
– 1.54 (1H, m, H-4), 0.98 (3H, d, $J = 6.7$ Hz, H-7), 0.96 (3H, d, $J = 6.7$ Hz, H-7) ppm; ^{13}C NMR (101 MHz, Chloroform- d): δ 182.59 (C-8), 137.93 (C-2), 115.26 (C-1), 51.96 (C-5), 31.97 (C-3), 30.51 (C-6), 28.44 (C-4), 20.48-20.10 (C-7) ppm ; **HRMS (ESI)**: 179.1038 ($M^+ \text{Na}^+$, $\text{C}_9\text{H}_{16}\text{NaO}_2$ requires 179.1043). IR (ATR) characterisation was not obtained due to the Spring 2020 COVID-19 shutdown of laboratory facilities.

Benzyl (1-phenylpent-4-en-1-yl)carbamate (**115a**)



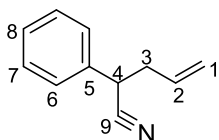
To a solution of acid **116a** (287.26 mg, 1.51 mmol) in dry toluene (5 ml) under N_2 was added Et_3N (0.32 ml, 1.82 mmol) and DPPA (0.36 ml, 1.66 mmol) and the reaction was heated to 90°C for 2 hours. Benzyl alcohol (0.26 ml, 2.27 mmol) was added and reaction was stirred at 90°C for 48 hours. The reaction was then quenched with H_2O (20 ml) and extracted with EtOAc (2 x 30 ml). The combined organics were washed with saturated brine solution (2 x 30 ml), dried with MgSO_4 , filtered and concentrated *in vacuo*. The crude residue was purified by flash column chromatography (10 % EtOAc/hexane) to give **115a** as colourless oil (444.5 mg, 1.5 mmol, 99% yield). ^1H NMR (400 MHz, Chloroform- d): δ 7.32 – 7.14 (10H ,m, H-Ar), 5.73 (1H, dddd, $J = 17.1, 12.2, 6.5, 6.5$ Hz, H-2), 5.18 (1H, d, $J = 8.0$ Hz, N-H), 5.09 – 4.89 (4H, m, H-1,H-11), 4.65 (1H, ddd, $J = 14.3, 7.0$ Hz, H-5), 2.09 – 1.88 (2H, m , H-3), 1.86 – 1.69 (2H, m, H-4); ^{13}C NMR (101 MHz, Chloroform- d): δ 155.0 (C-10), 142.41 (C-6), 137.63 (C-2) , 136.61 (C-12) , 128.5 - 126.3 (C-Ar), 115.2 (C-1), 66.64 (C-11), 54.8 (C-5), 35.6 (C-4), 30.2 (C-3) ppm; **IR (ATR)**: ν_{max} 3320, 3064, 2935, 2854, 1619, 1529, 1496, 1453, 1330, 1289, 1241, 1108, 1027, 911, 748, 696, 483 cm^{-1} ; **HRMS (ESI)**: 296.1645 ($M+\text{H}^+$. $\text{C}_{19}\text{H}_{22}\text{NO}_2$ requires 296.1645)

Benzyl (2-methylhept-6-en-3-yl)carbamate (**115b**)



Compound **115b** was synthesised using the same procedure as **115a** with acid **116b** (251.53 mg, 1.61 mmol), Et₃N (1.46 ml, 1.93 mmol), DPPA (1.36 ml, 1.77 mmol) and benzyl alcohol (1.00 ml, 2.41 mmol). **3b** yielded as a colourless oil (167.29 mg, 1.07 mmol, 66% yield) after flash column chromatography (10 % EtOAc/hexane). ¹H NMR (400 MHz, Chloroform-*d*): δ 7.30 – 7.19 (5H, m, H-Ar), 5.72 (1H, dddd, *J* = 16.8 Hz, 10.0 Hz, 6.5 Hz, 6.5 Hz, H-2), 5.00 (2H, s, H-9), 4.91 (1H, d, *J* = 17.5 Hz H-1trans), 4.86 (1H, d, *J* = 9.9 Hz, H-1cis), 4.46 (1H, d, *J* = 8.0 Hz, N-H), 3.45 (1H, ddd, *J* = 14.3 Hz, 9.5 Hz, 4.4 Hz, H-5), 2.09 – 1.91 (2H, m, H-3), 1.70 – 1.60 (1H, m, H-6), 1.54 – 1.44 (1H, m, H-4), 1.33 – 1.22 (1H, m, H-4), 0.82 (3H, d, *J* = 6.8 Hz, H-7), 0.78 (3H, d, *J* = 6.8 Hz, H-7) ppm; ¹³C NMR (101 MHz, Chloroform-*d*): δ 156.51 (C-8), 138.26 (C-2), 136.81 (C-10), 128.63 (C-12), 128.17 (C-11), 127.89 (C-13), 114.98 (C-1), 66.69 (C-9), 55.99 (C-5), 32.19 (C-6), 31.90 (C-4), 30.60 (C-3), 19.21 (C-7), 17.63 (C-7) ppm; HRMS (ESI): 262.1799 (M+H⁺ . C₁₆H₂₄NO₂ requires 262.1802). IR (ATR) characterisation was not obtained due to the Spring 2020 COVID-19 shutdown of laboratory facilities.

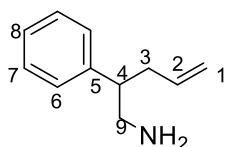
2-phenylpent-4-enenitrile (**122**)



To a solution of diisopropylamine (1.54 ml, 11.00 mmol) in dry THF (5 ml) at -78 °C under N₂ was added n-BuLi (1.81 M , 11.00 mmol) and the solution was stirred for 45 mins. A solution of phenylacetonitrile (1.15 ml, 10.00 mmol) in THF (5 ml) was added at -78 °C over 2 minutes and the reaction was stirred for 45 mins. Allyl bromide (0.86 ml, 10.00 mmol) was added at -78 °C over 1 minute and the reaction was warmed to room temperature. The reaction was stirred overnight and quenched with 1 M aq. HCl (10 ml). The reaction was extracted with diethyl ether (3 x 30 ml), Organic fractions were combined, washed with saturated brine solution (2 x 30 ml), dried with MgSO₄, filtered and concentrated *in vacuo*. The crude residue was purified by flash column chromatography (1 % EtOAc/hexane) to give **122** as a colourless oil (583.48 mg, 3.30 mmol, 30% yield). ¹H NMR (400 MHz, Chloroform-*d*): δ 7.42 – 7.28 (5H, m, H-Ar), 5.79 (1H, dddd, *J* = 17.3 Hz,

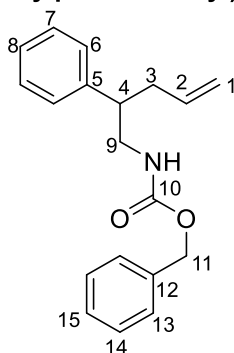
10.5 Hz, 6.9 Hz, 6.9 Hz, H-2), 5.26 – 5.12 (2H, m, H-1), 3.86 (1H, dd, $J = 7.12$ Hz, 7.12 Hz, H-4), 2.57–2.47 (2H, m, H-3) ppm; ^{13}C NMR (101 MHz, Chloroform-*d*): δ 135.39 (C-5), 132.78 (C-2), 129.20(C-8), 128.28 (C-7), 127.48(C-6), 120.51 (C-9), 119.45 (C-1), 39.92 (C-3), 37.53 (C-4) ppm; IR (ATR): ν_{max} 3033, 2921, 2241, 1643, 1600, 1495, 1454, 1077, 994, 925, 754, 698, 623, 554, 510 ; HRMS (APCI): 158.096736 ($\text{M} + \text{H}^+$, $\text{C}_{11}\text{H}_{12}\text{N}$ requires 158.096426)

2-phenylpent-4-en-1-amine (121)



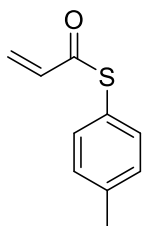
To a suspension of LiAlH_4 (188.23 mg, 4.96 mmol) in dry diethyl ether (10 ml) at 0 °C under N_2 was added nitrile **122** (583.00 mg, 3.30 mmol) in dry diethyl ether (10 ml) over 5 mins and the reaction was stirred at 0 °C for 30 mins. The reaction was then warmed to room temperature and stirred overnight. The reaction was cooled to 0 °C and quenched with H_2O (0.2 ml), followed by NaOH solution (15% w/w aq, 0.2 ml), followed by H_2O (0.6 ml) and then warmed to room temperature. MgSO_4 was added to the reaction and the suspension was filtered through Celite®. The filtrate was concentrated *in vacuo* to give **121** as a colourless oil (499.97 mg, 3.10 mmol, 93% yield). ^1H NMR (400 MHz, Chloroform-*d*): δ 7.54 – 7.05 (5H, m, H-Ar), 5.76 (1H, dddd, $J = 17.0$ Hz, 10.0 Hz, 7.0 Hz, 7.0 Hz, H-2), 5.11 – 4.94 (2H, m, H-1), 3.01 (1H, dd, $J = 12.6$ Hz, 5.1 Hz, H-9), 2.90 (1H, dd, $J = 12.6$ Hz, 8.7 Hz, H-9), 2.78 – 2.70 (1H, m, H-4), 2.52 – 2.38 (2H, m, H-3) ppm ; ^{13}C NMR (101 MHz, Chloroform-*d*): δ 143.10 (C-5), 136.65 (C-2), 128.64 (C-7), 128.05 (C-6), 126.63 (C-8), 116.25 (C-1), 49.43 (C-4), 47.49 (C-9), 38.48 (C-3) ppm; HRMS (ESI): 162.1278 ($\text{M} + \text{H}^+$, $\text{C}_{11}\text{H}_{16}\text{N}$ requires 162.1277). IR (ATR) characterisation was not obtained due to the Spring 2020 COVID-19 shutdown of laboratory facilities.

Benzyl (2-phenylpent-4-en-1-yl)carbamate (115c)



To a solution of **121** (677.25 mg, 4.20 mmol) in dioxane (20 ml) was added K₂CO₃ solution (696.52 mg, 5.04 mmol) followed by benzyl chloroformate (1.19 ml, 5.04 mmol) and the reaction was stirred at room temperature for 3 hours. The reaction was quenched with H₂O (20 ml) and extracted with CH₂Cl₂ (3 x 20 ml). The combined organics were washed with saturated brine solution (20 ml), dried with Na₂SO₄, filtered and concentrated *in vacuo*. The crude residue was purified by flash column chromatography (5 % EtOAc/hexane) to afford **115c** as colourless oil (876.46 mg, 2.96 mmol, 70% yield). ¹H NMR (400 MHz, Chloroform-*d*): δ 7.35 – 7.07 (10H, m, H-Ar), 5.63 (1H, ddt, *J* = 16.9 Hz, 7.2 Hz, H-2), 5.00 (2H, s, H-11), 4.95 (1H, d, *J* = 17.2 Hz, H-1trans), 4.91 (1H, d, *J* = 10.2 Hz H-1cis), 4.63 – 4.51 (1H, m, N-H), 3.62 – 3.54 (1H, m, H-9), 3.20 (1H, ddd, *J* = 13.7 Hz, 9.1 Hz, 4.8 Hz, H-9), 2.82 (1H, apparent pentet, *J* = 7.5 Hz, H-4), 2.37 – 2.31 (2H, m, H-3) ppm; ¹³C NMR (101 MHz, Chloroform-*d*): δ 156.40 (C-10), 142.08 (C-5), 136.64 (C-12), 135.94 (C-2), 130.17 – 125.79 (C-Ar), 116.84 (C-1), 66.76 (C-11), 46.10 (C-9), 45.82 (C-4), 38.27 (C-3) ppm; HRMS (ESI): 296.1644 (M+H⁺, C₂₄H₃₀NO₃S requires 296.1645); IR (ATR): ν_{max} 3337, 2926, 1708, 1520, 1454, 1250, 1141, 999, 756, 699

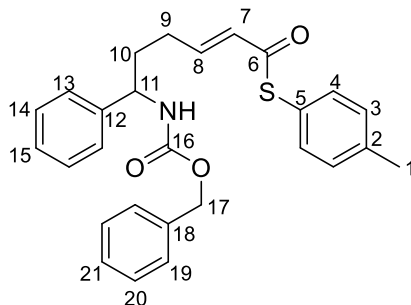
S-(*p*-tolyl) prop-2-enethioate (**118**)



To a solution of NaOH (15% w/w aq., 20 ml) was added NaBH₄ (0.04 g, 0.96 mmol) and *p*-thiocresol (4 g, 32 mmol) which was then stirred for 3 hours. A solution of butylated hydroxytoluene (1.05 g, 0.48 mmol) and acryloyl chloride (3.87 ml, 48 mmol) in cyclohexane (30 ml) was cooled to 0 °C. The aqueous solution of *p*-thiocresol was added dropwise to the acryloyl chloride solution and the reaction warmed to room temperature. The reaction was then heated to 55 °C for 35 minutes. Then, the reaction was cooled to room temperature and extracted with Et₂O (2x 80 ml). The combined organics were washed with saturated NaHCO₃ solution (100 ml) and saturated brine solution (100 ml), dried with MgSO₄, filtered and concentrated *in vacuo*. The crude material was purified by column chromatography (2 % Et₂O/hexane) to afford **118** as yellow oil (3 g, 16mmol, 52% yield). ¹H NMR (400 MHz, CDCl₃): δ 7.36 (d, *J*=8.4 Hz, 2H, H-5), 7.26 (d, *J*=8.4 Hz, 2H, H-6), 6.48 (dd, *J*=17.5, 10.0 Hz, 1H, H-2), 6.40 (dd, *J*=17.5, 1.5 Hz, 1H, H-1), 5.78 (dd, *J*=10.0, 1.5 Hz, 1H, H-1), 2.41 (s, 3H, H-8) ppm; ¹³C NMR (101 MHz, CDCl₃): δ 188.9 (C-3), 139.7 (C-7), 134.5 (C-5), 134.3 (C-2), 130.0 (C-6), 127.2 (C-1), 123.5 (C-4), 21.3 (C-8) ppm; HRMS (ESI) 179.0536 (M +

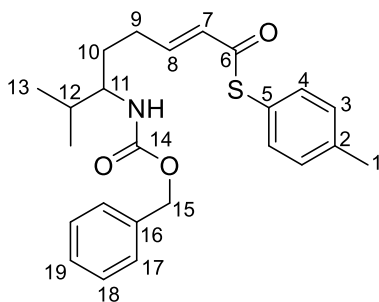
H⁺. C₁₀H₁₁OS requires 179.0536). IR (ATR) characterisation was not obtained due to the Spring 2020 COVID-19 shutdown of laboratory facilities.

S-(*p*-tolyl) (*E*)-6-(((benzyloxy)carbonyl)amino)-6-phenylhex-2-enethioate (113a)



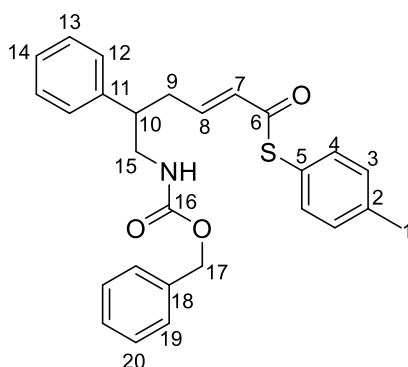
A solution of Cbz-amine **115a** (202.92 mg, 0.68 mmol) in 1,2-DCE (10 ml) and a solution of thioester **118** (367.19 mg, 2.06 mmol) in 1,2-DCE (10 ml) were added under N₂ to a dry flask containing Hoveyda-Grubbs Catalyst™ 2nd generation (43.86 mg, 0.07 mmol) and copper iodide (129.50 mg, 0.68 mmol) in 10 ml 1,2-DCE and the reaction was heated to 50 °C for 24 hours. The reaction was cooled to room temperature, and concentrated *in vacuo*. The crude residue was purified by flash column chromatography (15% EtOAc/hexane) to afford **113a** as pale yellow oil (236.15 mg, 0.53 mmol, 77% yield). ¹H NMR (400 MHz, Chloroform-*d*): δ 7.29 – 7.13 (14H, m, H-Ar), 6.84 (1H, ddd, *J* = 14.5 Hz, 6.5 Hz, H-8), 6.07 (1H, d, *J* = 15.1 Hz, H-7), 5.33 (1H, d, *J* = 8.2 Hz, N-H), 5.08 – 4.96 (2H, m, H-17), 4.64 (1H, dd, *J* = 7.2, 7.2 Hz, H-11), 2.30 (3H, s, H-1), 2.18 – 2.00 (2H, m, H-9), 1.93 – 1.74 (2H, m, H-10) ppm; ¹³C NMR (101 MHz, Chloroform-*d*): δ 188.57(C-6), 155.93 (C-16), 145.18 (C-8), 141.88 (C-12), 139.80 (C-2), 136.55 (C-18), 134.97 – 126.26 (C-Ar, C-7), 124.12 (C-5), 66.99 (C-17), 55.27 (C-11), 34.82 (C-10), 29.27 (C-9), 21.52 (C-1) ppm; IR (ATR): ν_{max} 3031, 2925, 1691, 1631, 1526, 1243, 1045, 808, 699; HRMS (ESI): 446.1795 (M+H⁺, C₂₇H₂₈NO₃S requires 446.1784)

S-(*p*-tolyl) (*E*)-6-(((benzyloxy)carbonyl)amino)-7-methyloct-2-enethioate (113b)



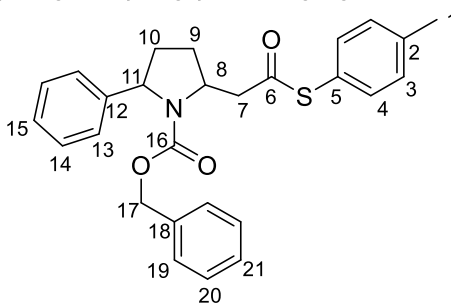
Compound was synthesised using the same procedure as **113a** with thioester **118** (342.27 mg, 1.92 mmol), Hoveyda-Grubbs Catalyst™ 2nd generation (40.10 mg, 0.06 mmol), copper iodide (121.8 mg, 0.64 mmol) and Cbz-amine **115b** (167.29 mg, 0.64 mmol). **113b** yielded as a pale yellow oil (218.12 mg, 0.53 mmol, 84% yield) after flash column chromatography (20% EtOAc/hexane). ¹H NMR (400 MHz, Chloroform-*d*): δ 7.28 – 7.10 (9H, m, H-Ar), 6.85 (1H, ddd, *J* = 14.1 Hz, 6.9 Hz, H-8), 6.17 (1H, d, *J* = 15.5 Hz, H-7), 5.09 (2H, s, H-15), 4.57 (1H, d, *J* = 8.0 Hz, N-H), 3.54 (1H, ddd, *J* = 14.5 Hz, 9.8 Hz, 4.3 Hz, H-11), 2.37 (3H, s, H-1), 2.34 – 2.17 (2H, m, H-9), 1.79 – 1.62 (2H, m, H-10, H-12), 1.50 – 1.37 (1H, m, H-11), 0.92 (3H, d, *J* = 6.8 Hz, H-13), 0.88 (3H, d, *J* = 6.8 Hz, H-13) ppm; ¹³C NMR (101 MHz, CDCl₃): δ 188.61 (C-6), 156.54 (C-14), 145.77 (C-8), 139.73 (C-15), 136.66 (C-16), 134.73-128.68 (C-Ar), 128.16 (C-7), 124.12 (C-2), 66.87 (C-15), 56.19 (C-11), 32.40 (C-12), 31.25 (C-10), 29.45 (C-9), 21.48 (C-1), 19.26- 17.71 (C-13) ppm; IR (ATR): ν_{max} 2958, 1693, 1240, 807; HRMS (ESI): 412.1948 (M+ H⁺, C₂₄H₃₀NO₃S requires 412.1941)

S-(*p*-tolyl) (E)-6-(((benzyloxy)carbonyl)amino)-5-phenylhex-2-enethioate (113c)



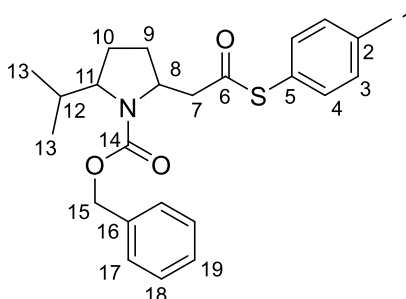
Compound **113c** was synthesised using the same procedure as **113a** with thioester **118** (361.85 mg, 2.03 mmol), Hoveyda-Grubbs Catalyst™ 2nd generation (31.33 mg, 0.05 mmol), copper iodide (100.36 mg, 0.53 mmol) and Cbz-amine **115c** (155.26 mg, 0.53 mmol). **113c** yielded as pale yellow oil (101.58 mg, 0.22 mmol, 42% yield) after flash column chromatography (20% EtOAc/hexane). ¹H NMR (400 MHz, Chloroform-*d*): δ 7.35 – 7.14 (15H, m, H-Ar), 6.83 – 6.74 (1H, ddd, *J* = 15.0 Hz, 7.2 Hz, H-8), 6.13 (1H, d, *J* = 15.4 Hz, H-7), 5.07 (2H, s, H-17), 4.71 – 4.54 (1H, m, N-H), 3.64 – 3.57 (1H, m, H-15), 3.30 (1H, ddd, *J* = 13.6 Hz, 8.6 Hz, 4.9 Hz, H-15), 3.03 – 2.94 (1H, apparent pentet, *J* = 8.4 Hz, H-10), 2.63 – 2.47 (2H, m, H-9), 2.37 (3H, s, H-1) ppm; ¹³C NMR (101 MHz, Chloroform-*d*): δ 188.37 (C-6), 156.43 (C-16), 143.26 (C-8), 140.88 (C-11), 139.75 (C-2), 136.53 (C-18), 134.68-127.30 (C-Ar, C-7), 124.03 (C-5), 66.89 (C-17), 46.25 (C-15), 45.24 (C-10), 36.50 (C-9), 21.47 (C-1) ppm; HRMS (ESI): 468.1605 (M+ Na⁺, C₂₇H₂₇NNaO₃S requires 468.1604). IR (ATR) characterisation was not obtained due to the Spring 2020 COVID-19 shutdown of laboratory facilities.

Benzyl 2-(2-oxo-2-(*p*-tolylthio)ethyl)-5-phenylpyrrolidine-1-carboxylate (**114a**)



A solution of **113a** (22.28 mg, 0.05 mmol) in 1,2-DCE (5 ml) was added under N₂ to a dry flask containing CSA (32.75 mg, 0.14 mmol) and the reaction was heated to 60 °C for 24 hours. The reaction was cooled down to room temperature, diluted with saturated NaHCO₃ solution (5 ml) and extracted with CH₂Cl₂ (3 x 5 ml). The combined organics were washed with saturated brine solution (5 ml), dried with MgSO₄, filtered and concentrated *in vacuo*. The crude material was purified by column chromatography (20 % Et₂O/hexane) to afford **114a** as a colourless oil (11.14 mg, 0.02 mmol, 61% yield) as a 2:1 mixture of rotomers. ¹H NMR (400 MHz, Chloroform-*d*): δ 7.46 – 6.79 (14H, m, H-Ar), 5.17 (1H, minor rotamer, d, *J*=16.0 Hz, H-17), 5.13 (1H, minor rotamer, d, *J*=16.0 Hz, H-17), 5.06-5.00 (1H, both rotomers, m, H-11), 5.01 (1H, major rotamer, d, *J*=12.0 Hz, H-17), 4.87 (1H, major rotamer, d, *J*=12.0 Hz, H-17), 4.65- 4.55 (1H, m, H-8), 3.47 (1H, major rotamer dd, *J*=3 Hz, 3 Hz, H-7), 3.22 (1H, major rotamer, dd, *J*=3 Hz, 3 Hz, H-7), 2.81 (1H, minor rotamer, dd, *J* = 9.6 Hz, 9.6 Hz, H-7), 2.73 (1H, minor rotamer, dd, *J* = 10.1 Hz, 10.1 Hz, H-7), 2.46 - 2.32 (4H, m, H-1, H-10), 2.22 - 2.12 (1H, m, H-10), 1.91 – 1.83 (1H, m, H-9), 1.81- 1.78 (1H, m, H-9) ppm; ¹³C NMR (101 MHz, Chloroform-*d*) δ 194.21 (C-6), 153.84 (C-16), 136.54 – 121.73 (C-Ar), 66.29 (C-17), 61.63 (C-11), 56.08 (C-8), 46.16 (C-7), 32.70 (C-10), 26.73 (C-9), 21.46 (C-1) ppm; HRMS(ESI): 446.1786 (M + H⁺, C₂₇H₂₈NO₃S requires 446.1784); IR (ATR) ν_{max} 2924, 1698, 1494, 1451, 1404, 1347, 1281, 1201, 1114, 1073, 994, 807, 773, 699, 606, 475

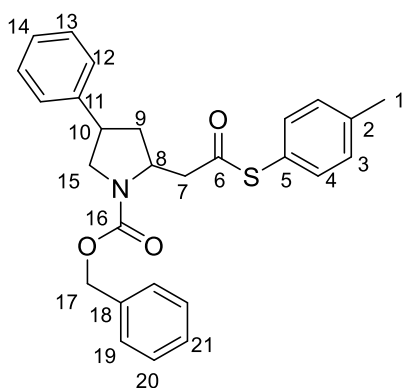
Benzyl 2-isopropyl-5-(2-oxo-2-(*p*-tolylthio)ethyl)pyrrolidine-1-carboxylate (**114b**)



Compound **114b** was synthesised using the same procedure as **114a** with **113b** (33.08 mg, 0.08 mmol) and CSA (56.20 mg, 0.24 mmol). **114b** yielded as a colourless oil (16.46 mg, 0.04 mmol, 45% yield) after flash column chromatography (20% EtOAc/hexane) as a 2:1 mixture of rotomers.

$^1\text{H NMR}$ (400 MHz, Chloroform-*d*): δ 7.43 – 7.18 (9H, m, H-Ar), 5.25 – 5.12 (2H, both rotamers, m, H-15), 4.38 – 4.32 (1H, m, H-8), 3.83 – 3.75 (1H, m, H-11), 3.40 (1H, minor rotamer, dd, $J = 3.2, 3.2$ Hz, H-7), 3.06 (1H, minor rotamer, dd, $J = 3.0, 3.0$ Hz, H-7), 2.72 (1H, major rotamer, dd, $J = 9.6, 9.6$ Hz, H-7), 2.60 (1H, major rotamer, dd, $J = 9.6, 9.9$ Hz, H-7), 2.52 – 2.44 (1H, m, H-12), 2.36 (3H, s, H-1), 2.26 – 2.20 (2H, m, H-10), 2.08 – 1.95 (2H, m, H-9) ppm; $^{13}\text{C NMR}$ (101 MHz, Chloroform-*d*) δ 196.02 (C-6), 154.17 (C-16), 134.74 – 127.39 (C-Ar), 66.86 (C-15), 63.17 (C-11), 56.05 (C-8), 47.47 (C-7), 21.49 (C-1) ppm; **HRMS (ESI)**: 434.1768 ($\text{M} + \text{Na}^+$, $\text{C}_{24}\text{H}_{29}\text{NNaO}_3\text{S}$ requires 434.1760). IR (ATR) characterisation was not obtained due to the Spring 2020 COVID-19 shutdown of laboratory facilities.

Benzyl 2-(2-oxo-2-(*p*-tolylthio)ethyl)-4-phenylpyrrolidine-1-carboxylate (114c)



Compound **114c** was synthesised using the same procedure as **114a** with **113c** (13.36 mg, 0.02 mmol) and CSA (23.00 mg, 0.98 mmol). **114c** yielded as colourless oil (14.00 mg, 0.03 mmol, 90% yield) after flash column chromatography (20% EtOAc/hexane). $^1\text{H NMR}$ (500 MHz, Chloroform-*d*): δ 7.47 – 7.06 (14H, m, H-Ar), 5.23 – 5.15 (2H, m, H-17), 4.20 – 4.15 (1H, minor rotamer, m, H-15), 4.09 – 4.04 (1H, major rotamer, m, H-15), 3.58 (1H, dd, $J = 2.9, 2.9$ Hz, H-7), 3.36 – 3.21 (2H, m, H-10, H-15), 2.69 – 2.61 (1H, m, H-9), 2.37 (3H, s, H-1), 2.08 – 1.94 (1H, m, H-9) ppm; $^{13}\text{C NMR}$ (126 MHz, Chloroform-*d*) δ 195.72 (C-6), 154.61 (C-16), 141.96 – 121.76 (C-Ar), 66.85 (C-17), 55.36 (C-8), 53.00 (C-15), 47.01 (C-7), 42.95 (C-10), 38.90 (C-9), 21.32 (C-1) ppm; **HRMS (ESI)**: 446.1795 ($\text{M} + \text{H}^+$, $\text{C}_{27}\text{H}_{28}\text{NO}_3\text{S}$ requires 446.1784). IR (ATR) characterisation was not obtained due to the Spring 2020 COVID-19 shutdown of laboratory facilities.

11. Abbreviations

| | |
|----------------------|---|
| (R)-anth-cat | (R)-3,3'-Bis(9-anthracenyl)-1,1'-binaphthyl-2,2'-diyl hydrogenphosphate |
| (R)-FeSulPhos | (R _p)-2-(<i>tert</i> -Butylthio)-1-(diphenylphosphino)ferrocene |
| (R)-phen-cat | (R)-2,6-Di-9-phenanthrenyl-4-hydroxy-dinaphtho[2,1-d:1',2'-f][1,3,2]dioxaphosphepin-4-oxide |
| (R)-TiPSY | (R)-3,3'-Bis(triphenylsilyl)-1,1'-binaphthyl-2,2'-diyl hydrogenphosphate |
| (R)-TRIP | (R)-3,3'-Bis(2,4,6-triisopropylphenyl)-1,1'-binaphthyl-2,2'-diyl hydrogenphosphate |
| (S)-SEGPPOS | (S)-(-)-5,5'-Bis(diphenylphosphino)-4,4'-bi-1,3-benzodioxole |
| 1,2-DCE | 1,2-dichloroethane |
| Å MS | Ångström molecular sieves |
| aq | aqueous |
| Ar | aryl |
| BINOL | 1,1'-bi-2-naphthol |
| BiPhePhos | 6,6'-[(3,3'-Di- <i>tert</i> -butyl-5,5'-dimethoxy-1,1'-biphenyl-2,2'-diyl)bis(oxy)]bis(dibenzo[d,f][1,2,3]dioxaphosphenin |
| BHT | butylated hydroxy toluene (2,6-di- <i>t</i> -butyl-4-methylphenol) |
| Bn | benzyl |
| Boc | <i>tert</i> -butyloxycarbonyl |
| Bp | boiling point |
| cat. | catalyst |
| Cbz | carboxybenzyl |
| CPA | chiral phosphoric acid |
| CSA | camphorsulfonic acid |
| DABCO | 1,4-diazabicyclo[2.2.2]octane |
| DBU | 1,8-diazabicyclo[5.4.0]undec-7-ene |
| DIAD | diisopropyl azodicarboxylate |
| DME | dimethoxyethane |
| DPPA | diphenylphosphoryl azide |
| dr | diastereomeric ratio |

| | |
|------------------------|--|
| ee | enantiomeric excess |
| eq | equivalent |
| er | enantiomeric ratio |
| ESI | electrospray ionization |
| Et | ethyl |
| Et₂O | diethyl ether |
| Et₃N | triethylamine |
| EtOAc | ethyl acetate |
| FDA | U.S. Food and Drug Administration |
| gem | geminal |
| HPLC | High Performance Liquid Chromatography |
| IPA | isopropanol |
| <i>i</i>-Pr | isopropyl |
| IR | infra-red |
| LDA | lithium diisopropylamide |
| LiHMDS | lithium bis(trimethylsilyl)amide |
| Me | methyl |
| MeOH | methanol |
| MTBE | methyl tert-butyl ether |
| <i>n</i>-Bu | <i>n</i> -butyl |
| NMR | nuclear magnetic resonance |
| Ns | nitrobenzenesulfonyl |
| OAc | acetate |
| OMe | methoxy |
| OTf | trifluoromethanesulfonate |
| PG | protecting group |
| Ph | phenyl |
| rt | room temperature |
| <i>s</i>-Bu | sec-butyl |

| | |
|--------------------|--------------------------------|
| TBAF | tetra-n-butylammonium fluoride |
| <i>t</i>-Bu | tert-butyl |
| THF | tetrahydrofuran |
| THP | tetrahydropyran |
| TMS | trimethylsilyl |
| Ts | toluenesulfonyl |
| TFA | trifluoroacetic acid |

12. References

- 1) E. Vitaku, D. T. Smith, J. T. Njardarson, *J. Med. Chem.*, 2014, **57**, 10257-10274.
- 2) (a) C. Bhat and S. G. Tilve, *RSC Adv.*, 2014, **4**, 5405-5452; (b) J. P. Michael, *Nat. Prod. Rep.*, 2008, **25**, 139-165; (c) J. W. Daly, T. F. Spande and H. M. Garraffo, *J. Nat. Prod.*, 2005, **68**, 1556-1575; (d) Seneca, in *Alkaloids - Secrets of Life*, 2007.
- 3) (a) L. Zhou, C. Luo, in *Studies in Natural Products Chemistry*, 2012; (b) X. Zhang, J. Ji, Y. Zhu, C. Jing, M. Lia and W. Hu, *Org. Biomol. Chem.*, 2012, **10**, 2133-2138.
- 4) Pearson, W. H. In *Studies in Natural Product Chemistry*; Atta-Ur-Rahman, Ed.; Elsevier: New York, 1998; p **323**. Vol. 1.
- 5) M. G. Vinogradov, O. V. Turova S. G. Zlotin, *Org. Biomol. Chem.*, 2019, **17**, 3670-3708.
- 6) Man-Yi Han, Ju-Ying Jia, Wei Wang, *Tetrahedron Lett.*, 2014, **55**, 784-794.
- 7) S. Wu, S. Lee and P. R. Beak, *J. Am. Chem. Soc.*, 1996, **118**, 715-721.
- 8) G. Carbone, P. O'Brien and G. Hilmersson, *J. Am. Chem. Soc.*, 2010, **132**, 15445-15450.
- 9) P. O'Brien, *Chem. Commun*, 2008, 655-667.
- 10) (a) J. R. Adrio, J. C. Carretero, *Chem. Commun.*, 2019, **55**, 11979-11991; (b) I. Arrastia, A. Arrieta and F. P. Cossio, *Eur. J. Org. Chem.*, 2018, 5889-5904; (c) J. Adrio and J. C. Carretero, *Chem. Commun.*, 2014, **50**, 12434-12446.
- 11) (a) L. M. Castello, C. Najera, J. M. Sansano, O. Larranaga, A. de Cozar and F. P. Cossio, *Adv. Synth. Catal.*, 2014, **356**, 3861; (b) L. M. Castello, C. Najera, J. M. Sansano, O. Larranaga, A. de Cozar and F. P. Cossio, *Synthesis*, 2015, 934.
- 12) S. Cabrera, R. G. Arrayas and J. C. Carretero, *J. Am. Chem. Soc.*, 2005, **127**, 16394-16395.
- 13) L. E. Burgess and A. I. Meyers, *J. Org. Chem.*, 1992, **57**, 1656-1662.
- 14) Y. Yu, C. Shu, T. Tan, L. Li, S. Rafique and L. Ye, *Org. Lett.*, 2016, **18**, 5178-5181.
- 15) G. Luo, M. Xiang, and M. J. Krische, *Org. Lett.*, 2019, **21**, 2493-2497.
- 16) (a) M. D. McReynolds, J. M. Dougherty and P. R. Hanson, *Chem. Rev.*, 2004, **104**, 2239-2258; (b) R. R. Schrock, A. H. Hoveyda, *Angew. Chem., Int. Ed.*, 2003, **42**, 4592-4663; (c) S. T. Diver, A. J. Giessert, *Chem. Rev.*, 2004, **104**, 1317-1382.
- 17) Q. Yang, H. Alper and W. Xiao, *Org. Lett.*, 2007, **9**, 769-771.
- 18) H. Zhou, W. Zhao, T. Zhang, H. Guo, H. Huang, M. Chang, *Synthesis*, 2019; **51(13)**, 2713-2719.
- 19) (a) Z. Amara, J. Caron and D. Joseph, *Nat. Prod. Rep.*, 2013, **30**, 1211-1225; (b) P. R. Krishna, A. Sreeshailam and R. Srinivas *Tetrahedron*, 2009, **65**, 9657-9672.

- 20) (a) S. Fustero, J. Moscardo, D. Jimenez, M. D. Perez-Carrion, M. Sanchez-Rosello and C. del Pozo, *Chem. Eur. J.*, 2008, **14**, 9868 – 9872; (b) S. Fustero, D. Jimenez, J. Moscardo, S. Catalan and C. del Pozo, *Org. Lett.*, 2007, **9**, 5283-5286.
- 21) S. Fustero, C. del Pozo, C. Mulet, R. Lazaro and M. Sanchez-Rosello, *Chem.–Eur. J.*, 2011, **17**, 14267-14272.
- 22) S. Fustero, J. Moscardo, M. Sanchez-Rosello, S. Flores, M. Guerola and C. del Pozo, *Tetrahedron*, 2011, **67**, 7412.
- 23) (a) E. C. Carlson, L. K. Rathbone, H. Yang, N. D. Collett and R. G. Carter, *J. Org. Chem.*, 2008, **73**, 5155; (b) N. Veerasamy, E. C. Carlson and R. G. Carter, *Org. Lett.*, 2012, **14**, 1596.
- 24) T. Azuma, A. Murata, Y. Kobayashi, T. Inokuma and Y. Takemoto, *Org. Lett.* 2014, **16**, 4256-4259.
- 25) E. C. Carlson, L. K. Rathbone, H. Yang, N. D. Collett and R. G. Carter, *J. Org. Chem.* 2008, **73**, 5155-5158.
- 26) A. Farwick and G. Helmchen, *Adv. Synth. Catal.*, 2010, **352**, 1023-1032.
- 27) Z. Sun, G. A. Winschel, P. M. Zimmerman and P. Nagorny, *Angew. Chemie - Int. Ed.*, 2014, **53**, 11194–11198.
- 28) (a) J. M. Keith, J. F. Larrow and E. N. Jacobsen, *Adv. Synth. Catal.*, 2001, **343**, No. 1; (b) E. Vedejs and M. Jure, Efficiency in Nonenzymatic Kinetic Resolution. *Angew. Chem. Int. Ed.*, 2005, **44**, 3974–4001; (c) H. B. Kagan and J. C. Fiaud, *Top. Stereochem.*, 1998, **18**, 249; (d) R. E. Gawley, *J. Org. Chem.*, 2006, **71**, **6**, 2411-2416; (e) J. M. Goodman, A. K. Köhler and S. C.M. Alderton, *Tetrahedron Lett.*, 1999, **40**, 8715-8718.
- 29) (a) T. O. Luukas, C. Girard, D. R. Fenwick and H. B. Kagan, *J. Am. Chem. Soc.*, 1999, **121**, 9299-9306; (b) D. W. Johnson Jr. and D. A. Singleton, *J. Am. Chem. Soc.*, 1999, **121**, 9307-9312.
- 30) (a) J. M. Keith, J. F. Larrow and E. N. Jacobsen: Practical Considerations in Kinetic Resolution Reactions, *Adv. Synth. Catal.*, 2001, **343**, 5-26 (b) M. Tokunaga, J. F. Larrow, F. Kakiuchi and E. N. Jacobsen: Asymmetric Catalysis with Water: Efficient Kinetic Resolution of Terminal Epoxides by Means of Catalytic Hydrolysis, *Science* 1997, **277**, 936–938.
- 31) S. Bellemin-Lapponnaz, J. Tweddell, J. C. Ruble, F. M. Breitling and G. C. Fu, *Chem. Commun.*, 2000, 1009-1010
- 32) (a) M. Binanzer, S.Y. Hsieh and J.W. Bode: Catalytic Kinetic Resolution of Cyclic Secondary Amines. *J. Am. Chem. Soc.*, 2011, **133**, 19698–19701 (b) S.Y. Hsieh, M. Binanzer, I. Kreituss and J. W. Bode: Expanded Substrate Scope and Catalyst Optimization for the Catalytic Kinetic Resolution of N-Heterocycles. , *Chem. Commun.*, 2012, **48**, 8892–8894.
- 33) A. Viso, N. E. Lee and S. L. Buchwald, *J. Am. Chem. Soc.*, 1994, **116**, 9373-9374.
- 34) K. Ermanis, Y. Hsiao, U. Kaya, A. Jeuken and P. Clarke, *Chem. Sci.*, 2017, **8**, 482-490.
- 35) P. Clarke and K. Ermanis, *Org. Lett.*, 2012, **14**, 5550.

- 36) N. S. P. Chakravarthy, *MSc(Research) Thesis*, University of York, 2018.
- 37) C. J. Maddocks, K. Ermanis and P. A. Clarke, Unpublished results
- 38) S. Hanessian, A. Tehim and P. Chen, *J. Org. Chem.*, 1993, **58**, 7768–7781.
- 39) C. Zhong, Y. Wang, A. W. Hung, S. L. Schreiber and D. W. Young, *Org. Lett.* 2011, **13**, 5556.
- 40) (a) M. Beaudoin Bertrand, J. D. Neukom and J. P. Wolfe, *J. Org. Chem.*, 2008, **73**, 8851–8860; (b) H. Boufroua, M. Mauduit, E. Drege and D. Joseph, *J. Org. Chem.*, 2013, **78**, 2346–2354; (c) C. Legeay, W. Lewis and R. A. Stockman, *Chem. Commun.*, 2009, 2207–2209.
- 41) M. Walborsky, M. Topolski, C. Hamdouchi and J. Pankowskif, *J. Org. Chem*, 1992, **57**, 6188–6191.
- 42) L. F. Fieser, *Reagents for Organic Synthesis*, 1967, **1**, 581–595.
- 43) P. Kiviranta, T. Suuronen, E. Walleen, J. Leppanen, J. Tervonen, S. Kyrlylenko, A. Salminen, A. Poso and E. Jarho, *J. Med. Chem.*, 2009, **52**, 2153–2156.
- 44) H. Fuwa, N. Ichinokawa, K. Noto and M. Sasaki, *J. Org. Chem.*, 2011, **77**, 2588–2607.
- 45) J. Kingsbury, J. Harrity, P. Bonitatebus and A. Hoveyda, *J. Am. Chem. Soc.*, 1999, **121**, 791–799.
- 46) K. Ermanis, *PhD Thesis*, University of York, 2014.
- 47) (a) H. Fuwa, N. Ichinkawa, K. Noto and M. Sasaki, *J. Org. Chem.*, 2012, **77**, 2588; (b) L. S. Liebeskind, J and Srogl, *J. Am. Chem. Soc.*, 2000, **122**, 11260.
- 48) H. Wang, B. J. Shuhler and M. Xian, *Synlett*, 2008, 2651–2654.
- 49) Y. Yu and L. S. Liebeskind, *J. Org. Chem.*, 2004, **69**, 3554–3557.
- 50) Y.T Hsiao, *PhD Thesis*, University of York, 2017.
- 51) J. R. Dehli and V. Gotor, *Chem. Soc. Rev.*, 2002, **31**, 365–370.